Quantum Groups and Integralities in Chern-Simons Theory

Thesis by
Sungbong Chun

In Partial Fulfillment of the Requirements for the
Degree of
Doctor of Philosophy

CALIFORNIA INSTITUTE OF TECHNOLOGY
Pasadena, California

2019
Defended June 3rd, 2019

Sungbong Chun
ORCID: 0000-0003-3594-2690

To my family.

ACKNOWLEDGEMENTS

I have spent six academically exciting years at Caltech and I thank all my friends with whom I shared this wonderful experience.

First and foremost, I owe everything that I have learned and achieved to my advisor, Professor Sergei Gukov. I was extremely fortunate to have him as my advisor, who was always open to share his experience, vision and academic mentorship. His advices marked the milestones of my graduate studies and expanded my horizons to the greatest extent. Also, I could only complete my graudate studies because of his consistent support and encouragement throughout the six years. I truly wish I could return the debt by contributing interesting developments and novel ideas to the scientific community, however many years it may take.

I am grateful to Professors Yi Ni, Hirosi Ooguri, Cumrun Vafa and Mark B. Wise, not only for serving as my thesis/candidacy committee and providing invaluable advices, but also for preparing the exciting academic environment in which I was nurtured. I also find myself extremely fortunate to have opportunities to collaborate with: Ning Bao, Miranda C. N. Cheng, Francesca Ferrari, Sarah M. Harrison, Sunghyuk Park, Daniel Roggenkamp, and Nikita Sopenko. I have not only learned a lot, but also enjoyed working with you.

I would also like to thank those with whom I had interesting discussions and conversations: Jørgen Andersen, Christian Blanchet, Hee-Joong Chung, Mykola Dedushenko, Tudor Dimofte, Dongmin Gang, Siqi He, Matthew T. Heydeman, Matthew Hogancamp, Gahye Jeong, Saebyeok Jeong, Dominic Joyce, Murat Koloğlu, Petr Kravchuk, Piotr Kucharski, Aaron Lauda, Ciprian Manolescu, Antun Milas, Satoshi Nawata, Chan Youn Park, Onkar Parrikar, Du Pei, William Petersen, Pavel Putrov, You Qi, David E. V. Rose, Ingmar Saberi, John H. Schwarz, Allic Sivaramakrishnan, Jaewon Song, Piotr Sułkowski, Yuuji Tanaka, Jaroslav Trnka, Alex Turzillo, Zitao Wang, Paul Wedrich, Masahito Yamazaki, Minyoung You, Ke Ye and Don Zagier. I should also thank Carol Silberstein for her help with all the administrative works. This dissertation was in part supported by DEPARTMENT OF ENERGY Award No: DE-SC0011632, and also by the Samsung Scholarship.

Lastly, I would like to thank my family. My father Kwangsuk Jeon and my mother Sunjin Hong have always encouraged me to be a scientist, and I could complete this degree program due to their support. Words are simply not enough, and I instead

dedicate this thesis to them.

ABSTRACT

In this dissertation, we investigate integralities in Chern-Simons theory. The integralities of interest arise from non-local observables (Wilson lines) in Chern-Simons theory and the partition function itself. In the associated supersymmetric gauge theories (via 3d-3d correspondence), they encode certain BPS spectrum, which are often identified with homological invariants of links and three-manifolds. In this dissertation, we observe that all of them are equipped with non-trivial algebraic structures, such as quantum group actions, modularity, and logarithmic vertex algebras. In the first half of this dissertation, we identify quantum group representations with the dynamics of line operators and their lift to surface operators. In the second half, Chern-Simons partition functions on Seifert manifolds are studied in detail, and its "hidden" integralities are identified with quantum modular forms and the characters of logarithmic vertex operator algebra. From the latter, we also observe that quantum group actions control the "dynamics" of characters.

PUBLISHED CONTENT AND CONTRIBUTIONS

This thesis is based on the following publications, which are available on arXiv.

S. Chun, S. Gukov and D. Roggenkamp, "Junctions of surface operators and categorification of quantum groups," arXiv:1507.06318 [hep-th]. S.C computed Wilson line relations, identified them with quantum group relations, and participated in the writing of the manuscript.

S. Chun, "Junctions of refined Wilson lines and one-parameter deformation of quantum groups," arXiv:1701.03518 [hep-th].

S. Chun, "A resurgence analysis of the $SU(2)$ Chern-Simons partition functions on a Brieskorn homology sphere $\Sigma(2,5,7)$," arXiv:1701.03528 [hep-th].

S. Chun and N. Bao, "Entanglement entropy from SU(2) Chern-Simons theory and symmetric webs," arXiv:1707.03525 [hep-th]. S.C participated in the conception of the project, computed link states using web relations, and participated in the writing of the manuscript.

M. Cheng, S. Chun, F. Ferrari, S. Gukov and S. Harrison, "3d Modularity," arXiv:1809.10148 [hep-th]. S.C participated in the construction of modularity dictionary, analyzed transseries expansions, participated in the proof of convergence criteria, and participated in the writing of the manuscript.

TABLE OF CONTENTS

LIST OF ILLUSTRATIONS

LIST OF TABLES

Chapter 1

INTRODUCTION

Chern-Simons theory is a three-dimensional topological field theory (TQFT) of Schwarz type. Due to its topological nature, it is exactly solvable [134]. At the same time, it is a pure gauge theory, and one can study it perturbatively [62, 75, 93, 128]. The theory is naturally equipped with non-local observables supported on one-dimensional defects, called Wilson lines. For certain choice of gauge groups, their expectation values are identified with known polynomial links invariants, while the partition function itself is a 3-manifold invariant.

Curiously, the former exhibits non-trivial integrality. The theory was embedded in string theory [139], and the integrality was understood as BPS degeneracies in topological string theory [71–73, 78, 80, 82, 122]. Meanwhile in the context of quantum algebra, the integrality of polynomial link invariants were understood as graded dimensions of homological invariants [102, 104, 107]. Consequently, homological invariants (Q-cohomology of BPS states) are strictly stronger than the polynomial invariants (supersymmetric indices). In observance of the pattern, one may expect that higher algebraic structures would encode more information about the system. "Categorification" is such a mathematical process in which one associates a higher algebraic structure to a given invariant: numbers to vector spaces, vector spaces to categories, and so on.

This thesis summarizes the author's attempts with his collaborators towards the categorification of Chern-Simons theory, and the role played by various quantum groups therein. In Chapter 2, we focus on categorification of line defects in $SU(N)$ Chern-Simons theory. Utilizing categorical skew Howe duality [125], we associate surface defects and their singular cobordisms to Khovanov-Rozansky homologies which categorify $\mathfrak{sl}_N$ link polynomials. We also consider their possible refinements and applications in quantum information. This chapter is an adaptation of [42, 43].

In Chapter 3, we explore categorification of Witten-Reshetkhin-Turaev (WRT) invariants, which is simply $SU(2)$ Chern-Simons partition function. This chapter not only lies in the development of [84, 85], but it also reveals a novel viewpoint towards the "hidden" integrality of WRT invariants via modularity and logarithmic conformal field theories. This chapter is an adaptation of [38].

Chapter 2

NETWORKS OF DEFECTS AND HOMOLOGICAL LINK INVARIANTS

In this chapter, we consider networks of Wilson lines in $SU(N)$ Chern-Simons theory and their categorifications.

2.1 Polynomial invariants

Chern-Simons theory of interest is supported on S^3. It is a pure gauge theory whose partition function is given by:

$$Z_{CS} = \int \mathcal{D}A\, e^{iS_{CS}}, \quad \text{where} \quad S_{CS} = \frac{k}{4\pi}\int_{S^3} \mathrm{tr}\left(A\wedge dA + \frac{2}{3}A\wedge A\wedge A\right). \quad (2.1)$$

The partition function comes with an anomaly which can be fixed by restricting $k \in \mathbb{Z}$. The classical equation of motion is the flat connection condition $F_A = dA + A\wedge A = 0$. Around them, one can compute the partition function perturbatively in terms of the gauge coupling $k^{-1/2}$ *e.g.* [93, 120, 121, 128].

Besides the partition function, one can also introduce "Wilson line" operators. They are non-local gauge invariant observables supported on one-dimensional manifold C. When C is closed, the Wilson loop operator is defined as:

$$W_R(C) = \mathrm{Tr}_R \int_C A \quad (2.2)$$

by taking a holonomy of gauge field A along a prescribed loop C.

To be well-defined, we must specify representation R of the gauge group and the "framing" of the Wilson line. Framing is a choice of normal vector field on Wilson line in S^3. By slightly displacing the line along the vector field, we may compute the self-linking number. When the self-linking number vanishes, we say that the Wilson line is *canonically* framed. In the canonical framing, expectation values of Wilson lines are invariant under isotopies (Reidemeister moves, in particular), hence topological invariants.

The expectation values of canonically framed Wilson loops can be identified with $\mathfrak{sl}_N$ link polynomials for $G = SU(N)$ and $R = \square$ (the fundamental, N-dimensional representation) [134]. In fact, they are exactly computable by a virtue of TQFT

axioms. Consider a neighborhood (solid torus) of a Wilson loop. By performing path integral, one fixes a vector in the Hilbert space H_{T^2} associated to the boundary torus. Segal's modular functor tells us what the Hilbert space is: the space of conformal blocks in $\hat{G}_k$ Wess-Zumino-Witten model. Next, glue it with another

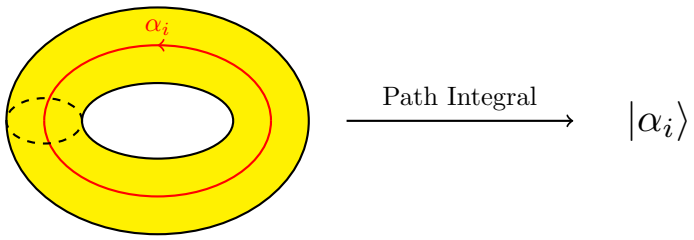

Figure 2.1: A solid torus (colored in yellow) containing a Wilson loop (colored in red). When the Wilson loop carries a representation α_i of the gauge group, the path integral fixes a vector $|\alpha_i\rangle$ in H_{T^2}.

solid torus along the boundary by an element of modular group, $S = \begin{pmatrix} 0 & -1 \\ 1 & 0 \end{pmatrix}$. Then, modular group action on H_{T^2} determines the expectation value of Wilson loop inside S^3, supported on an unknot:

$$\langle W_{\alpha_i}(C)\rangle = \frac{Z_{CS}(S^3;C)}{Z_{CS}(S^3)} = \frac{\langle 0|S|\alpha_i\rangle}{\langle 0|S|0\rangle} = \dim_q \alpha_i \tag{2.3}$$

which is the quantum dimension of α_i. For instance,

$$\dim_q \Lambda^i \square = \begin{bmatrix} N \\ i \end{bmatrix}, \quad \text{where} \quad \begin{bmatrix} N \\ i \end{bmatrix} = \frac{[N]\cdots[N-i+1]}{[i]\cdots[1]}, \quad [i] = \frac{q^i - q^{-i}}{q - q^{-1}}. \tag{2.4}$$

Alternatively, one can consider Wilson lines in a closed 3-ball. Suppose Wilson lines end on n points on the boundary S^2 with representations $\alpha_1, \cdots, \alpha_n$. By a simple charge conservation argument, one can show that the associated Hilbert space has dimension:

$$\dim H_{\{S^2;\{\alpha_i\}_{i=1}^n\}} = \dim \mathrm{Inv}_G \left(\otimes_{i=1}^n \alpha_i\right). \tag{2.5}$$

Diffeomorphisms on S^2 also determine the expectation values. Among them, it is particularly useful to consider the configurations shown in Figure 2.2. Each term of Figure 2.2 represents a pair of Wilson lines in a closed 3-ball, colored by $\square$. For each Wilson line configuration, the path integral fixes a vector in the associated Hilbert space $H_{\{S^2;\square,\square,\bar{\square},\bar{\square}\}}$. Since the Hilbert space is two-dimensional, they must satisfy a linear relation, called a *skein* relation as shown above.

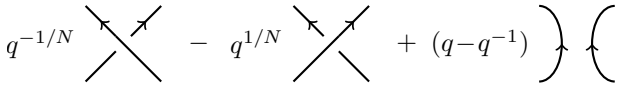

Figure 2.2: Skein relation among *vertically framed* Wilson lines in ordinary $SU(N)$ Chern-Simons theory. Wilson lines are in a closed 3-ball, colored by $\square$. Here, $q = e^{\pi i/(N+k)}$.

It is important to note that the Wilson lines in Figure 2.2 are *vertically* framed. In canonical framing, we only need to replace the first two coefficients by q^{-N} and $-q^N$. The canonically framed skein relation and Equation (2.3) are precisely the defining relations of $\mathfrak{sl}_N$ link polynomials.

2.2 Networks of Wilson lines

Besides Wilson loops, one can introduce junctions of Wilson lines [136, 137]. Consider a Wilson line colored by R, supported on an open interval Γ. Path-ordered integral on Γ yields:

$$(U_R)^i_j = \int_\Gamma \rho(A) \ \in \ \mathrm{Hom}_G(R, R) = R \otimes \bar{R} \tag{2.6}$$

where i, j are the representation indices of R. For $G = SU(N)$, the path-ordered integral is invariant under reversing the orientation of Γ and exchanging $R \leftrightarrow \bar{R}$.

Next, consider junctions of open Wilson lines (Figure 2.3). When Wilson lines colored by $R_1, \cdots R_n$ form a junction, we can place a gauge invariant tensor $\epsilon \in \mathrm{Hom}_G(R_1 \otimes \cdots \otimes R_n, \mathbb{C})$ and contract the representation indices as shown in Figure 2.3(a). Just like braided Wilson lines, networks of Wilson lines would fix a

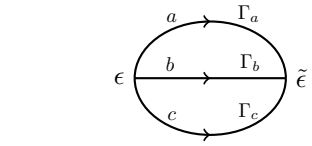

(a)

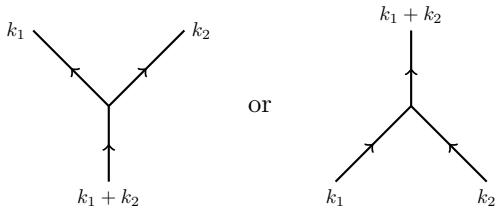

(b)

Figure 2.3: Junctions of Wilson lines. (a) A network of Wilson lines and the corresponding gauge invariant observable. (b) Trivalent junctions of Wilson lines in antisymmetric representations: Labels k refer to representations $\Lambda^k \square$.

vector in the associated Hilbert space. Indeed, Wilson lines in Figure (2.3)(b) would

fix a vector in the associated Hilbert space which is one-dimensional:

$$\dim \mathrm{Hom}_G(\Lambda^{k_1}\square \otimes \Lambda^{k_2}\square, \Lambda^{k_1+k_2}\square) = 1.$$

Since the Hilbert space is one-dimensional, any Wilson line with open ends colored by $\Lambda^{k_1}\square, \Lambda^{k_2}\square, \overline{\Lambda^{k_1+k_2}\square}$ would fix a vector proportional to Figure 2.3.

The proportionality is one example of linear relations satisfied by networks of Wilson lines. Indeed, we will soon observe their relations reproduce quantum group relations of our interest. Of course, it is necessary to properly fix the normalization of invariant tensors. Different choices of normalization lead to different quantum group relations (*c.f.*, [43] and [137]).

Let us remark that the presence of junction requires vertical framing, as self-linking of graphs are quite obscure. Also, we will mostly consider Wilson lines in totally antisymmetric representations $\Lambda^k\square$. For simplicity, they are labeled by k.

Normalizations and some techniques

Before proceeding to quantum group relations, we fix the normalization ambiguity and review some necessary techniques from [135–137].

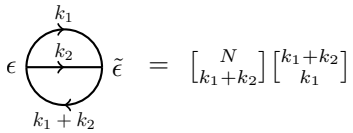

Figure 2.4: Evaluation of a "θ-web" that determines the normalization of invariant tensors ϵ and $\tilde{\epsilon}$.

Normalizations. In what follows, the invariant tensors of type $\mathrm{Hom}_G(k_1 \otimes k_2, k_1 + k_2)$ are normalized as in Figure 2.4. Our choice not only provides a consistent normalization of Wilson line networks (up to a sign which is unimportant), but it also produces quantum group relations of our interest.

Connected sum formula. Consider the LHS of Figure 2.5. Wilson lines are depicted by thick, solid lines, and the two shaded spheres contain non-trivial Wilson line networks as well. They lie in S^3, and a separating S^2 intersects two Wilson lines colored by R and R'. Cutting the three-sphere along S^2, we obtain two closed three-balls with boundary punctures colored by R and R'. Considering the invariant subspace of $R \otimes R'$, the associated Hilbert space is non-trivial if and only if $R' = \bar{R}$. So suppose $R' = \bar{R}$, and perform a path integral on the two separated three-balls.

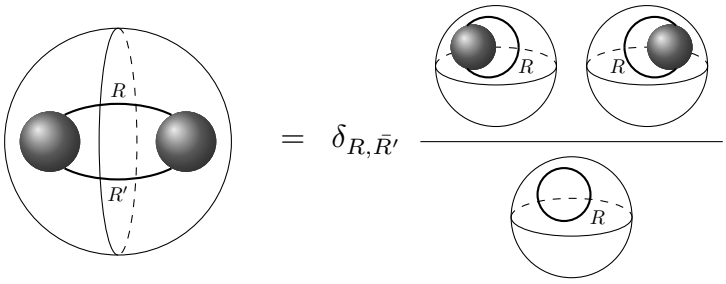

Figure 2.5: An illustration of the connected sum formula, which is satisfied by four different Wilson line configurations.

Denoting the resultant vectors as $|\psi\rangle$ and $|\chi\rangle$, the LHS can be compactly written as $\langle\chi|\psi\rangle$.

Next, consider a Wilson loop colored by R in S^3. Let the loop intersect a separating S^2 at two points. Cutting the three-sphere along S^2 again, we obtain two identical vectors $|\phi\rangle$. Then, the connected sum formula is written as follows:

$$\langle\chi|\psi\rangle\langle\phi|\phi\rangle = \delta_{\bar{R},R'}\langle\phi|\psi\rangle\langle\chi|\phi\rangle. \tag{2.7}$$

The equation holds because when $R' \cong \bar{R}$, all vectors belong to the one-dimensional vector space $H_{\{S^2;R,R'\}}$. This proves the connected sum formula.

Braids. Since Wilson lines are vertically framed in this thesis, they follow the relations in Figure 2.6. In addition, braiding Wilson lines colored by $\Lambda^{k_1}\square$ and $\Lambda^{k_2}\square$ permutes the representation indices of gauge invariant tensors. Therefore, when braiding Wilson lines colored by antisymmetric representations, we must include an extra sign factor $(-1)^{k_1 k_2}$.

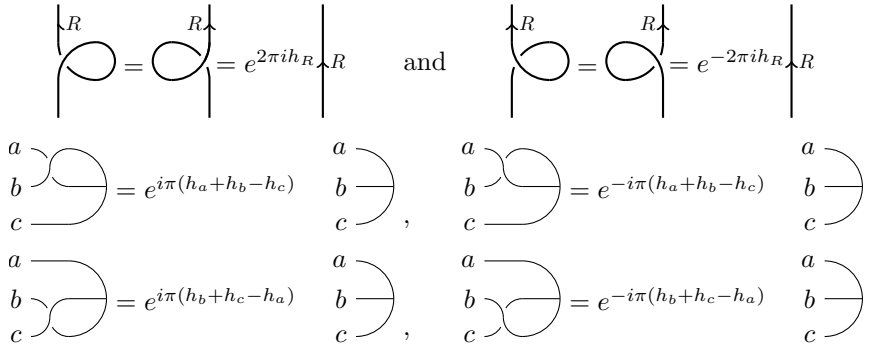

Figure 2.6: Braiding relations among vertically framed Wilson lines. (Above) Reidemeister one moves. (Below) braiding at junctions following the conventions of [136].

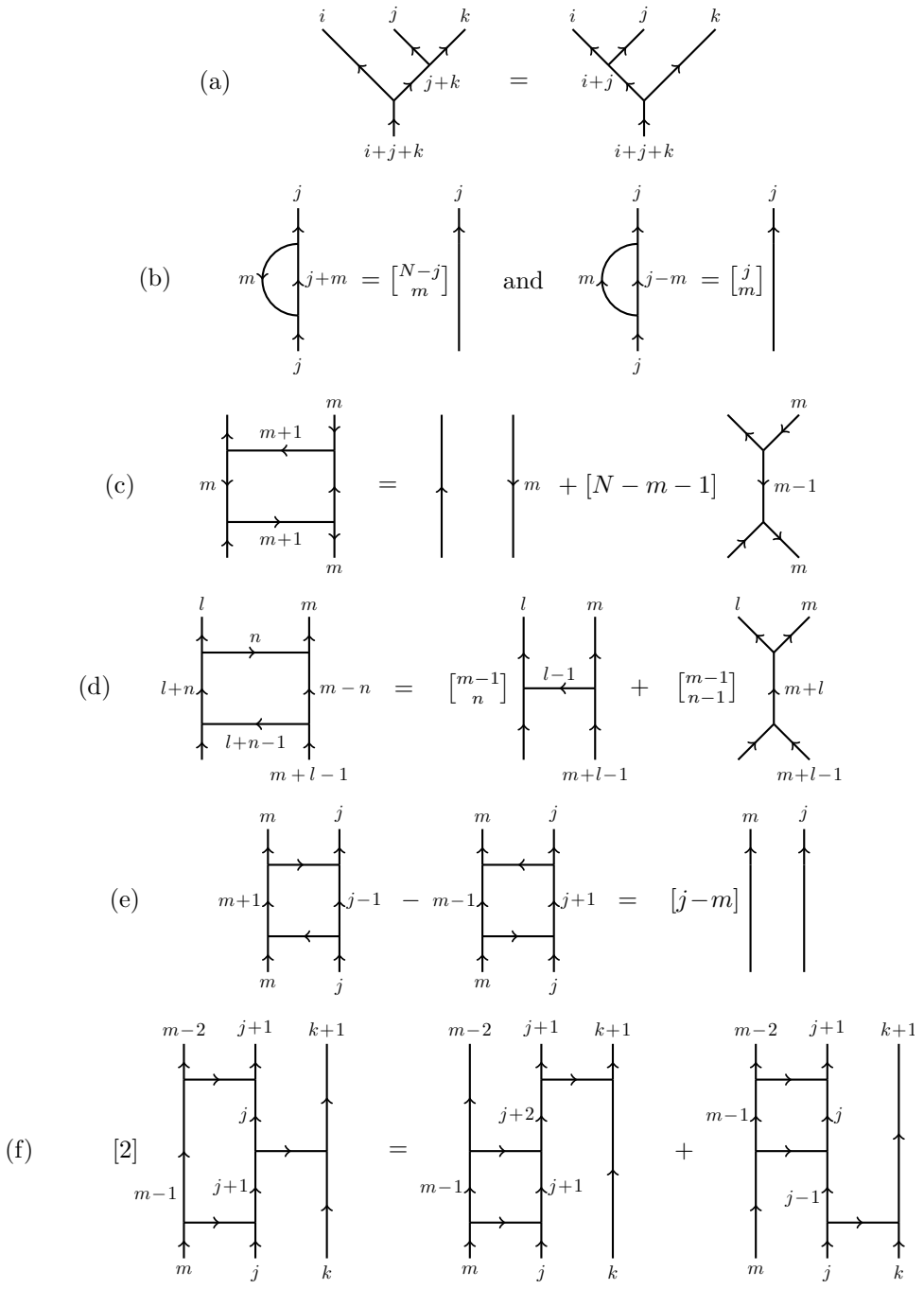

Figure 2.7: Relations among networks of Wilson lines.

Quantum group relations

From the dimensionality 2.5 and the techniques from the previous section, we can derive linear relations among networks of Wilson lines shown in Figure 2.7 (see Appendix A for the proof.) In fact, they not only coincide with relation among

Murakami-Ohtsuki-Yamada (MOY) graph polynomials [143], but also with the defining relations of the diagrammatic quantum group $\dot{\mathbf{U}}_q(\mathfrak{sl}_m)$ [30].

The quantum group of interest $\mathbf{U}_q(\mathfrak{sl}_2)$ is usually defined by means of generators E, F, K, K^{-1} and relations:

$$\begin{gathered} KK^{-1} = 1 = K^{-1}K, \\ KE = q^2EK, \quad KF = q^{-2}FK, \\ [E,F] = \frac{K - K^{-1}}{q - q^{-1}}. \end{gathered} \tag{2.8}$$

In finite-dimensional $\mathbf{U}_q(\mathfrak{sl}_2)$ representations, one can diagonalize K such that its eigenvalue is q^n. In the eigenbasis of K, E and F raises and lowers $\mathfrak{sl}_2$-weights by 2.

To make a direct connection with Wilson lines, one can define idenpotents 1_n which project onto q^n-eigenspace of K. As a result, one obtains an idempotented quantum group $\dot{\mathbf{U}}_q(\mathfrak{sl}_2)$ [13]:

$$\begin{gathered} 1_n 1_m = \delta_{n,m} 1_n, \\ E1_n = 1_{n+2}E = 1_{n+2}E1_n, \quad F1_n = 1_{n-2}F = 1_{n-2}F1_n, \\ [E,F]\,1_n = [n]\,1_n. \end{gathered} \tag{2.9}$$

Then, we have the following identification between Wilson lines and quantum group generators $E, F, 1_n$:

$1_{k_2-k_1} \mapsto$ 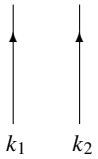

, $E \mapsto$ 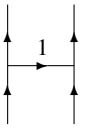

, $F \mapsto$ 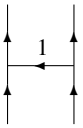

. (2.10)

Upon the identification, Figure 2.7(a) is interpreted as the associativity of $\dot{\mathbf{U}}_q(\mathfrak{sl}_2)$, and Figure 2.7(e) as the commutation relation shown in Equation (2.9).

It must be noted that the rank of quantum group is identified with the number of parallel Wilson lines. Indeed, upon the above identification, $\dot{\mathbf{U}}_q(\mathfrak{sl}_2)$ relations would appear from $SU(N)$ Chern-Simons theory. The choice of gauge group $SU(N)$ only restricts labels k_i of individual Wilson lines, because they represent totally antisymmetric representations $\Lambda^{k_i}\square$. Therefore, one can realize quantum group relations of higher rank under the following identification:

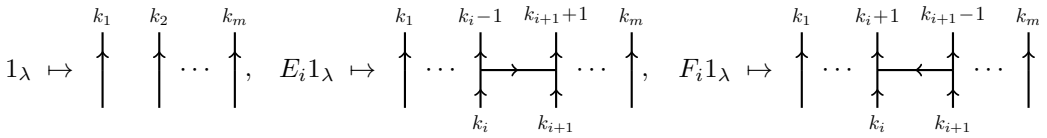

Figure 2.8: $\dot{\mathbf{U}}_q(\mathfrak{sl}_m)$ idempotents and generators in terms of Wilson lines and their junctions.

Then, Figure 2.7(a)-(f) translate to the defining relations of $\dot{\mathbf{U}}_q(\mathfrak{sl}_m)$:

$$\begin{aligned} &1_\lambda 1_{\lambda'} = \delta_{\lambda,\lambda'} 1_\lambda, \quad E_i 1_\lambda = 1_{\lambda+l_i} E_i, \quad F_i 1_\lambda = 1_{\lambda-l+i} F_i, \\ &[E_i, F_j] 1_\lambda = \delta_{i,j} [\lambda_i] 1_\lambda, \quad [E_i, E_j] 1_\lambda = 0 \quad \text{for} \quad |i-j| > 1, \\ &\text{and} \quad E_i E_j E_i 1_\lambda = E_i^{(2)} E_j 1_\lambda + E_j E_i^{(2)} 1_\lambda \quad \text{for} \quad |i-j| = 1. \end{aligned} \tag{2.11}$$

Here $\lambda = (k_2 - k_1, \cdots, k_m - k_{m-1}) \in \mathbb{Z}^{m-1}$ denotes an $\mathfrak{sl}_m$ weight, and E_i (resp. F_i) are simple roots of $\mathfrak{sl}_m$ raising (resp. lowering) the weights λ by an addition (resp. subtraction) of $l_i = (0, \cdots, 0, -1, 2, -1, 0, \cdots, 0)$ where 2 appears in the i^{th} position.

Thus, we have described a physical realization of *skew Howe duality*:

$$\Lambda^k(\mathbb{C}^m \otimes \mathbb{C}^N) \cong \bigoplus_{k_1+\cdots+k_m=k} \Lambda^{k_1}\mathbb{C}^N \otimes \cdots \otimes \Lambda^{k_m}\mathbb{C}^N \,. \tag{2.12}$$

On $\mathbb{C}^m$ and $\mathbb{C}^N$ respectively, $\mathfrak{sl}_m$ and $\mathfrak{sl}_N$ act commutatively. On the RHS, we have decomposed the representation by $\mathfrak{sl}_m$ weights. The equality is obviously true in classical Lie algebra, but it also generalizes to quantum groups $\dot{\mathbf{U}}_q(\mathfrak{sl}_m)$ [30]. The quantum group is by itself a category and admits a very simple diagrammatic representation. Indeed, one can represent each weight space by a dot labeled by n, and the "morphisms" E_i and F_i by arrows mapping from n to $n \pm 2$.

In Chern-Simons theory, one can identify $\wedge^{k_i}\mathbb{C}^N$ as the k_i-th antisymmetric power of $SU(N)$ fundamental representation. Therefore, each summand on the RHS is identified with m Wilson lines in the k_i-th totally antisymmetric representations. In fact, the identification of Figure 2.8 exactly corresponds to the skew Howe duality functor from an idempotent quantum group $\dot{\mathbf{U}}_q(\mathfrak{sl}_m)$ to the category $N\text{Web}_m$ [30]. The latter category has m-tuples $(k_1, \cdots, k_m)$ as objects, and morphisms (called "$\mathfrak{sl}_N$-webs") are generated by morphisms in Figure 2.8. $\mathfrak{sl}_N$-webs naturally satisfy the relations of Figure 2.7.

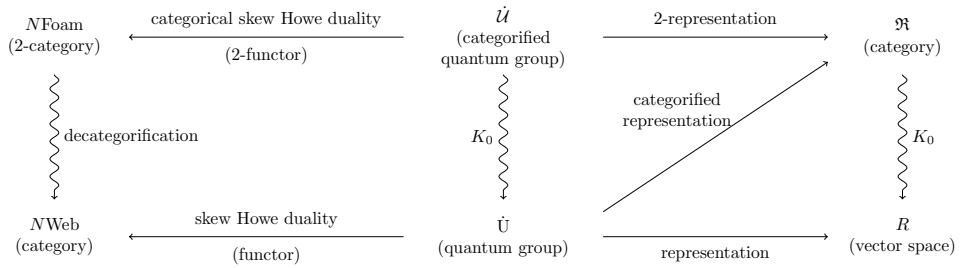

Figure 2.9: Categorification of skew Howe duality.

2.3 Categorification and *N*Foam categories

In the previous section, we have seen that Wilson lines in $SU(N)$ Chern-Simons theory realize *N*Web category. In fact, the latter admits categorification via *categorical* skew Howe duality [125]. Upon categorification, both the quantum group $\dot{\mathbf{U}}_q(\mathfrak{sl}_m)$ (which is itself a category) and its representation category *N*webs are lifted to higher algebraic structures (2-categories).

Just like *N*Web category, *N*Foam 2-category has a diagrammatic presentation [125] in terms of singular cobordisms. Furthermore, just as *N*Web category is a representation of $\dot{\mathbf{U}}_q(\mathfrak{sl}_m)$, *N*Foam 2-category is a representation of the categorified quantum group, $\dot{\mathcal{U}}$. Indeed, the above construction is a $\mathfrak{sl}_N$ generalizations of Bar-Natan category of tangles and cobordisms [12] which encode Khovanov homology for links in S^3. Recall that in Khovanov homology, one encodes the skein relation by associating to each crossing of the given link, a two-dimensional complex which is a mapping from one trivial tangle into another. For a link L with n crossings, therefore, one associates a 2^n-dimensional complex $[[L]]$. By introducing cobordism among tangles to encode such a mapping, one arrives at the Bar-Natan category. To recover homological invariants, one only needs to apply the representable functor $\oplus_{k\in\mathbb{Z}}\mathrm{Hom}(q^{-k}\emptyset,\cdot)$ from degree-shifted empty tangles to the complex $[[L]]$. As a result, one obtains a complex of q-graded vector spaces which is precisely the Khovanov homology of L.

The $\mathfrak{sl}_3$ generalization of Khovanov homology also admits a similar construction [103, 114, 117]. However, one must introduce "thick" edges, because one cannot resolve crossings via skein relation even when the edges are colored by fundamental representations. As a result, one naturally associates to each crossing a complex between *networks* of edges instead of trivial tangles. Consequently, $\mathfrak{sl}_3$ generalization of the Bar-Natan category is a 2-category of singular cobordisms.

Generalizations to other $n \geq 3$ are more delicate. Homological invariants themselves were constructed by utilizing matrix factorizations [104]. The singular cobordism category was also constructed [115], but it had several technical issues. First of all, the singular cobordism category does not accommodate "colored" version of Khovanov-Rozansky homologies whose edges carry representations other than $\square$ [143, 144]. Secondly, it was rather obscure how to extract link invariants from the relations among foams. Instead, closed Foams were evaluated by using Kapustin-Li formula from topological Landau-Ginzburg models [96, 105].

It is by virtue of categorical skew Howe duality [125] that all such issues were resolved. The structure of higher representation is particularly useful, because the categorified quantum group controls morphisms in a higher category (which is typically difficult to study). Furthermore, there is an induced representation from NFoams to the homotopy category of matrix factorizations, which enables us to compute homological link invariants without ambiguity.

In physics, the above observation implies that networks of Wilson lines must be lifted to junctions of surface defects, as shown in Figure (2.10). Indeed, this is consistent with "dimensional oxidation" in TQFT, which promotes a d-dimensional TQFT to a $(d+1)$-dimensional one [46] (see also [77]). Since Chern-Simons theory

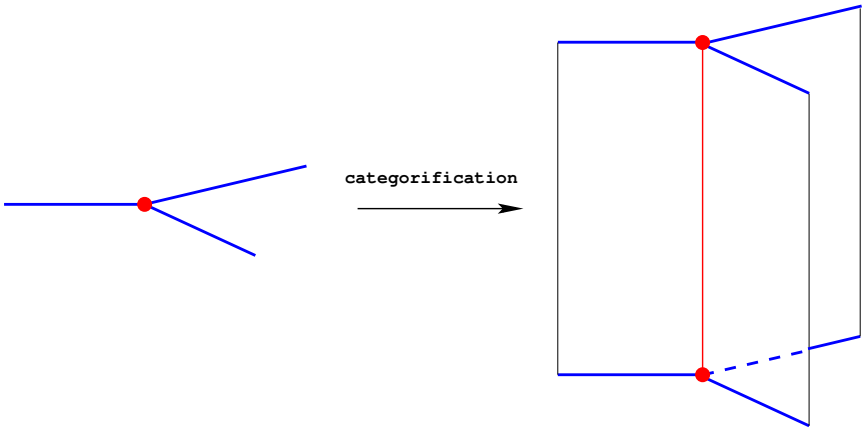

Figure 2.10: Categorification by lifting a given TQFT to one dimension higher.

is a 3d TQFT with line defects, Figure 2.10 suggests that its categorification would involve junctions of surface defects in 4d TQFT, where the fourth dimension is vertical. Indeed, the cobordism shown in Figure 2.10 depicts a 1-morphism in the NFoam 2-category, acting *horizontally* on a set of parallel surfaces (colored blue) to another set of surfaces across a junction (colored red).

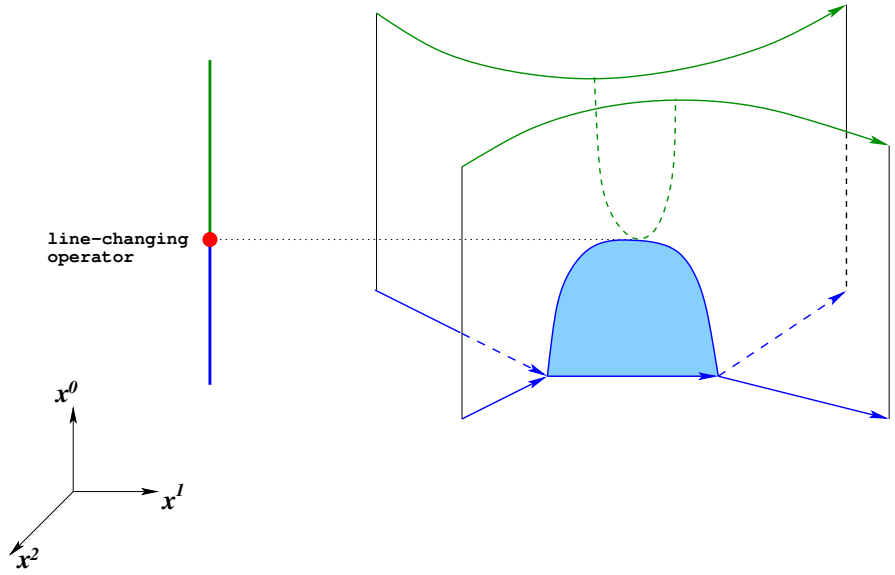

Figure 2.11: A singular cobordism which represents a 2-morphism of $\dot{\mathcal{U}}$.

The novel features of NFoam 2-category are 2-morphisms, which is a *vertical* mapping between NWebs. The "seamed line" of the singular cobordism encodes 2-morphisms of $\dot{\mathcal{U}}$, which realizes the NFoam 2-category as a 2-representation of $\dot{\mathcal{U}}$.

Therefore, we wish to identify a 4d TQFT with surface defects whose kinematics realizes NFoam 2-category. In fact, a clue is provided by the "decategorification" process. Our candidate 4d TQFT associates a vector space $H(K)$ to (colored) knots or links K embedded in the boundary 3-manifold. Then, we associate a linear map to a cobordism Σ between knots / links K_1 and K_2 extending in the fourth dimension:

$$Z(\Sigma) : H(K_1) \ \rightarrow \ H(K_2).$$

Next, consider $K_1 = K \cup C$ (a disjoint union of a knot K and an unknot C) and $K_2 = K \# C \cong K$. For simplicity, color K, C by the same representation R of the gauge group. Then,

$$Z(\Sigma) : H^R(C) \otimes H^R(K) \ \rightarrow \ H^R(K). \tag{2.13}$$

Denote $A = H^R(C)$. Equation (2.13) implies that $H^R(C)$ are A-modules, and pair-of-pants cobordisms among disjoint union of unknots determine a Frobenius algebra. For example, $N = 2$ leads to the original Khovanov homology, where

$$A = \mathbb{C}[x]/\langle x^2 \rangle.$$

The Frobenius algebra determines a 2d TQFT supported on Σ. When one obtains such a 2d TQFT from a supersymmetric theory by performing a topological twist, A corresponds to a chiral ring of the untwisted theory on $\Sigma = \mathbb{R} \times C$.

2.4 Junctions of surface operators

Surface operators are supported on surfaces Σ in 4d QFT on M_4. In this thesis, we are particularly interested in surface operators supported on singular surfaces (2-morphisms of NFoams), or equivalently, junctions of surface operators. It thus provides a natural home in physics for a microscopic realization of the ideas advocated in [6, 105, 129].

Just as Wilson and 't Hooft line operators can be regarded as the worldline of infinitely massive electric / magnetic sources in 3d, we may consider surface operators as non-dynamical flux tubes (or vortices). In many examples, surface operators can be described either (1) as singularities for the gauge fields along Σ, or (2) as 4d-2d coupled systems, $S_{\text{tot}} = \int_{M_4} d^4x \ (\mathcal{L}_{\text{4d}} + \delta_\Sigma \cdot \mathcal{L}_{\text{2d}})$.

Surface operators and conservation of charges

From the first viewpoint, a surface operator $F = 2\pi\alpha\delta_\Sigma + \cdots$ with non-zero α can be thought as a worldsheet of Dirac string of a magnetic monopole with charge α. Then, the surface operator would be visible only if the monopole violates the Dirac quantization condition that α belongs to the root lattice of G [81]. Thus, we require that $\alpha \in \mathfrak{t}$, the Lie algebra of the maximal torus of G (modulo the action of root lattice). In particular, when $G = U(1)$, $\alpha \in \mathbb{R}/\mathbb{Z}$.

To consider "charge conservation" across junctions of surface operators, we first recall that Wilson lines colored by R are oriented. Physically, a Wilson line is equivalent to its orientation reversal colored by the dual representations $\bar{R}$. Upon categorification, the orientations are naturally identified with magnetic fluxes along Σ. Therefore, two surface operators with opposite orientations are equivalent if the gauge holonomies $U = \exp(2\pi i\alpha) \in G$ around the Dirac string are related by $U \leftrightarrow U^{-1}$. We will soon observe that the gauge fields restricted on a "static slice" of $M_4 = \mathbb{R}_t \times M_3$ often satisfy the flat connection condition $F_{\mu\nu} = 0$ as BPS equations. When the BPS condition is satisfied away from the singularity Σ, the magnetic fluxes are conserved at every junction. In particular, when $G = U(1)$,

$$\alpha = \alpha' + \alpha'' \pmod 1 \tag{2.14}$$

for a basic junction depicted in Figure 2.3. Note the analogy to the "charge conser-

vation" witnessed in Equation (2.5). The analogy extends to non-abelian cases:

$$1 \in C \cdot C' \cdot C'' \tag{2.15}$$

where C, C', C'' are conjugacy classes of the holonomies U, U', U''. Here, we have oriented surface operators forming a trivalent junction such that they are all "incoming." Equation (2.15) has a natural meaning as OPE of surface operators, whose coefficients are valued in the moduli space of flat G-bundles on a S^2 with three punctures.

For $G = SU(N)$, the "selection rules" for the OPE of surface operators can be most conveniently written in terms of $\alpha = \frac{1}{2\pi i} \log U$ in the fundamental alcove of G,

$$\alpha \in \mathcal{U}, \quad \text{where} \quad \mathcal{U} = \{\alpha_1 \geq \cdots \alpha_N \geq \alpha_1 - 1 \mid \sum_i \alpha_i = 0\}. \tag{2.16}$$

When $G = SU(2)$, Equation (2.15) becomes a "triangular inequality" [94]:

$$|\alpha' - \alpha''| \leq \alpha \leq \min\{\alpha' + \alpha'', 1 - \alpha' - \alpha''\}.$$

For $G = SU(N)$, the inequalities are more delicate, but they can still be explicitly written [4, 15]:

$$\sum_{i \in I} \alpha_i + \sum_{j \in J} \alpha'_J + \sum_{k \in K} \alpha''_k \leq d, \tag{2.17}$$

for each $d \geq 0$, $r = 1, \cdots, N$, and I, J, K running over all r-elements subsets of $\{1, \cdots, N\}$ such that the degree-d Gromov-Witten invariant of $Gr(r, n)$ satisfies:

$$GW_d(\sigma_I, \sigma_J, \sigma_K) = 1.$$

Above, σ_I's are Schubert cycles of $Gr(r, N)$ defined with respect to a complete flag. Regarding OPE coefficients for junctions of totally antisymmetric-colored surface operators, Equation (2.17) can be solved by U_k in the following form [43]:

$$U_k = \exp 2\pi i \alpha_k = \exp 2\pi i \left(\underbrace{\frac{k}{2N}, \cdots, \frac{k}{2N}}_{N-k}, \underbrace{\frac{k-N}{2N}, \cdots, \frac{k-N}{2N}}_{k} \right).$$

Surface operators in a 4d-2d coupled system

Now, consider a configuration where $\Sigma = \mathbb{R}_t \times \Gamma$ is a foamed surface (Γ being a trivalent, colored graph) embedded in $\mathbb{R}_t \times S^3$. Holonomies of the gauge fields around

an edge colored by k is fixed by U_k. Then, the moduli space of flat connections is the representation variety:

$$\mathcal{M}(\Gamma) \;=\; \mathrm{Rep}\left(\pi_1(S^3 \setminus \Gamma); SU(N)\right) . \tag{2.18}$$

In fact, one can model the above moduli space in the following way [74, 111]. Consider associating a point in Grassmannian $Gr(k, N)$ to each edge colored by k. At each junction of lines colored by k_1, k_2, $k = k_1 + k_2$, we impose the condition that "incoming" k_1- and k_2- planes are orthogonal in $\mathbb{C}^N$ and span the "outgoing" k-plane. Let us call such decorations *admissible*. Then, the space of all admissible decorations on Γ is homeomorphic to $\mathcal{M}(\Gamma)$. In other words, surface operators of interest are naturally labeled by the "Levi types" $\mathbb{L} = S(U(k) \times U(N-k))$ for $k = 1, \cdots, N-1$, so that for a k-colored facet, we can asscociate:

$$\mathcal{F}_k \;=\; G/\mathbb{L} \;=\; Gr(k, N) \;=\; SU(N)/S(U(k) \times U(N-k)). \tag{2.19}$$

A simple example of Γ would be an unknot colored by k, whose moduli space is $Gr(k, N)$ itself. One can easily observe that the cohomology ring is isomorphic to the k-colored cohomology of an unknot.

Notice that the above construction tells us that the moduli space for a trivalent junction is precisely the partial flag variety $Fl(k_1, k, N)$ of k_1-planes in $k = (k_1 + k_2)$-planes in $\mathbb{C}^N$

$$\begin{array}{ccccc} Gr(k,N) & \longleftarrow & Fl(k_1,k,N) & \longrightarrow & Gr(k_1,N) \times Gr(k_2,N) \\ V & \longleftarrow & (V_1 \subset V) & \longmapsto & (V_1, V_1^{\perp} \subset V). \end{array} \tag{2.20}$$

Although it would be extremely interesting to investigate the explicit solution to the supersymmetric gauge theory with prescribed boundary conditions (the holonomies U around Σ), it can be a difficult task in general. To study the kinematics of surface operators in a 4d TQFT, however, we only need to know their existence and their moduli spaces. So far, we have discussed the effective 2d theory on $\Sigma = \mathbb{R}_t \times \Gamma$ which lifts networks of Wilson lines Γ. In the next section, we will consider them as Landau-Ginzburg theories with B-type defects to physically realize 2-morphisms NFoam 2-category in terms of matrix factorizations. Still, it remains to lift Chern-Simons theory to higher dimensions. One can achieve this by embedding the gauge theory to string / M-theory.

Brane constructions

We can engineer various supersymmetric field theories on M_4 from coincident fivebranes supported on:

$$N \text{ M5-branes}: \qquad M_4 \times C. \tag{2.21}$$

Various choices of 2d surfaces C and the 11d spacetime yield different effective four-dimensional theories on M_4. In particular, we may preserve different amount of supersymmetries: $\mathcal{N} = 4, 2$, or 1 supersymmetry on M_4. In [43], all three cases are discussed in detail, and we restrict ourselves to $\mathcal{N} = 4$ and 2 cases which are directly relevant to the *N*Foam 2-category.

To include defects, we introduce additional M5-branes or M2-branes which intersect the above N M5-branes along $\Sigma \subset M_4$. It turns out that the coloring $\Lambda^k\square$ of the seamed facets can be obtained from k coincident fivebranes (denote M5'-branes) intersecting N M5-branes along Σ. Then, the junctions of surface operators have a natural interpretation, where k coincident branes splitting into k_1- and k_2- coincident branes across the junction.

Junctions in 4d $\mathcal{N} = 4$ theories. When the surface C is flat (T^2 or $\mathbb{R}^2$), we can preserve maximal amount of $\mathcal{N} = 4$ supersymmetry on M_4. Including surface defects along Σ, we may break supersymmetry further depending on the geometry of Σ.

In the simplest case where M_4 and Σ are both flat, we can again preserve maximal amount of SUSY and introduce half-BPS surface operators supported on Σ. The relevant brane construction can be summarized as follows:

	0	1	2	3	4	5	6	7	8	9	10
M5	×	×	×	×			×				×
M5′	×	×					×		×	×	×

(2.22)

Following conventions of [140], M_4 is parametrized by (x^0, x^1, x^2, x^3), Σ by (x^0, x^1), and C by x^6 and x^{10}.

Since the surface operators are half-BPS in 4d $\mathcal{N} = 4$ theory, their junctions are $\frac{1}{4}$-BPS. Identify $\mathbb{R}_t = x^0$ and $\Gamma \subset (x^1, x^2)$ which form a seamed surface $\Sigma = \mathbb{R}_t \times \Gamma$. In fact, we may choose $M_4 = \mathbb{R}_t \times M_3$ for a 3-manifold M_3 whose local coordinates are (x^1, x^2, x^3). Perform partial topological twist along M_3, (x^7, x^8, x^9) fiber over M_3 as a cotangent bundle. As a result, we can preserve four real supercharges, and junctions are 1/4-BPS. M5-branes are supported on $\mathbb{R}_t \times M_3 \times C$, while M5'-branes

are supported on $\mathbb{R}_t \times L_\Gamma \times C$. Here, L_Γ is a special Lagrangian submanifold in the local Calabi-Yau manifold T^*M_3 intersecting M_3 along Γ.

Note that $\Sigma = \mathbb{R}_t \times \Gamma$ is a "static" configuration and represents a 1-morphism in NFoam 2-category. For "dynamical" configurations and non-trivial 2-morphisms, we must replace $\mathbb{R}_t \times M_3$ with a four-manifold M_4 and $\mathbb{R}_t \times \Gamma$ with a generic seamed surface Σ. To preserve supersymmetry on generic $\Sigma \subset M_4$, we must perform topological twist on M_4, in which (x^7, x^8, x^9) directions fiber over M_4 as a bundle of self-dual 2-forms. As a result, the spacetime is $\Lambda^2_+(M_4) \times \mathbb{R}^4$, and L_Σ, M_4 are coassociative submanifolds in a local G_2-holonomy manifold $\Lambda^2_+(M_4)$. As a result, we can preserve two real supercharges, hence $\mathcal{N} = (0, 2)$ supersymmetry on C.

Junctions in 4d $\mathcal{N} = 2$ theory. Consider C, an arbitrary Riemann surface of genus $g \neq 1$ (boundaries and punctures allowed). To preserve 4d $\mathcal{N} = 2$ SUSY, we must perform a topological twist along C and fiber (x^4, x^5) over C, so that C is a holomorphic Lagrangian submanifold in a CY_2 manifold which is locally T^*C. Topological twists identify the $U(1)_r \times SU(2)_R$ R-symmetry group with rotations in the fiber, $U(1)_{45} \times SU(2)_{789}$. Restricting ourselves to $M_4 = \mathbb{R}_t \times M_3$ and "static" $\Sigma = \mathbb{R}_t \times \Gamma$, we obtain junctions of half-BPS surface operators whose junctions are quarter-BPS, hence two real supercharges preserved.

Next, we consider the brane setup for the categorification of line defects in $SU(N)$ Chern-Simons theory. Soon after the construction of the first homological knot invariants [102, 123, 127], it was proposed [77, 82] that knot homology should be interpreted as a Q-cohomology of the suitable physical system,

$$\text{knot homology} \;=\; Q\text{-cohomology} \;\equiv\; \mathcal{H}_{\text{BPS}}. \tag{2.23}$$

The proposal has been advocated by many physical realizations of different knot homologies. In particular, for a $\Lambda^k\square$-colored, doubly graded $\mathfrak{sl}_N$ homological knot invariants, the five-brane configuration was described in [141]:

$$\begin{aligned} \text{space-time:} \quad & \mathbb{R}_t \times T^*S^3 \times TN_4 \\ N \text{ M5-branes:} \quad & \mathbb{R}_t \times\; S^3 \;\times\; \mathbb{R}^2_\epsilon \\ k \text{ M5}'\text{-branes:} \quad & \mathbb{R}_t \times\; L_K \;\times\; \mathbb{R}^2_\epsilon \end{aligned} \tag{2.24}$$

where $C = \mathbb{R}^2_\epsilon$ is a cigar in the Taub-NUT space $TN_4 \cong T^*C$. Keeping track of the $U(1) \times U(1)$ quantum numbers associated with the rotation symmetry of the base and fiber in $C \subset TN_4$, we obtain two gradings, namely the q-grading and the homological t-grading.

Therefore, a natural home for NFoam 2-category is a brane setup similar to Equation (2.24) in which we replace K by Γ. Indeed, it provides a variant of brane constructions of junctions in 4d $\mathcal{N} = 2$ theory, where we specify $M_3 = S^3$ and $C = \mathbb{R}^2_\epsilon$.

2.5 Landau-Ginzburg phases and matrix factorizations

So far, we have identified the brane setup in which the junctions of surface defects carry 2d sigma models on Σ whose target spaces are partial flag varieties. The purpose of this section is to relate them with interfaces of LG models which naturally arise from the singular cobordisms $\Sigma = \mathbb{R}_t \times \Gamma$. We find that the relevant matrix factorizations indeed coincide with those of [125, 143, 144].

LG theories on R-colored facets

As was briefly mentioned above, matrix factorizations were utilized to construct homological knot invariants [104, 107] and their colored variants [143, 144]. Physically, matrix factorizations describe boundary conditions and interfaces in 2d Landau-Ginzburg models [24–27, 92, 96].

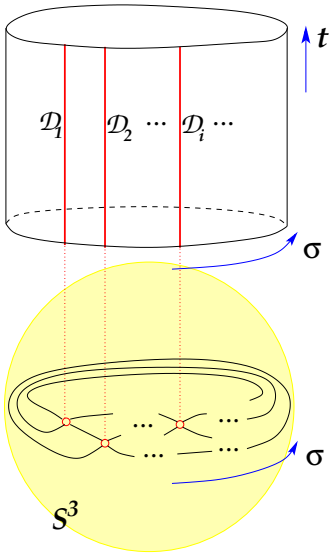

Figure 2.12: 2d LG theories and their interfaces supported on $\mathbb{R}_t$ times strands of links and the crossings.

Furthermore, it was argued [29, 78, 79] that the matrix factorizations of Khovanov-Rozansky homology (*i.e.*, when edges are colored by $\square$) should be identified with those which appear on the interfaces of 2d Landau-Ginzburg (LG) models. To elaborate, consider a braid group representation of a knot / link K. As depicted in

Figure 2.12, one considers its 1d projection S^1_σ along the direction of braid closure. Then, the support of LG models are the facets between the interfaces in $\mathbb{R}_t \times S^1_\sigma$, which appear at the crossings.

Dualities in string / M-theory allow us to study the degrees of freedom on Σ, and one associates to each facet colored by R a 2d theory whose chiral ring is isomorphic to the R-colored homology of an unknot (as discussed in Section 2.3). This way, one not only reproduces the superpotential $W_{\mathfrak{sl}_N,\square}$ used in [104, 107] but also obtains $W_{\mathfrak{sl}_N,R}$ for $R = \mathrm{Sym}^l \square$ or $\Lambda^k \square$. More general superpotentials were considered in [79], which do coincide with the potentials used in colored Khovanov-Rozansky homologies [55, 106, 143, 144].

In all of the above constructions, a facet in $\mathbb{R}_t \times S^1_\sigma$ corresponds to n parallel strands of the braid representation of K. If the strands are colored by $R_1, \cdots, R_n$, one associates the category of matrix factorizations $\mathrm{MF}(W)$, given by:

$$W = W_{R_1} + \ldots + W_{R_n}, \quad \mathrm{MF}(W) = \mathrm{MF}(W_{R_1}) \otimes \cdots \otimes \mathrm{MF}(W_{R_n}) \tag{2.25}$$

where $\mathrm{MF}(W_R)$ is the category of matrix factorization for a superpotential W_R.

The choice of W_R can be constrained by the functoriality. Indeed, when W_R is appropriately chosen, the Hochschild homology of $\mathrm{MF}(W_R)$ would coincide with the R-colored homology of an unknot:

$$\mathcal{A} \;=\; HH^*\big(\mathrm{MF}(W_R)\big) \;=\; \mathcal{H}^R\big(\text{unknot}\big) \tag{2.26}$$

as we have discussed in Section 2.3. On the category of matrix factorizations, the Hochschild homology is computed as the homology of the Koszul complex associated with the sequence of partial derivatives of W_R. In fact, it not only contains, but also equals the Jacobi ring $J(W_R)$ if and only if W_R has only isolated singularities. This way, we obtain the following constraint on the superpotential W_R:

$$J(W_R) = \text{chiral ring of the LG model on a } R\text{-colored facet} = \mathcal{H}^R\big(\text{unknot}\big).$$

In fact, one could have obtained a similar constraint from the effective 2d theory on surface operators in 4d $\mathcal{N} = 4$ theories. Since we are studying the 2d physics of R-colored facets, we can take (locally) $M_4 = \mathbb{R}^4$ and $\Sigma = \mathbb{R}^2$ in the brane construction of the 2d-4d coupled system we have previously discussed. When $G = SU(N)$ and $R = \Lambda^k \mathbb{C}^N$, the surface operators are labeled by Levy types $\mathbb{L} = S(U(k) \times U(N-k))$,

and the 2d theory on Σ is a $\mathcal{N} = (4,4)$ sigma-model with hyper-Kähler target space $T^*(G/\mathbb{L}) = T^*Gr(k,N)$. Performing a topological twist along M_4, we have an induced topological twist along Σ, and the 2d theory comes with the chiral ring

$$\mathcal{H}^{\Lambda^k \square}(\text{unknot}) \;=\; H^*(Gr(k,N)) \tag{2.27}$$

given by the *classical* cohomology of the Grassmannian.

The same chiral ring can be obtained by performing a topological B-twist of the $\mathcal{N} = (2,2)$ Landau-Ginzburg model with k chiral superfields $x_1, \cdots, x_k$ of $U(1)_R$-charge $q = \frac{2}{N+1}$ and the superpotential

$$W_0(x_1, \ldots, x_k) = x_1^{N+1} + \ldots + x_k^{N+1}\,. \tag{2.28}$$

One may also consider the change of variables $X_i = \sigma_i(x_1, \ldots, x_k)$ where $\sigma_j(x_1, \ldots, x_k)$ represents the j-th elementary symmetric polynomial, $\sum_{1 \le i_1 < \ldots < i_k \le k} x_{i_1} \ldots x_{i_j}$. Then, the symmetrization procedure

$$(x_1, \ldots, x_k) \longmapsto (X_1 = \sigma_1(x_1, \ldots, x_k), \ldots, X_k = \sigma_k(x_1, \ldots, x_k)) \tag{2.29}$$

gives rise to a new Landau-Ginzburg model denoted by LG_k (see e.g. section 8.3 of [31].) The latter has chiral superfields X_i with $U(1)_R$-charge $q_i = \frac{2i}{N+1}$, and its superpotential $W = W(X_1, \ldots, X_k)$ is just W_0 expressed in terms of the X_i. It is still quasi-homogeneous, and LG_k flows to a superconformal field theory of central charge:

$$c = 3\sum_i (1 - q_i) = \frac{3k(N-k)}{N+1}. \tag{2.30}$$

It is believed to be the level-1 Kazama-Suzuki model associated to the Grassmannian $Gr(k,N)$. The chiral ring of LG_k is the Jacobi ring of $W(X_1, \ldots, X_k)$ which agrees with the classical cohomology ring $H^*(Gr(k,N))$ of the Grassmannian [138]. One can identify the chiral superfields X_i with the Chern classes c_i of the tautological bundle over $Gr(k,N)$. Therefore, we propose LG_k as the effective 2d theory on the surface operators on k-colored facets.

Junctions and LG interfaces

Let us now turn to the junctions of surface operators. As was discussed before, we consider the junctions across which a stack of $k = k_1 + k_2$ M5'-branes split into two stacks of k_1 and k_2 M5'-branes, *c.f.*, Figure 2.13.

Interfaces and chiral rings. As we have discussed below Equation (2.18), the junction imposes a condition on the Grassmannian sigma model that the "incoming" k_1-

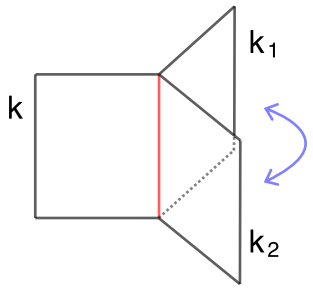

Figure 2.13: Junction between $LG_{k_1+k_2}$, LG_{k_1} and LG_{k_2}. Upon folding, it can be described by an interface $\mathcal{I}_k^{k_1,k_2}$ between LG_k and $LG_{k_1} \otimes LG_{k_2}$.

and k_2-dimensional subspaces should span the "outgoing" k-dimensional subspace in $\mathbb{C}^N$. The condition can be cast into the language of Chern classes $c_1^{(k)}, \ldots, c_k^{(k)}$ which correspond to $X_i^{(k)}$'s:

$$c_i^{(k)} = \sum_{j=0}^{i} c_j^{(k_1)} c_{i-j}^{(k_2)}. \tag{2.31}$$

In terms of Landau-Ginzburg models, Equation (2.31) can be interpreted as an interface $\mathcal{I}_k^{k_1,k_2}$ between LG_k and $LG_{k_1} \otimes LG_{k_2}$. On the LG_k side, the chiral superfields X_i are obtained from $LG_1^{\otimes k}$ via total symmetrization. On the other side, the chiral superfields Z_i, Z_i' are obtained by symmetrizing $(x_1, \cdots, x_{k_1})$ and $(x_{k_1+1}, \cdots, x_k)$ separately. Then,

$$X_i = \sum_{j=0}^{i} Z_i Z_i'. \tag{2.32}$$

It is important to note that the above discussion generalizes to junctions of higher valency. In terms of Grassmannian sigma models, when there are r incident $k_1, \cdots, k_r$-planes, the partial flag variety $Fl(k_1, k, N)$ generalize to $Fl(k_1, k_1+k_2, \ldots, k_1+\ldots+k_r = k, N) = G/\mathbb{L}$ with the Levi subgroup $\mathbb{L} = S\big(\prod_i U(k_i)\big)$ [65],

$$\mathbb{C}^{k_1} \subset \mathbb{C}^{k_1+k_2} \subset \cdots \subset \mathbb{C}^N. \tag{2.33}$$

In terms of LG models, the interface $\mathcal{I}_k^{k_1,\ldots,k_r}$ has LG_k on one side, and $\otimes_{i=1}^r LG_{k_i}$ on the other side. In terms of the M5'-branes, a stack of k coincident branes split into r stacks of k_i coincident branes.

Now, consider a junction across which r stacks of $k_1, \cdots, k_r$ coincident M5'-branes splitting into s stacks of $l_1, \cdots, l_s$ coincident M5'-branes, where $\sum_i k_i = \sum_j l_j = k$.

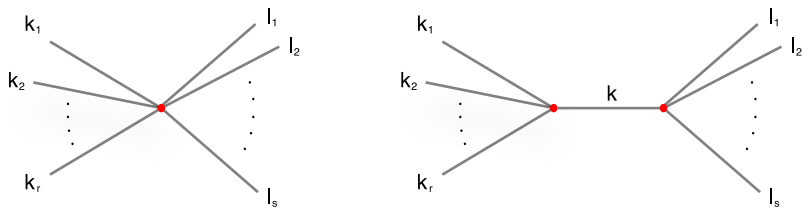

Figure 2.14: Junction described by $\mathcal{I}^{l_1,\ldots,l_s}_{k_1,\ldots,k_r}$ (left) factorizes as $\mathcal{I}^{k}_{k_1,\ldots,r_r} * \mathcal{I}^{l_1,\ldots,l_s}_{k}$ over LG_k (right).

The interface $\mathcal{I}^{l_1,\ldots,l_s}_{k_1,\ldots,k_r}$ has $LG_{k_1} \otimes \ldots \otimes LG_{k_r}$ on one side and $LG_{l_1} \otimes \ldots \otimes LG_{l_s}$ on the other. In terms of elementary symmetric polynomials, the chiral superfields of $LG_1^{\otimes k}$ are partially symmetrized along each facets. They satisfy relations generalizing Equation (2.32), and consequently, the interface $\mathcal{I}^{l_1,\ldots,l_s}_{k_1,\ldots,k_r}$ factors through interfaces $\mathcal{I}^{k}_{k_1,\ldots,k_r}$ and $\mathcal{I}^{l_1,\ldots,l_s}_{k}$ (*c.f.*, Figure 2.14). It has a natural meaning as a "fusion" of interfaces of LG models:

$$\mathcal{I}^{l_1,\ldots,l_s}_{k_1,\ldots,k_r} = \mathcal{I}^{k}_{k_1,\ldots,r_r} * \mathcal{I}^{l_1,\ldots,l_s}_{k}. \tag{2.34}$$

One can inductively reduce the valency of junctions by the above procedure. Therefore, matrix factorizations associated to junctions of higher valencies can be described by those associated to the trivalent junctions.

Interfaces and matrix factorizations. In fact, the LG interfaces have an elegant description in terms of matrix factorizations [23]. A matrix factorization of a potential $W \in \mathcal{R}$ is defined over a polynomial ring $\mathcal{R}$ by a pair of $r \times r$ square matrices p_0 and p_1 satisfying $p_1 p_0 = W\mathrm{Id}_r$ and $p_0 p_1 = W\mathrm{Id}_r$ where Id_r is the identity $r \times r$ matrix. A matrix factorization is often represented as follows:

$$\mathcal{P}: \quad P_1 \cong \mathcal{R}^r \underset{p_0}{\overset{p_1}{\rightleftarrows}} \mathcal{R}^r \cong P_0, \quad p_1 p_0 = W\mathrm{Id}_{P_0}, \quad p_0 p_1 = W\mathrm{Id}_{P_1}. \tag{2.35}$$

Now, consider a LG model on the upper half-plane with B-type boundary condition on the real axis. The boundary therefore obtains the supercoordinates:

$$x^{\pm} = t, \quad \theta^{\pm} = \theta, \quad \bar{\theta}^{\pm} = \bar{\theta}. \tag{2.36}$$

Due to the boundary, the 2d $\mathcal{N} = 2$ supersymmetry is broken, and the B-type boundary conditions preserve the B-twisted supercharge:

$$\bar{Q}_B = \bar{Q}_+ + \bar{Q}_- \tag{2.37}$$

and its complex conjugate. Some boundary superfields nautrally arise by the limit of the bulk fields. Indeed, one can see that the variation $\delta_B = \epsilon Q - \bar{\epsilon}\bar{Q}$ of the bulk D-term can be compensated by those of inherited boundary superfields. However, $\delta_B S_F$ cannot be compensated unless we introduce extra non-chiral Fermi superfields whose lowest components are $\pi_1, \cdots \pi_r$ satisfying:

$$\bar{D}\pi_i = E_i(\phi) \tag{2.38}$$

where ϕ's represent the lowest components of the (boundary restricted) chiral superfields and $E_i(\phi)$ is holomorphic in ϕ. Then, we can introduce boundary F-terms to cancel the bulk variation of F-terms:

$$i\int_{\text{boundary}} dtd\theta J_i(\Phi)\pi_i|_{\bar{\theta}=0} + \text{ c.c.}, \quad \text{such that} \quad \sum_i J_i E_i = W. \tag{2.39}$$

Performing a B-twist (which is of course compatible with the B-type boundary conditions), one can define the boundary BRST charge:

$$Q_{\text{bd}} = \sum_i (J_i\pi_i + E_i\bar{\pi}_i), \quad \text{such that} \quad Q_{\text{bd}}^2 = W. \tag{2.40}$$

The space P where the boundary superfields act is graded by the fermion number $P = P_0 \oplus P_1$. Then, one can further study the action of Q_{bd} in the basis of Clifford algebra generated by r boundary Fermi superfields π_i's:

$$Q_{\text{bd}} = \begin{pmatrix} 0 & p_1 \\ p_0 & 0 \end{pmatrix} \tag{2.41}$$

as a $2^{r+1} \times 2^{r+1}$ matrix. Here, p_i's are $2^r \times 2^r$ whose entries are polynomials in the bulk chiral superfields X_i satisfying Equation (2.35). Then, the boundary chiral ring is given by the Q_{bd}-cohomology on $\text{End}_{\mathcal{R}}(P_0 \oplus P_1)$. For $\Phi \in \text{End}_{\mathcal{R}}(P_0 \oplus P_1)$, Q_{bd} acts as a graded commutator:

$$Q\Phi = p\,\Phi - \sigma\Phi\sigma\, p, \quad p = \begin{pmatrix} 0 & p_1 \\ p_0 & 0 \end{pmatrix}, \tag{2.42}$$

where the $\mathbb{Z}_2$-grading (fermion number) is given by

$$\sigma = \begin{pmatrix} \text{id}_{P_0} & 0 \\ 0 & -\text{id}_{P_1} \end{pmatrix}. \tag{2.43}$$

The boundary condition has a natural meaning in terms of interfaces between two LG models. Consider LG_k and LG_l with superpotentials $W(X_1, \cdots, X_k)$, $W(Y_1, \cdots, Y_l)$

and a B-type interface between them. To characterize the latter in terms of matrix factorization, we consider a "folded" LG model as in Figure 2.13. As a result, we obtain $LG_k \otimes \overline{LG_l}$. Here, $\overline{LG_l}$ is the orientation reversal of LG_l, hence with a superpotential $-W(Y_1, \cdots, Y_l)$. Thus, the matrix factorization for the interface is described by the following data:

$$\mathcal{R} = \mathbb{C}[X_1, \ldots, X_k, Y_1, \ldots, Y_l], \quad W = W(X_1, \cdots, X_k) - W(Y_1, \cdots, Y_l). \tag{2.44}$$

Properties. Based on the above observations, we can now explore properties of the interface matrix factorizations. First of all, we may consider the "fusion" of LG interfaces shown in Figure 2.15.

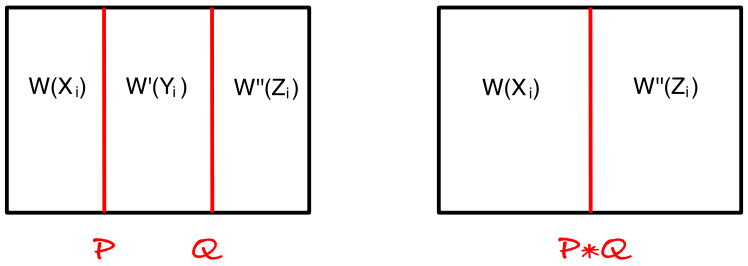

Figure 2.15: Fusion of interfaces $\mathcal{P}$ and $\mathcal{Q}$ into an equivalent interface, $\mathcal{P} * \mathcal{Q}$.

Consider two interfaces $\mathcal{P}$ separating LG models with superpotentials $W(X_i)$ and $W'(Y_i)$ and $\mathcal{Q}$ between LG models with superpotentials $W'(Y_i)$ and $W''(Z_i)$. And consider the matrix factorizations of $W(X_1, \ldots, X_r) - W'(Y_1, \ldots, Y_s)$ and $W'(Y_1, \ldots, Y_s) - W''(Z_1, \ldots, Z_t)$ they represent:

$$\mathcal{P}: \; P_1 \underset{p_0}{\overset{p_1}{\rightleftarrows}} P_0 \quad \text{and} \quad \mathcal{Q}: \; Q_1 \underset{q_0}{\overset{q_1}{\rightleftarrows}} Q_0. \tag{2.45}$$

Then, one can described their fusion $\mathcal{P} * \mathcal{Q}$ by the tensor product matrix factorization:

$$(\mathcal{P} \otimes \mathcal{Q})_1 := \begin{pmatrix} P_1 \otimes Q_0 \\ \oplus \\ P_0 \otimes Q_1 \end{pmatrix} \begin{pmatrix} p_1 \otimes \mathrm{id}_{Q_0} & -\mathrm{id}_{P_0} \otimes q_1 \\ \mathrm{id}_{P_1} \otimes q_0 & p_0 \otimes \mathrm{id}_{Q_1} \end{pmatrix} \rightleftarrows \begin{pmatrix} p_0 \otimes \mathrm{id}_{Q_0} & \mathrm{id}_{P_1} \otimes q_1 \\ -\mathrm{id}_{P_0} \otimes q_0 & p_1 \otimes \mathrm{id}_{Q_1} \end{pmatrix} \begin{pmatrix} P_0 \otimes Q_0 \\ \oplus \\ P_1 \otimes Q_1 \end{pmatrix} =: (\mathcal{P} \otimes \mathcal{Q})_0 \; . \tag{2.46}$$

Obviously, this is a matrix factorization of the sum

$$\begin{aligned} (W(X_1, \ldots, X_r) - W'(Y_1, \ldots, Y_s)) + (W'(Y_1, \ldots, Y_s) - W''(Z_1, \ldots, Z_t)) \\ = W(X_1, \ldots, X_r) - W''(Z_1, \ldots, Z_t), \end{aligned} \tag{2.47}$$

and describes an interface between two Landau-Ginzburg models with superpotentials $W(X_1, \ldots, X_r)$ and $W''(Z_1, \ldots, Z_t)$. Of course, the matrix factorization is taken over the polynomial ring involving Y_i's. Nevertheless, one can drop them by moding out the "trivial" matrix factorization of the form $1 \cdot W$ (See [23] for further details.)

It is important to note that the matrix factorizations are graded. Indeed, LG models of our interest have a $U(1)_R$-symmetry, which are also preserved in the presence of interfaces. The superpotentials have $U(1)_R$ charges 2, and p_0, p_1 are homogeneous of charge 1. Consequently, $\mathcal{R}$-modules P_0, P_1 carry representations ρ_0 and ρ_1 of $U(1)_R$. In what follows, we rescale the R-charges so that it naturally matches with the degree-shifts in matrix factorizations which appear in the homological knot invariants. For $\mathfrak{sl}_N$ examples, we rescale them by $N + 1$, so that the superpotentials $W_{\mathfrak{sl}_n,k}$'s have charges $2N + 2$.

After the above general considerations, we can construct matrix factorizations for the interface $\mathcal{I}_k^{k_1,k_2}$ which separates LG_k and $LG_{k_1} \otimes LG_{k_2}$. Recall that relevant superpotentials are partial symmetrizations of the same superpotential $\sum_{i=1}^k x_i^N$. Then, the relevant matrix factorizations are Koszul types, *c.f.* [23], and there are homogeneous polynomials $U_i\left(\{X_i\}_{i=1}^k, \{Z_i\}_{i=1}^{k_1}, \{Z_i'\}_{i=1}^{k_2}\right)$ such that:

$$\begin{aligned} &W(X_1, \ldots, X_k) - W(Z_1, \ldots, Z_{k_1}) - W(Z_1', \ldots, Z_{k_2}') \\ &\qquad = \sum_{i=1}^{k} \left(X_i - \sum_{j=1}^{k} Z_j Z_{i-j}'\right) U_i\left(\{X_i\}_{i=1}^k, \{Z_i\}_{i=1}^{k_1}, \{Z_i'\}_{i=1}^{k_2}\right). \end{aligned} \tag{2.48}$$

Explicitly, one can choose (matrix factorizations from different choices are equivalent):

$$U_i = \frac{1}{X_i - f_i}\left(W(f_1, \ldots, f_{i-1}, X_i, \ldots, X_k) - W(f_1, \ldots, f_i, X_{i+1}, \ldots, X_k)\right), \tag{2.49}$$

where we have defined $f_i = \sum_{j=1}^k Z_j Z_{i-j}'$ for the ease of notation. Then, we associate to $\mathcal{I}_k^{k_1,k_2}$ a rank $r = 2^{k-1}$ matrix factorization given by the tensor product:

$$\mathcal{I}_k^{k_1,k_2} = \left(\bigotimes_{i=1}^{k} \mathcal{P}^i\right)\{-k_1 k_2\} \tag{2.50}$$

of the rank-1 matrix factorizations

$$\mathcal{P}^i: \quad P_1^i \cong \mathcal{R}\{2i - N - 1\} \underset{p_0^i = U_i}{\overset{p_1^i = (X_i - f_i)}{\rightleftarrows}} \mathcal{R}\{0\} \cong P_0^i \tag{2.51}$$

over $\mathcal{R} = C[\{X_i\}_{i=1}^{k}, \{Z_i\}_{i=1}^{k_1}, \{Z_i'\}_{i=1}^{k_2}]$. By $\mathcal{R}\{a\}$, we consider $\mathcal{R}$ as a module over itself with an overall degree shift a (the degree being the $U(1)_R$ charge). By $\{-k_1k_2\}$ in $\mathcal{I}_k^{k_1,k_2}$, we shift the degrees of the $\mathcal{R}$-modules in $\mathcal{I}_k^{k_1,k_2}$ by $\{-k_1k_2\}$.

The above construction is compatible with the fusion of interfaces, and therefore, naturally generalizes to the junctions of higher valency.

Junctions and categorification of quantum groups

We are now ready to identify features of categorified quantum groups from LG interfaces. Here we present two basic and important relations, "digon removal" relations and the "$[E, F]$" relations.

First, let us consider the digon removal relation. This is a categorified version of Figure 2.7(b). In terms of interfaces, we can consider the fusion of interfaces depicted in Figue 2.16.

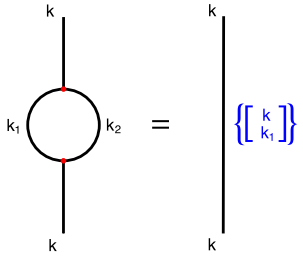

Figure 2.16: Fusion of $\mathcal{I}_{k_1,k_2}^{k}$ and $\mathcal{I}_k^{k_1,k_2}$ in $LG_{k_1} \otimes LG_{k_2}$ produces copies of the identity defect in LG_k.

In terms of LG interfaces, Figure 2.16 represents a fusion of $\mathcal{I}_{k_1,k_2}^{k}$ and $\mathcal{I}_k^{k_1,k_2}$. As was exhibited in [23], it is convenient to associate to matrix factorization of a potential W over $\mathcal{R}$, a $\hat{\mathcal{R}} := \mathcal{R}/(W)$-module. Explicitly, to $\mathcal{I}_k^{k_1,k_2}$, we associate:

$$M = \hat{\mathcal{R}}/\mathcal{J}\hat{\mathcal{R}}\{-k_1k_2\}. \tag{2.52}$$

As before, $\mathcal{R}$ is the chiral ring of partially symmetrized superfields X_i, Z_i, Z_i', $W = W(X_1, \ldots, X_k) - W(f_1, \ldots, f_k)$, and $\mathcal{J}$ is the ideal generated by $\{(X_i - f_i)\}_{i=1}^{k}$.

Similarly, $\mathcal{I}_{k_1,k_2}^{k}$ is related to the $\mathcal{R}'$-module

$$M' = \hat{\mathcal{R}}'/\mathcal{J}'\hat{\mathcal{R}}', \tag{2.53}$$

where $\mathcal{R}$ is the chiral ring of partially symmetrized superfields X_i', Z_i, Z_i'. Definition of superpotentials and $\mathcal{J}'$ are analogous to those of $\mathcal{I}_{k_1,k_2}^{k}$.

The matrix factorization of the fusion product $\mathcal{I}^{k}_{k_1,k_2} * \mathcal{I}^{k_1,k_2}_{k}$ is now given by the 2-periodic part [54] of the free resolution of the module $M'' := M \otimes M'$ considered as a module over $\hat{\mathcal{R}}'' := \mathbb{C}[X_1, \ldots, X_k, X'_1, \ldots, X'_k]/(W(X_1, \ldots, X_k) - W(X'_1, \ldots, X'_k))$. But

$$\begin{aligned} M'' &\cong \hat{\mathcal{R}}'' \otimes \left(\mathbb{C}[\{Z_i\}_{i=1}^{k_1}, \{Z'_i\}_{i=1}^{k_2}]/\left(\{(X_i - f_i), (X'_i - f_i)\}_{i=1}^{k}\right)\right)\{-k_1k_2\} \\ &\cong \left(\hat{\mathcal{R}}''/(X_i - X'_i)\right) \otimes \left(\mathbb{C}[\{Z_i\}_{i=1}^{k_1}, \{Z'_i\}_{i=1}^{k_2}]/(f_1, \cdots, f_k)\right)\{-k_1k_2\}\,. \end{aligned}$$

Recall that $f_1, \cdots, f_k$ span a basis of the totally symmetrized $(x_1, \cdots, x_k)$, while Z_i, Z'_i's are partially symmetrized in k_1 and k_2 variables, respectively. Therefore, we obtain:

$$\begin{aligned} &\left(\mathbb{C}[\{Z_i\}_{i=1}^{k_1}, \{Z'_i\}_{i=1}^{k_2}]/(f_1, \cdots f_k)\right)\{-k_1k_2\} \\ &\qquad \cong \left(\frac{\mathbb{C}[x_1, \ldots, x_k]^{S_{k_1} \times S_{k_2}}}{\mathbb{C}[x_1, \ldots, x_k]^{S_k}}\right)\{-k_1k_2\} \\ &\qquad \cong H^*(Gr(k_1, k))\{-k_1k_2\} \cong \mathbb{C}\left\{\begin{bmatrix} k \\ k_1 \end{bmatrix}\right\}. \end{aligned} \tag{2.54}$$

Here, we use the notation $\mathcal{P}\{q^{a_1} + \ldots + q^{a_r}\} := \mathcal{P}\{a_1\} \oplus \ldots \oplus \mathcal{P}\{a_r\}$ for a matrix factorization $\mathcal{P}$. The 2-periodic part of the Koszul resolution of $\left(\hat{\mathcal{R}}''/(X_i - X'_i)\right)$ is the matrix factorization corresponding to the identity defect $\mathcal{I}^{k}_{k}$ of LG_k. As a result, we obtain:

$$\mathcal{I}^{k}_{k_1,k_2} * \mathcal{I}^{k_1,k_2}_{k} = \mathrm{Id}_k \left\{\begin{bmatrix} k \\ k_1 \end{bmatrix}\right\}. \tag{2.55}$$

Next, we consider the "$[E, F]$" relation in $\dot{\mathcal{U}}$, the categorification of $\dot{U}_q(\mathfrak{sl}_2)$:

$$\mathcal{E}_{k_1+1,k_2-1} * \mathcal{F}_{k_1,k_2} \cong \mathcal{F}_{k_1-1,k_2+1} * \mathcal{E}_{k_1,k_2} \oplus \mathrm{Id}_{k_1,k_2}\{[k_2 - k_1]\} \tag{2.56}$$

for $k_1 \leq k_1$ and

$$\mathcal{F}_{k_1-1,k_2+1} * \mathcal{E}_{k_1,k_2} \cong \mathcal{E}_{k_1+1,k_2-1} * \mathcal{F}_{k_1,k_2} \oplus \mathrm{Id}_{k_1,k_2}\{[k_1 - k_2]\} \tag{2.57}$$

for $k_1 \geq k_2$. Observe that the rank of quantum group depends only on the number of "stacks" of M5'-branes, and not on the rank of the gauge group $SU(N)$. This is precisely the behavior of categorical skew Howe duality.

In terms of LG interfaces, we define:

$$\begin{aligned} \mathcal{E}_{k_1,k_2} &:= \quad \left(\mathrm{Id}_{k_1-1} \otimes \mathcal{I}^{k_2+1}_{1,k_2}\right) * \left(\mathcal{I}^{k_1-1,1}_{k_1} \otimes \mathrm{Id}_{k_2}\right) \\ \mathcal{F}_{k_1,k_2} &:= \left(\mathcal{I}^{k_1+1}_{k_1,1} \otimes \mathrm{Id}_{k_2-1}\right) * \left(\mathrm{Id}_{k_1} \otimes \mathcal{I}^{1,k_2-1}_{k_2}\right), \end{aligned}$$

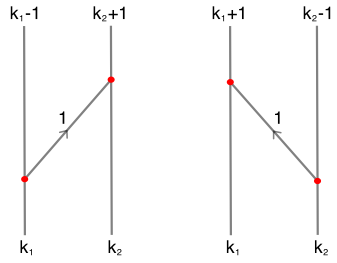

Figure 2.17: Configurations of surface operators categorifying the quantum group generators: $\mathcal{E}_{k_1,k_2}$ (left) and $\mathcal{F}_{k_1,k_2}$ (right).

as depicted in Figure 2.17. Through a similar but more involved procedure, one can show that the interfaces satisfy [43]:

$$\mathcal{E}_{k_1+1,k_2-1} * \mathcal{F}_{k_1,k_2} \cong \mathcal{F}_{k_1-1,k_2+1} * \mathcal{E}_{k_1,k_2} \oplus \mathrm{Id}_{k_1,k_2}\{[k_2 - k_1]\} \tag{2.58}$$

for $k_1 \leq k_1$ and

$$\mathcal{F}_{k_1-1,k_2+1} * \mathcal{E}_{k_1,k_2} \cong \mathcal{E}_{k_1+1,k_2-1} * \mathcal{F}_{k_1,k_2} \oplus \mathrm{Id}_{k_1,k_2}\{[k_1 - k_2]\} \tag{2.59}$$

for $k_1 \geq k_2$. Here, $\mathrm{Id}_{k_1,k_2} = \mathrm{Id}_{k_1} \otimes \mathrm{Id}_{k_2}$ denotes the identity defect in the tensor product $LG_{k_1} \otimes LG_{k_2}$. This is precisely the Equation (2.56), which categorifies Figure 2.7(e).

2.6 Generalizations and discussions

Super q-Howe duality

First of all, recall that the skew Howe duality (categorified or not) involves two quantum groups of independent ranks. One may ask, then, whether one can also consider Howe dualities involving supergroups instead of $\dot{U}_q(\mathfrak{sl}_m)$'s. In fact, it turns out to be the case, at least in the decategorified setup.

The super q-Howe duality is also represented diagrammatically [133]. Similar to the skew Howe duality functor in which NWebs are constructed from $k \in \mathbb{Z}$ colored edges, the super q-Howe duality functor maps to the so-called *green-red web category*, which is generated by the following colored webs: The webs in the green-red web category satisfy the relations shown in Figure 2.19. Notice that, for monochromatic webs, the relations in Figure 2.7 hold the same way *except* for the relations that involve the edges which are oriented downwards. Only the mixed-color relations are the novel features.

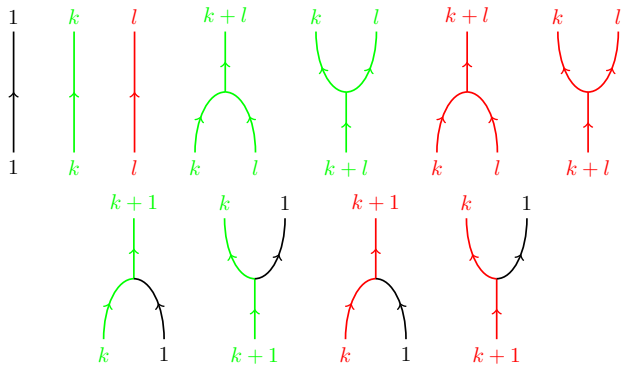

Figure 2.18: Junctions that appear in the super Howe duality functor. Above: monochromatic edges and their trivalent junctions. Below: mixed-color trivalent junctions. Mirror images are also generators.

In fact, the super q-Howe duality functor also has a natural meaning as networks of Wilson lines in $SU(N)$ Chern-Simons theory [40]. In addition to the totally antisymmetric representations, we include Wilson lines colored by totally symmetric representations. Let us distinguish the Wilson lines colored by totally symmetric / totally antisymmetric / fundamental representations by the red / green / black edges.

First of all, Equation (2.5) shows that the junctions of Figure 2.18 are allowed. Then, by a proper normalization of gauge invariant tensors, one can obtain Figure 2.19(a) and (b) for the $\mathrm{Sym}^l\square$-colored Wilson lines as well. The proof of Figure 2.19(c) is also similar to its counterpart in the NWeb category, and this is because the fusion rules among totally symmetric representations are almost identical to those of $\Lambda^k\square$. Based on these observations, the diagrammatic proof [133] of Figure 2.19(d) can be immediatly translated to the relations among green and red Wilson lines.

To categorify the super q-Howe duality to obtain relations among surface defects still remains an open problem. Physically, the practical difficulty lies in the construction of matrix factorizations for $LG_{\mathrm{Sym}^l\square}$. Unlike $LG_{\Lambda^k\square}$ whose superpotentials have a polynomial degree $N+1$, the candidate potentials [78, 79] have degrees $N+l$. Due to the inhomogeneity, the factorization (Equation (2.49)) across interfaces must be modified in a non-trivial way, which is subject of the stated open problem.

Entanglement entropies of "link states"

Another application of NWebs is the computation of entanglement entropies of "link states" [42]. As we have discussed before, a path integral on a link complement determines a vector in the associated Hilbert space. For a m-component link, the

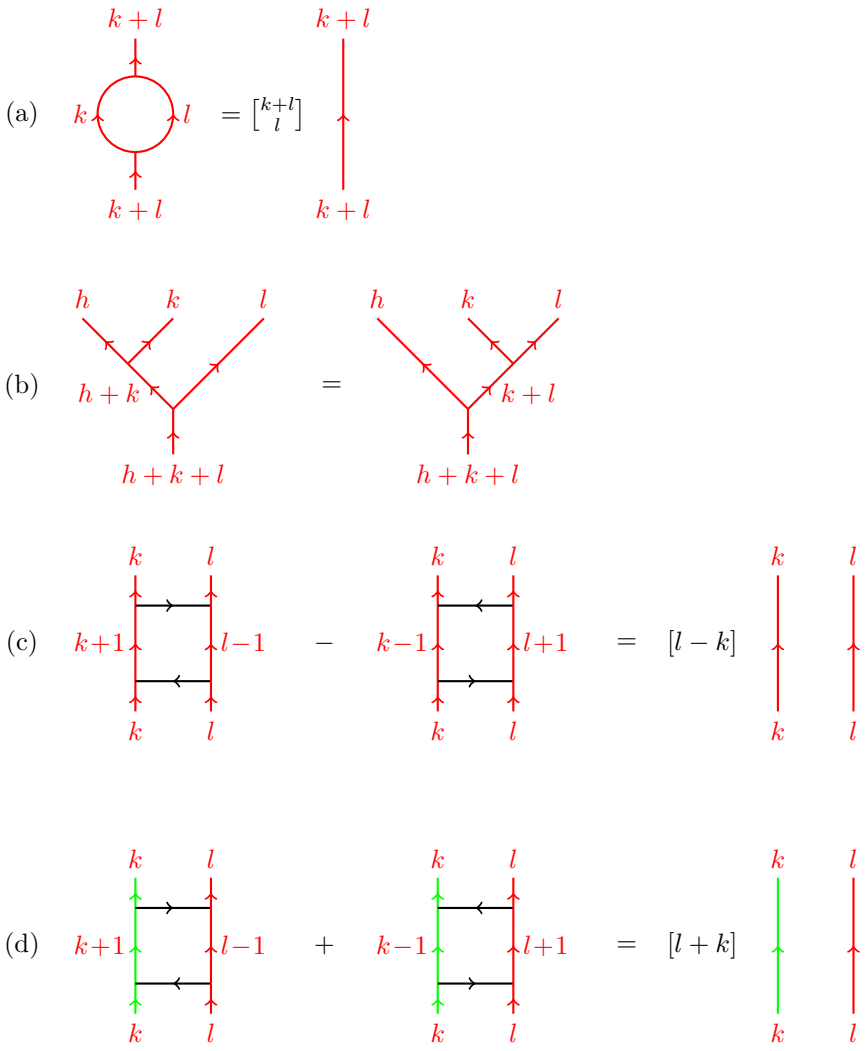

Figure 2.19: Monochromatic relations (the same holds for green edges): (a) digon removal, (b) associativity, and (c) the monochromatic [E,F] relation. Mixed-color relation: (d) the mixed-color [E,F] relation.

vector lives in the associated Hilbert space $H_{T^2}^{\otimes m}$. As a result, one can study the entanglement property of the "link state" [11, 130]:

$$|\mathcal{L}\rangle = \sum_{\alpha_1,\cdots,\alpha_m} C(\alpha_1,\cdots,\alpha_m)|\alpha_1\rangle \otimes \cdots \otimes |\alpha_m\rangle,$$

where $\mathcal{L}$ is a m-component link, and α_i's are integrable representations of the gauge group at level k. The vectors $|\alpha_i\rangle$ span the 2d Hilbert space H_{T^2}, and they are fixed by a path integral on a solid torus with a Wilson loop colored in α_i.

The work [42] mainly corroborated [11, 130] by an additional technique to compute the coefficients $C(\alpha_1,\cdots,\alpha_m)$. Of course, these are the colored Jones polynomials, which can be computed in multiple ways. Besides the computational advantage, the author and his collaborator also conjectured that [42]:

Conjecture. *Given a m-component link $\mathcal{L}$, suppose there exist two sub-links $\mathcal{L}_1$ and $\mathcal{L}_2$, each with i and $(m-i)$ components. Suppose the two sub-links satisfy the following:*

$$J_{\alpha_1,\cdots,\alpha_m}(\mathcal{L}) = J_{\alpha_1,\cdots,\alpha_i}(\mathcal{L}_1)J_{\alpha_{i+1},\cdots,\alpha_m}(\mathcal{L}_2)$$

for all colorings $\alpha_1,\cdots,\alpha_m$, then $\mathcal{L}_1$ and $\mathcal{L}_2$ are unlinked.

The intuition behind the conjecture is extremely simple. It was observed in [11, 42, 130] and many other related papers that non-trivial topology of $\mathcal{L}$ implies that the corresponding link state exhibits non-trivial entanglement. Then, we may ask whether the converse is true. Namely, given a link state which is bi-partite in terms of its sub-links, can we determine whether the link itself decomposes into unlinked $\mathcal{L}_1$ and $\mathcal{L}_2$? The idea transcribes to the constraints on the coefficients $C(\alpha_1,\cdots,\alpha_m)$, which is the shown condition for the conjecture. For large enough level k, the condition would impose a large number of constraints on the coefficients $C(\alpha_1,\cdots,\alpha_m)$, hence on the link state $\mathcal{L}$ as well.

Chapter 3

MODULAR FORMS AND THREE-MANIFOLD INVARIANTS

In this chapter, we explore the "hidden" integralities of Chern-Simons partition functions [84, 85]. Furthermore, it is shown that the corresponding "homological blocks" admit interpretations from various angles: as topological invariants of a three-manifold, as supersymmetric indices in three-dimensional physics, and as quantum modular forms in number theory [38]. The relations among three different viewpoints are summarized in Figure 3.1. Lastly, we observe that homological blocks naturally arise from chiral algebras of logarithmic CFTs, which are in turn related to the quantum groups at roots of unity.

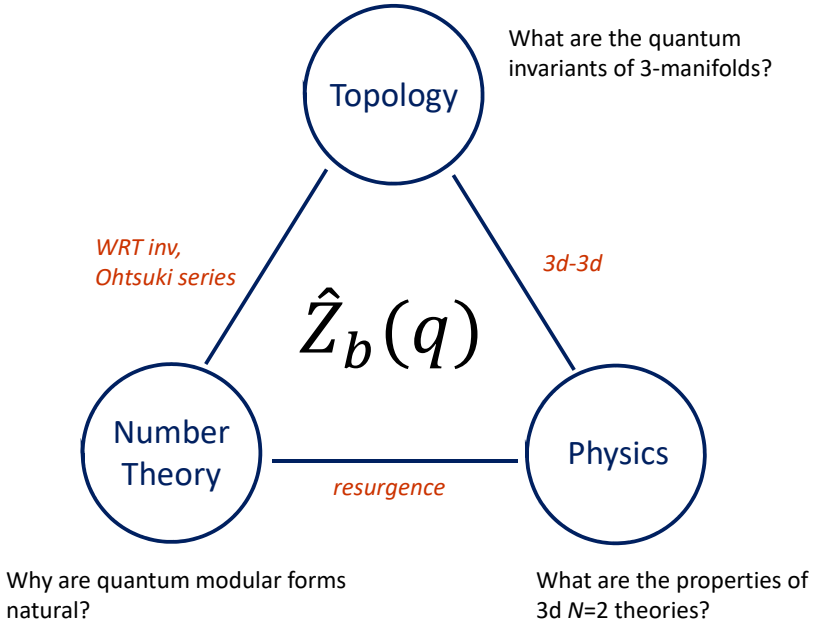

Figure 3.1: The different topics involved in this chapter.

3.1 Integralities of Chern-Simons partition function

The "hidden" integralities of Chern-Simons partition functions can be observed in multiple ways, but they are *a priori* not so obvious. As a TQFT, Chern-Simons

partition function can be computed from the surgery description of the base 3-manifold M_3. Indeed, the Lickorish-Wallace theorem states that any closed 3-manifold can be obtained by ± 1 surgeries on a framed link embedded in S^3. Surgeries define the actions of modular group elements on the Hilbert space associated to the link complements, $H_{T^2}^{\otimes L}$. When H_{T^2} is finite-dimensional in an appropriate sense, TQFT axioms give the exact partition function.

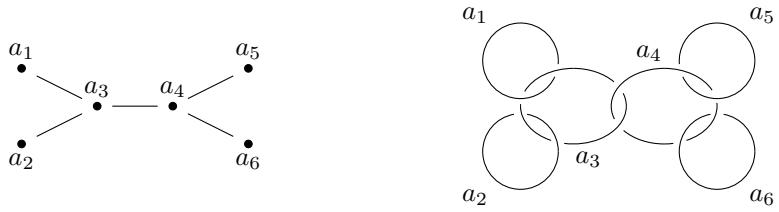

Figure 3.2: A plumbing graph (left) and the associated surgery link (right).

Concretely, consider a special class of 3-manifolds, called "plumbed" manifolds [119]. Their surgery presentations are particularly simple, because all the link components are unknots which are Hopf-linked. Due to the simplicity, we can translate the surgery presentation as a "plumbing graph" as illustrated in Figure 3.2.[1]

$$-p/q \quad = \quad \overset{a_1}{\bullet}\!\!-\!\!\!-\overset{a_2}{\bullet}\!\!-\!\!\!-\overset{a_3}{\bullet}\!\!-\!\!\!-\cdots \quad \text{where} \quad \frac{q}{p} = -\cfrac{1}{a_1 - \cfrac{1}{a_2 - \cfrac{1}{a_3 - \cdots}}}. \tag{3.1}$$

There can be multiple plumbing descriptions which are equivalent, as shown in (3.1). It turns out that when two 3-manifolds have plumbing descriptions related by 3d Kirby moves (Figure 3.3), they are homeomorphic to each other.

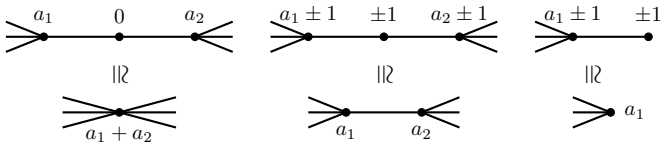

Figure 3.3: 3d Kirby moves for plumbed manifolds.

Such a simple surgery presentation enables us to write Z_{CS} of a plumbed manifold in a closed form. Concretely, when $G = SU(2)$ and the Chern-Simons level is k

[1] In fact, the linking number of the Hopf link also matters, especially when plumbing graphs involve loops. In this chapter, however, we focus on tree-shaped plumbings, for which the sign of a Hopf link is unimportant.

[84, 134],

$$\begin{aligned} Z_{CS}[M_3] &= \sqrt{\frac{2}{k}} \sin\frac{\pi}{k} \frac{F(\Gamma)}{F(+1\bullet)^{b_+} F(-1\bullet)^{b_-}}, \\ F(\Gamma) &= \sum_{n_1,\cdots,n_L=1}^{k-1} J_{n_1,\cdots,n_L}(\mathcal{L}(\Gamma)) \prod_{v=1}^{L} \frac{q^{n_v/2} - q^{-n_v/2}}{q^{1/2} - q^{-1/2}} \end{aligned} \tag{3.2}$$

where $\mathcal{L}(\Gamma)$ is the link associated to a plumbing graph Γ, and $J_{n_1,\cdots,n_L}(\mathcal{L})$ is the colored Jones polynomial of a link $\mathcal{L}$ whose components are colored by $n_1, \cdots, n_L$.[2] Finally, (b_+, b_-) is the signature of the linking matrix associated to Γ:

$$M_{ij} = \begin{cases} a_i & \text{if} \quad i = j \\ 1 & \text{if} \quad (i,j) \in \text{Edges} \\ 0 & \text{otherwise,} \end{cases} \tag{3.3}$$

Observe that each summand of F has integral coefficients of q. However, the summation over k spoils the integrality, as $k \sim \log q$. Consequently, the integrality of Z_{CS} is totally obscured, but we can still employ one of the following techniques to recover it.

Resurgence analysis. First of all, one can observe the hidden integrality via resurgence analysis [83]. For instance, consider the Poincaré homology sphere $\Sigma(2,3,5)$. Since it is an integral homology sphere, the perturbative expansion around the trivial flat connection recovers the exact Chern-Simons partition function in the following form:

$$\begin{aligned} Z_{CS}(\Sigma(2,3,5)) = \frac{q^{-181/120}}{i\sqrt{2k}} \Big(q^{1/120} - \frac{1}{2}\Psi_{30,1}(q) - \frac{1}{2}\Psi_{30,11}(q) \\ - \frac{1}{2}\Psi_{30,19}(q) - \frac{1}{2}\Psi_{30,29}(q) \Big), \end{aligned} \tag{3.4}$$

where

$$\Psi_{m,r}(q) = \sum_{n \geq 0} \psi^a_{2m}(n) q^{n^2/4m}, \quad \psi^a_{2m}(n) = \begin{cases} \pm 1 & n \equiv \pm a \mod 2m \\ 0 & \text{otherwise.} \end{cases} \tag{3.5}$$

Obviously, $Z_{CS} \in \mathbb{Z}[[q]]$ up to an overall coefficient. Furthermore, $\Psi_{m,r}(q)$ is a *false theta function* which exhibits certain modular property. By its "modular" transform, one can easily recover the perturbative expansion (more precisely, the *transseries* when there are multiple abelian flat connections.)

[2] Here, we have implicitly incorporated the quantum correction to the level, $k \to k + N$.

We will soon witness that $\Psi_{m,r}(q)$ appears for *any* Seifert manifolds with three singular fibers. Indeed, false theta functions were first observed from 3-singular fibered Seifert manifolds [146], and the relation was further advocated in [88, 90, 91].

Gauss resummation formula. Following [84], one can also perform Gauss resummation on the expression (3.2) and free the RHS from summation which depends on k. When the plumbing graph is tree-shaped,

$$
\begin{gathered}
Z_{CS} = \frac{1}{2i\sqrt{2k}} \sum_a e^{2\pi i k \mathrm{CS}(a)} \left(\lim_{q \to e^{2\pi i/k}} \sum_b S^{(A)}_{ab}\, \widehat{Z}_b(q) \right), \\
a \in \mathrm{Coker} M_{ij}/\mathbb{Z}_2 \cong \mathrm{Tor} H_1(M_3, \mathbb{Z})/\mathbb{Z}_2 \quad (\text{see } e.g.\ [70]), \\
b \in (2\mathrm{Coker} M_{ij} + \delta)/\mathbb{Z}_2, \quad (\delta \in \mathbb{Z}^L \text{ s.t. } \delta_i \cong \deg v_i \bmod 2) \\
\mathrm{CS}(a) = -(a, M^{-1} a) \bmod \mathbb{Z}, \\
S^{(A)}_{ab} = \frac{\sum_{a' \in \{\mathbb{Z}_2\text{-orbit of } a\}} e^{2\pi i (a', M^{-1} b)}}{\sqrt{|\mathrm{Tor} H_1(M_3)|}},
\end{gathered}
\tag{3.6}
$$

and

$$
\begin{aligned}
\widehat{Z}_b(q) = q^{-\frac{\sum_v a_v - 3\sigma(M_{ij})}{4}} \cdot \mathrm{v.p.} \int_{|z_v|=1} \prod_{v \in \mathrm{Vertices}} \frac{dz_v}{2\pi i z_v} (z_v - 1/z_v)^{2-\deg_v} \\
\times \sum_{\ell \in 2M\mathbb{Z}^L + b} q^{-\frac{(\ell, M^{-1}\ell)}{4}} \prod_{v \in \mathrm{Vertices}} z_v^{\ell_v}
\end{aligned}
\tag{3.7}
$$

where the principal value integral "dodges" the singularities on $|z_i| = 1$, and the Weyl group actions (labeled $/\mathbb{Z}_2$) identify a and b indices via $a \sim -a$ and $b \sim -b$.

It turns out that $\widehat{Z}_b(q) \in 2^{-c} q^{\Delta_b} \mathbb{Z}[[q]]$ for some $c \in \mathbb{Z}_+, \Delta_b \in \mathbb{Q}$. The summations $\sum_a$ and $\sum_b$ are now independent of k. Thus, we have observed the hidden integrality in Z_{CS} via Gauss resummation.

3d-3d correspondence. In fact, the Gauss resummation is motivated by the 3d-3d correspondence which provides the physical reason why we should expect such integrality. Consider embedding $SU(N)$ Chern-Simons theory into the string / M-theory setup as in Equation (2.24). We can simply replace $M_3 \leftrightarrow S_3$ and remove the extra M5'-branes to reflect the absence of line defects. Compactifying M_3, the 6d $\mathcal{N} = (2, 0)$ worldvolume theory of M5-brane reduces to a 3d $\mathcal{N} = 2$ theory $T[M_3]$ on $S^1 \times D$ (D represents the Taub-NUT cigar.) Since the base manifold has a torus boundary, one must consider supersymmetric boundary conditions of $T[M_3]$. For $G = SU(2)$, these boundary conditions correspond to b-indices in Equation (3.7).

Let $H_b[M_3]$ denote the BPS spectrum of $T[M_3]$ compatible with a supersymmetric boundary condition b. The spectrum itself can be considered as a homological invariant of M_3. Just like the doubly graded homological link invariants, it is graded by the rotation symmetries $U(1)_q \times U(1)_t$ acting on $D \subset TN^4$.

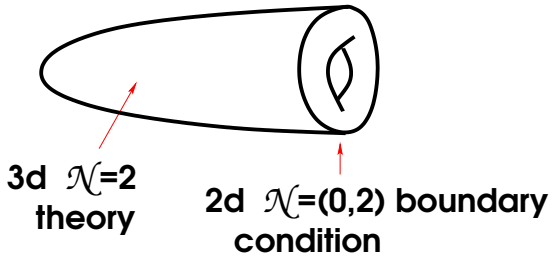

Figure 3.4: A 3d $\mathcal{N} = 2$ theory with a 2d $\mathcal{N} = (0, 2)$ boundary condition b.

The supersymmetric boundary conditions can preserve 2d $\mathcal{N} = (0, 2)$ supersymmetry. When the boundary 2d theory has massless degrees of freedom, one can compute the 2d-3d coupled index of the system to obtain Equation (3.7). Indeed, when M_3 is plumbed along a tree-shaped graph, the *homological blocks* $\widehat{Z}_b(q)$ have a form of a 3d-2d coupled indices:

$$\begin{aligned} \widehat{Z}_b &= \int \prod_v \frac{dz_v}{2\pi i z_v} F_{3d}(z)\, \Theta^{(b)}_{2d}(z) \\ F_{3d}(z) &= \prod_v (z_v - 1/z_v)^{2-\deg_v} \\ \Theta^{(b)}_{2d}(x) &= \sum_{\ell \in 2M\mathbb{Z}^L + b} q^{-\frac{(\ell, M^{-1}\ell)}{4}} \prod_{v \in \text{Vertices}} x_v^{\ell_v}. \end{aligned} \tag{3.8}$$

3.2 False theta functions and homological blocks

Let us note that the "generalized theta function" in Equation (3.8) is modular as an elliptic genus [67]. However, the bulk 3d theory (whose index is $F_{3d}(z)$) does not necessarily respect the modular invariance. As a result, we obtain "spoiled" modularity as one can see from the appearance of false theta functions in Equations (3.4) and (3.5). Depending on the bulk theory $T[M_3]$, we observe that the modular invariance is broken to different degrees. For example, when the bulk theory is completely gapped (*i.e.* $F_{3d}(x) = 1$), the homological blocks will enjoy the modular invariance. However, the bulk theory (although gapped) may have a non-trivial topological phase. We will mainly consider such examples in this chap-

ter, and because of the non-trivial contribution $F_{3d}(x) \neq 1$ from the bulk, we will observe the appearance of false theta functions and mock modular forms.

Before proceeding further, let us remark that we will encounter multiple modular S-transforms, besides the S-matrices which appear in computation of Z_{CS} via surgery presentations and TQFT axioms. First of all, $S_{ab}^{(A)}$ defined in Equation (3.6) is indeed an S-matrix, but it encodes the modular S-transform of *logarithmic* CFTs. It turns out that the latter is also connected to "baby" quantum groups which are close cousins of $\dot{U}_q(\mathfrak{sl}_2)$ from the previous chapter. We will discuss the connection later in this chapter. Secondly, for certain M_3, homological blocks $\widehat{Z}_b(q)$ themselves exhibit well-defined modular properties. Indeed, the modular S-transform of false theta functions $\Psi_{m,r}(q)$ will be particularly useful when we later "decode" the integrality of Z_{CS} to produce its transseries expansion. This will be the subject of the next section.

Convergence criteria

To explore the modular properties of $\widehat{Z}_b(q)$, we must first determine when the semi-infinite q-series converges. Seemingly pedantic, the convergence is crucial for the study of mock-false pairs which will appear later.

Since the false theta functions are observed in $\widehat{Z}_b(q)$ of Seifert manifolds, we first consider them. Any Seifert manifold $M_3 = M(b; \{q_i/p_i\}_i)$ can be represented by a plumbing graph with a unique vertex with degree > 2. In the relevant plumbing graph, we can represent the rational surgeries q_i/p_i along singular fibers by continued fractions, as in (3.1).

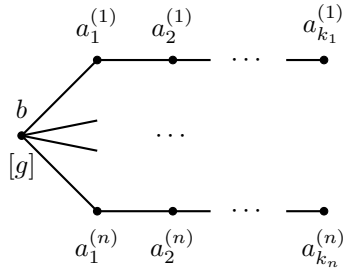

Figure 3.5: Plumbing graph for a Seifert manifold $M\big(b, g; \{\frac{q_i}{p_i}\}_{i=1}^n\big)$.

Next, consider the integral expression for $\widehat{Z}_b(q)$ in Equation (3.6). One can rewrite it in the following way [84]:

$$\widehat{Z}_b(q) = 2^{-L} q^{\Delta} \sum_{\ell \in 2M\mathbb{Z}^L + b} F_1^{\ell}\, q^{-\frac{(\ell, M^{-1}\ell)}{4}}, \quad b \in (2\mathrm{Coker}M + \delta)/\mathbb{Z}_2 \tag{3.9}$$

where the integer coefficients F_1^{ℓ} are generated as follows (note that $2M\mathbb{Z}^L + b$ is a sublattice of $2\mathbb{Z}^L + \delta$):

$$\sum_{\ell \in 2\mathbb{Z}^L + \delta} F_1^{\ell} \prod_{v \in \mathrm{Vertices}} x_v^{\ell_v} = \prod_{v \in \mathrm{Vertices}} \left\{ \underset{\text{at } x_v \to 0}{\text{Expansion}} \frac{1}{(x_v - 1/x_v)^{\deg v - 2}} + \underset{\text{at } x_v \to \infty}{\text{Expansion}} \frac{1}{(x_v - 1/x_v)^{\deg v - 2}} \right\}. \tag{3.10}$$

Observe that the power series expansion in x_v terminates at a finite order if and only if $\deg v \leq 2$. Therefore, it is only the vertices with "high-valency" (meaning, $\deg v > 2$) which contribute arbitrarily large q-powers. Explicitly,

$$F_1^{\ell} \neq 0 \quad \Leftrightarrow \quad \ell_v = \begin{cases} \ell_v & \text{if } \deg v > 2,\ \ell_{v_0} \in \mathbb{Z} \\ 0 & \text{if } \deg v = 2 \\ 1 & \text{if } \deg v = 1. \end{cases} \tag{3.11}$$

When the plumbing graph Γ has a unique high-valency vertex v_0, it is easy to write down its q-power growth, namely:

$$q^{-\frac{(\ell, M^{-1}\ell)}{4}} = q^{-\frac{(M^{-1})_{v_0 v_0} (\ell_{v_0})^2}{4} + O(1)}, \quad \text{as } |\ell| \to \infty. \tag{3.12}$$

Here, v_0 also denotes the coordinate which corresponds to the high-valency vertex in the linking matrix representation, M and $\mathbb{Z}^L$. Therefore, $\widehat{Z}_b(q)$ will be convergent *inside* the unit disc if $(M^{-1})_{v_0 v_0}$ is negative, but it will converge *outside* otherwise.

When there are multiple high-valency vertices (*e.g.*, Figure 3.2), the domain of convergence is determined by positive/negative-definiteness of the submatrix of M^{-1} spanned by high-valency vertices.

Example. Consider the Poincaré homology sphere $\Sigma(2,3,5)$. Since $|H_1| = 1$, there is only one homological block proportional to the Chern-Simons partition function shown in Equation (3.4).

$$Z_{CS}(\Sigma(2,3,5)) = \frac{q^{-181/120}}{i\sqrt{2k}} \Big(q^{1/120} - \frac{1}{2}\Psi_{30,1}(q) - \frac{1}{2}\Psi_{30,11}(q) - \frac{1}{2}\Psi_{30,19}(q) - \frac{1}{2}\Psi_{30,29}(q) \Big), \tag{3.13}$$

Note the appearance of false theta functions and their convergence inside the unit disk. Since the Poincaré homology sphere can be represented by a $-E_8$ plumbing graph, we can easily see that $(M^{-1})_{v_0v_0} = -30$, which is consistent with the above criteria.

Weil representations

Later, it turns out that $\widehat{Z}_b(q)$'s are naturally identified with certain linear combinations of false theta functions, $\Psi_{m,r}(q)$'s. The linear sum is controlled by the so-called "Weil representations."

Given a positive-definite lattice, one can associate a Weil representation. In this chapter, we focus on Weil representations associated to $\mathbb{Z}_{2m}$ equipped with a quadratic form $x \mapsto x^2/4m$. To construct the Weil representation, consider a unitary map $\widetilde{SL(2,\mathbb{Z})} \to GL_{2m}$. Here, $\widetilde{SL(2,\mathbb{Z})}$ is a metaplectic double cover of $SL(2,\mathbb{Z})$:

$$\widetilde{SL(2,\mathbb{Z})} = \left\{ (\gamma, \upsilon) \,\middle|\, \gamma = \begin{pmatrix} a & b \\ c & d \end{pmatrix} \in SL(2,\mathbb{Z}),\ \upsilon : \mathbb{H} \to \mathbb{C},\ \upsilon(\tau)^2 = (c\tau + d) \right\}, \tag{3.14}$$

with multiplication $(\gamma, \upsilon)(\gamma', \upsilon') = (\gamma\gamma', (\upsilon \circ \gamma')\upsilon')$. This group is generated by $\widetilde{T} := \left(\left(\begin{smallmatrix} 1 & 1 \\ 0 & 1 \end{smallmatrix}\right), 1\right)$ and $\widetilde{S} := \left(\left(\begin{smallmatrix} 0 & -1 \\ 1 & 0 \end{smallmatrix}\right), \sqrt{\tau}\right)$. The unitary map of interest has the following images of the generators:

$$\mathcal{S}_{rr'} := \frac{1}{\sqrt{2m}} e\left(-\frac{rr'}{2m}\right), \quad \mathcal{T}_{rr'} := e\left(\frac{r^2}{4m}\right)\delta_{r,r'}, \quad r, r' \in \{0, \cdots, 2m-1\}, \tag{3.15}$$

where we have set $e(x) := e^{2\pi i x}$. Then, the Weil representation ϱ_m is realized by the familiar theta functions:

$$\theta_{m,r}(\tau, z) := \sum_{\ell = r \bmod 2m} q^{\ell^2/4m} y^\ell, \quad q := e(\tau),\ y := e(z) \tag{3.16}$$

for $\tau \in \mathbb{H}$ and $z \in \mathbb{C}$. Regarding $\theta_m := (\theta_{m,r})_{r \in \mathbb{Z}_{2m}}$ as a $2m$-dimensional vector,

$$\begin{aligned} \theta_m\left(-\frac{1}{\tau}, \frac{z}{\tau}\right) \frac{1}{\sqrt{\tau}} e\left(-\frac{mz^2}{\tau}\right) &= \mathcal{S}\theta_m(\tau, z), \\ \theta_m(\tau + 1, z) &= \mathcal{T}\theta_m(\tau, z). \end{aligned} \tag{3.17}$$

Therefore, θ_m's span a $2m$-dimensional representation (denoted Θ_m) of $\widetilde{SL(2,\mathbb{Z})}$. However, this representation is reducible for all $m > 1$. One can decompose it into irreps by an aid of the orthogonal group action:

$$\theta_{m,r} \cdot a := \theta_{m,ra}, \quad a \in O_m := \{a \in \mathbb{Z}/2m \mid a^2 = 1 \bmod 4m\}. \tag{3.18}$$

The eigenspaces of O_m are indeed irreducible, which are directly relevant for us. In practice, it is convenient to use the fact that $O_m \cong \mathrm{Ex}_m = \{n \in \mathbb{Z}_+ : n|m, (n, \frac{m}{n}) = 1\}$. For the latter, the group multiplication is given by $n * n' = nn'/(n, n')^2$. The isomorphism $O_m \cong \mathrm{Ex}_m$ is then given by:

$$n \mapsto a(n), \quad \text{s.t.} \quad a(n) = -1 \bmod 2n,\ a(n) = 1 \bmod 2m/n. \tag{3.19}$$

Since such a is uniquely determined, the isomorphism is well-defined. One can compactly write the isomorphism as the *Omega matrix* which appears in the classification of modular invariant combinations of chiral and anti-chiral characters of the $SU(2)$ current algebra [28]:

$$\Omega_m(n)_{r,r'} := \begin{cases} 1 & \text{if } r = -r' \bmod 2n, \text{ and } r = r' \bmod 2m/n, \\ 0 & \text{otherwise,} \quad r, r' \in \mathbb{Z}/2m, \end{cases} \tag{3.20}$$

For reasons to become clear, we will mostly consider representations which are (-1)-eigenspaces of $\theta_{m,r} \cdot a(m)$, *e.g.*, combinations $\theta_{m,r} - \theta_{m,-r}$ (because $a(m) = -1$). Effectively, we will consider "non-Fricke" $K \subset \mathrm{Ex}_m$ such that $m \notin K$. Later, we observe that Seifert manifolds with four singular fibers exhibit "Fricke" ($m \in K$) properties.

Explicitly, the irreps (denoted Θ^{m+K} for $K \subset \mathrm{Ex}_m$) are projections of the $2m$-dimensional representation by the following projectors:

$$P^{m+K} = \left(\prod_{n \in K} P_m^+(n) \right) P_m^-(m), \quad \text{where} \quad P_m^\pm(n) = (\mathbb{I} \pm \Omega_m(n))/2 \tag{3.21}$$

when m is square-free. When $\mathrm{Ex}_m = K \cup (m * K)$, Θ^{m+K} represents an irrep:

$$\theta_r^{m+K} = 2^{|K|} \sum_{\ell \in \mathbb{Z}/2m} P_{r\ell}^{m+K} \theta_{m,\ell}. \tag{3.22}$$

Let us denote by $r \in \sigma^{m+K}$ the set of independent vectors θ_r^{m+K}.

When m is divisible by a square, the case is more subtle. Irreps are orthogonal complements of the images of $U_d : \Theta_m \to \Theta_{md^2}$, $\phi(\tau, z) \mapsto \phi(\tau, dz)$ with respect to the Petersson metric in $\{\phi \in \Theta \mid \phi \cdot a = \alpha(a)\phi\}$ [131]. Explicitly, when $m = p^2 m'$, m' is square-free, and p is prime, the projector is given by:

$$P^{m+K} = \left(\prod_{n \in K} P_m^+(n) \right) P_m^-(m) \left(\mathbb{I} - \Omega_m(p)/p \right). \tag{3.23}$$

Using the above prescriptions, one can explicitly write the S- and T-matrices of the irrep Θ^{m+K}:

$$\begin{aligned} \mathcal{S}^{m+K}_{rr'} &= \sum_{\ell\in\mathbb{Z}_{2m}} \frac{\mathcal{S}_{r\ell}P^{m+K}_{\ell r'}}{P^{m+K}_{r'r'}}, \quad r, r' \in \sigma^{m+K}, \\ \mathcal{T}^{m+K}_{rr'} &= e\left(\frac{r^2}{4m}\right)\delta_{r,r'}. \end{aligned} \tag{3.24}$$

Example. Consider $m = 6$ and $K = \{1, 3\}$. Since $\mathrm{Ex}_6 = \{1, 2, 3, 6\} = K \cup 6 * K$, see that the resulting representation Θ^{6+3} is irreducible. Following the above discussion, a simple calculation leads to $\sigma^{6+3} = \{1, 3\}$ and the corresponding basis vectors are

$$\begin{aligned} \theta^{6+3}_1 &= \theta_{6,1} + \theta_{6,5} - \theta_{6,-1} - \theta_{6,-5} \\ \theta^{6+3}_3 &= 2\left(\theta_{6,3} - \theta_{6,-3}\right), \end{aligned} \tag{3.25}$$

and the S-matrix is

$$\mathcal{S}^{6+3} = \frac{i}{\sqrt{3}}\begin{pmatrix} -1 & -1 \\ -2 & 1 \end{pmatrix}. \tag{3.26}$$

From the above theta functions $\theta_{m,r}$ and Θ^{m+K}, one obtains partial and false theta functions via Eichler integral. Therefore, one can also group false theta functions by means of the Weil representations. For instance, when $M_3 = \Sigma(2, 3, 5)$, $m + K = 30 + 6, 10, 15$.

Eichler integrals and false theta functions

Later, we will observe numerous identifications among Ψ^{m+K}_r and homological blocks. In fact, this is not a coincidence at all. Recall that integralities of Z_{CS} can often be recovered by resurgence analysis. In the following section, we will discuss how closely resurgence analysis and Eichler integrals are related. Then, the appearance of false theta functions is expected, because they arise as Eichler integrals of the weight $3/2$ "unary" theta functions:

$$\theta^1_{m,r}(\tau) \;:=\; \frac{1}{2\pi i}\frac{\partial}{\partial z}\theta_{m,r}(\tau, z)|_{z=0} \quad = \sum_{\substack{\ell\in\mathbb{Z} \\ \ell = r \bmod 2m}} \ell\, q^{\ell^2/4m}. \tag{3.27}$$

This is the subject of the current section.

Given a cusp form $g = \sum_{n>0} a_g(n)q^n$ of weight $w \in \frac{1}{2}\mathbb{Z}$, its *Eichler integral* is defined:

$$\widetilde{g}(\tau) := \sum_{n>0} n^{1-w}a_g(n)q^n = C\int_\tau^{i\infty} g(z')(z'-\tau)^{w-2}dz', \quad C = \frac{(2\pi i)^{w-1}}{\Gamma(w-1)} \tag{3.28}$$

where we have chosen the principal branch $-\pi < arg\, x \leq \pi$.

For weight-$3/2$ unary theta functions, the Eichler integral has the following Fourier expansion:

$$\Psi_{m,r}(\tau) := \widetilde{\theta^1_{m,r}}(\tau) = 2\sum_{n>0}(P^-_m(m))_{r,n}\, q^{n^2/4m}, \tag{3.29}$$

which is precisely the false theta function convergent in $|q| < 1$, since

$$2(P^-_m(m))_{r,n} = \begin{cases} \pm 1 & n = \pm r \bmod 2m \\ 0 & otherwise \end{cases}. \tag{3.30}$$

Note that $\theta^1_{m,r} = -\theta^1_{m,-r}$ and consequently $\Psi_{m,r} = -\Psi_{m,-r}$. Observe that this is the "non-Fricke' type that we have observed before.[3]

Similar to the ordinary theta functions, we can group them by the Weil representations:

$$\Psi^{m+K}_r := \widetilde{\theta^{m+K,1}_r} = 2^{|K|}\sum_{n\geq 0} P^{m+K}_{r,n}\, q^{n^2/4m}. \tag{3.31}$$

where similarly to $\theta^1_{m,r}$, we have defined $\theta^{m+K,1}_r(\tau) := \frac{1}{2\pi i}\frac{\partial}{\partial z}\theta^{m+K}_r(\tau, z)|_{z=0}$.

Now we are ready to explore the limit behaviors of $\Psi_{m,r}$ and observe how if "fails" to be modular. First of all, observe that the coefficients (Equation (3.30)) exhibit $2m$-periodicity with a vanishing mean value. For any such function $\psi : \mathbb{Z} \to \mathbb{C}$, the corresponding Dirichlet L-series

$$L(s, \psi) = \sum_{n\geq 1} n^{-s}\psi(n), \quad \mathrm{Re}(s) > 1 \tag{3.32}$$

can be holomorphically extended to all $s \in \mathbb{C}$. Furthermore, for $t > 0$ [146],

$$\sum_{n\geq 1}\psi(n)e^{-nt} \sim \sum_{\ell\geq 0} L(-\ell, \psi)\frac{(-t)^\ell}{\ell!}, \tag{3.33}$$

$$\sum_{n\geq 1}\psi(n)e^{-n^2t} \sim \sum_{\ell\geq 0} L(-2\ell, \psi)\frac{(-t)^\ell}{\ell!}. \tag{3.34}$$

The radial limit values (as $\tau \to 1/k$) of $\Psi_{m,r}$ can be computed by taking $\psi(n) = (P^-_m(m))_{r,n}e(-r^2/4mk)$. On the other hand, the asymptotic series can be computed if we take $\psi^{m+K}_r(n) := P^{m+K}_{r,n}$:

$$\Psi^{m+K}_r\left(\tau = \frac{it}{2\pi}\right) \sim \sum_{\ell\geq 0}\frac{L(-2\ell, \psi^{m+K}_\ell)}{\ell!}\left(\frac{-t}{4m}\right)^\ell. \tag{3.35}$$

[3]The nomenclature "false theta" follows [8]. They are often called partial theta functions as well [20, 21, 47].

The following identity between the Dirichlet L-series and ratio of sinh functions will be particularly useful :

$$\frac{\sinh((m-r)z)}{\sinh(mz)} = \sum_{\ell \geq 0} \frac{L(-2\ell, \psi_{m,r})}{(2\ell)!} z^{2\ell}. \tag{3.36}$$

Resurgence analysis and Eichler integrals

In this section, we discuss the close relation between the Borel resummation and Eichler integrals. For that purpose, we provide here a brief review of resurgence analysis in Chern-Simons theory, adapted from [41].

Consider a perturbatively computed Chern-Simons partition function at level k:

$$Z_{CS}(M_3) = \sum_{\alpha \in \mathcal{M}_{\text{flat}}(M_3, G)} e^{2\pi i k CS(\alpha)} Z_\alpha^{\text{pert}}. \tag{3.37}$$

Above, $\mathcal{M}_{\text{flat}}(M_3, G)$ is the moduli space of flat G-connections on M_3, which we have assumed to be discrete. To perform resurgence anlaysis, we first analytically continue k to complex values and apply the method of steepest descent on the Feynman path integral [9, 45, 68, 69, 97, 108–110, 116, 142]. Then, the integration domain is altered to a middle-dimensional cycle Γ in the moduli space of $G_{\mathbb{C}} = SL(2, \mathbb{C})$ connections, which is the union of the steepest descent flows from the saddle points. To elaborate, the moduli space is the universal cover of the space of $SL(2, \mathbb{C})$ connections modulo "based" gauge transformations, in which the gauge transformations are held to be 1 at the designated points. In sum, the partition function becomes:

$$Z_{CS}(M_3) = \int_\Gamma \mathcal{D}A \, e^{2\pi i k CS(A)}, \quad k \in \mathbb{C}. \tag{3.38}$$

Perturbative expansion of Equation 3.38 is a *transseries*, which can be Borel resummed. Let us provide here the basics of Borel resummation, following [116]. The simplest example of a transseries is a formal power series solution of Euler's equation:

$$\frac{d\varphi}{dz} + A\varphi(z) = \frac{A}{z}, \quad \varphi_0(z) = \sum_{n \geq 0} \frac{A^{-n} n!}{z^{n+1}}. \tag{3.39}$$

One may view the above transseries as a perturbative (in $1/z$) solution to the differential equation, but the solution has zero radius of convergence. By the Borel resummation, however, one can recover a convergent solution. When a transseries is of form $\varphi(z) = \sum_{n \geq 0} a_n / z^n$ with $a_n \sim n!$, its Borel transformation is defined as:

$$\hat{\varphi}(\zeta) = \sum_{n \geq 1} a_n \frac{\zeta^{n-1}}{(n-1)!}. \tag{3.40}$$

The Borel transformation $\hat{\varphi}(\zeta)$ is analytic near the origin of ζ-plane. If we can analytically continue $\hat{\varphi}(\zeta)$ to a neighborhood of the positive real axis, we can perform the Laplace transform:

$$S_0\varphi(z) = a_0 + \int_0^\infty e^{-z\zeta}\hat{\varphi}(\zeta)d\zeta, \tag{3.41}$$

where the subscript "0" indicates that the integration contour is along the positive real axis, $\{\arg(z) = 0\}$. It can be easily checked that the asymptotics of the above integral coincides with that of $\varphi(z)$. When $S_0\varphi(z)$ converges in some region in the z-plane, $\varphi(z)$ is said to be Borel summable, and $S_0\varphi(z)$ is called the Borel sum of $\varphi(z)$.

Saddle points of the complex Chern-Simons action form the moduli space of flat connections $\tilde{M}$, whose connected components $\tilde{M}_{\tilde{\alpha}}$ are indexed by their "instanton numbers,"

$$\tilde{\alpha} = (\alpha, CS(\tilde{\alpha})) \in \mathcal{M}_{\text{flat}}(M_3, SL(2,\mathbb{C})) \times \mathbb{Z}. \tag{3.42}$$

Here, $CS(\tilde{\alpha})$ denotes the value of Chern-Simons action at α, without moding out by 1. Following [83], we will call a flat connection *abelian* (*irreducible*, resp.), if its stabilizer is $SU(2)$ or $U(1)$ ($\{\pm 1\}$, resp.) action on $Hom(\pi_1(M_3), SU(2))$.

Now, let $\Gamma_{\tilde{\alpha}}$ be the union of steepest descent flows in $\tilde{M}$, starting from $\tilde{\alpha}$. The integration cycle Γ is then given by a linear sum of these "Lefshetz thimbles."

$$\Gamma = \sum_{\tilde{\alpha}} n_{\tilde{\alpha},\theta}\Gamma_{\tilde{\alpha},\theta}, \tag{3.43}$$

where $\theta = \arg(k)$, and $n_{\tilde{\alpha},\theta} \in \mathbb{Z}$ are the *transseries* parameters, given by the pairing between the submanifolds of steepest descent and ascent. The value of θ is adjusted so that there is no steepest descent flow between the saddle points. Let $I_{\tilde{\alpha},\theta}$ be the contribution from a Lefshetz thimble $\Gamma_{\tilde{\alpha},\theta}$ to $Z_{CS}(M_3)$ in Equation 3.38:

$$I_{\tilde{\alpha},\theta} = \int_{\Gamma_{\tilde{\alpha},\theta}} \mathcal{D}A e^{2\pi i k CS(A)},$$

which can be expanded in $1/k$ near $\tilde{\alpha}$ as:

$$I_{\tilde{\alpha},\theta} \sim e^{2\pi i k CS(\tilde{\alpha})} Z_\alpha^{\text{pert}}, \quad \text{where} \quad Z_\alpha^{\text{pert}} = \sum_{n=0}^{\infty} a_n^\alpha k^{-n+(d_\alpha-3)/2}, \quad d_\alpha = dim_{\mathbb{C}}\tilde{\mathcal{M}}_{\tilde{\alpha}}.$$

In sum, we can write the Chern-Simons partition function in the form:

$$Z_{CS}(M_3;k) = \sum_{\tilde{\alpha}} n_{\tilde{\alpha},\theta} I_{\tilde{\alpha},\theta} \sim \sum_{\tilde{\alpha}} n_{\tilde{\alpha},\theta} e^{2\pi i k CS(\tilde{\alpha})} Z^{\text{pert}}_{\alpha}(k), \tag{3.44}$$

which is a transseries expansion of the Chern-Simons partition function. From the asymptotics given by this transseries, we can apply Borel resummation and recover the full Chern-Simons partition function.

Concretely, one begins with a non-convergent (factorially divergent) series, and considers its Borel transform

$$Z^{\text{pert}}(k) = \sum_n \frac{a_n}{k^n} \quad \xrightarrow{\text{Borel transform}} \quad BZ^{\text{pert}}(z) = \sum_n \frac{a_n}{\Gamma(n)} z^{n-1} \tag{3.45}$$

which defines a function analytic near the origin. Then, we can perform Borel resummation,

$$\int e^{-\tau z} BZ_{pert}(z) dz, \tag{3.46}$$

where the contour of integration is unspecified at this stage.

Note that Equation 3.44 depends on the choice of $\theta = \arg(k)$. In fact, as we vary θ, the value of $I_{\tilde{\alpha},\theta}$ jumps (called "Stokes phenomenon") to keep the whole expression continuous in θ:

$$I_{\tilde{\alpha},\theta_{\tilde{\alpha}\tilde{\beta}}+\epsilon} = I_{\tilde{\alpha},\theta_{\tilde{\alpha}\tilde{\beta}}-\epsilon} + m^{\tilde{\beta}}_{\tilde{\alpha}} I_{\tilde{\beta},\theta_{\tilde{\alpha}\tilde{\beta}}-\epsilon}. \tag{3.47}$$

The "jump" happens near the Stokes rays $\theta = \theta_{\tilde{\alpha}\tilde{\beta}} \equiv \frac{1}{i}\arg(S_{\tilde{\alpha}} - S_{\tilde{\beta}})$. The transseries parameters $n_{\tilde{\alpha},\theta}$ jump accordingly to keep $Z_{CS}(M_3;k)$ continuous in θ. The coefficients $m^{\tilde{\beta}}_{\tilde{\alpha}}$ are called Stokes monodromy coefficients.

Now, suppose Z_{CS} is written in terms of false theta functions $\Psi_{m,r}$ (most likely, via homological blocks). When $b_1(M_3) = 0$, there is an overall factor of $k^{-1/2}$ multiplying the false theta functions evaluated at $\tau \to -1/k$. From the modular point of view, this $1/\sqrt{k}$ factor stems from the fact that $\Psi_{m,r}$ is a weight $1/2$ quantum modular form (see Section 3.4).

From the asymptotics (Equation (3.35) and (3.36)), one can obtain the Borel transform of false theta functions:

$$B\left(\frac{1}{\sqrt{k}}\Psi_{m,r}(\tfrac{1}{k})\right)(z) = \frac{1}{\sqrt{\pi z}} \frac{\sin((m-r)\sqrt{\frac{2\pi z}{m}})}{\sin(m\sqrt{\frac{2\pi z}{m}})}. \tag{3.48}$$

Consequently, its exact Borel resummation yields:

$$\frac{1}{\sqrt{k}}\Psi_{m,r}(\tfrac{1}{k}) = \frac{\sqrt{i}}{2}\left(\int_{e^{i\delta}\mathbb{R}_+} + \int_{e^{-i\delta}\mathbb{R}_+}\right) \frac{dz}{\sqrt{\pi z}} \frac{\sin((m-r)\sqrt{\frac{2\pi z}{m}})}{\sin(m\sqrt{\frac{2\pi z}{m}})} e^{-ikz}. \tag{3.49}$$

Note that the integral has poles at $z = 2\pi n^2/4m$ with residues:

$$\operatorname*{Res}_{z=2\pi n^2/4m}\left(\frac{\sqrt{i}}{2}\frac{1}{\sqrt{\pi z}}\frac{\sin((m-r)\sqrt{\frac{2\pi z}{m}})}{\sin(m\sqrt{\frac{2\pi z}{m}})}e^{-ikz}\right) = -\frac{\sqrt{i}}{\pi\sqrt{2m}}\sin\left(\frac{r\pi n}{m}\right)e\left(-k\frac{n^2}{4m}\right) \tag{3.50}$$

for $n \in \mathbb{Z}_+$. The RHS is (up to an overall constant) the S-matrix of Equation (3.24), when restricted to the -1 eigenspace of the action by $-1 = a(m)$:

$$\mathcal{S}^m_{r,n} = (\mathcal{S}P^-_m(m))_{r,n} = \frac{-i}{\sqrt{2m}}\sin\left(\frac{rn\pi}{m}\right). \tag{3.51}$$

The zeta-function regularization $\sum_{n\equiv\pm r\,(mod\,2m)} \pm 1 = 1 - \frac{r}{m}$ allows us to sum the infinitely many poles:

$$\sum_{n\geq 0}(P^-_m(m))_{r,n} = \lim_{t\to 0^+}\sum_{n\geq 0}(P^-_m(m))_{r,n}e^{-nt} = \lim_{t\to 0^+}\frac{\sinh((m-r)t)}{\sinh(mt)} = 1 - \frac{r}{m}. \tag{3.52}$$

In sum, Ψ^{m+K}_r has poles in the Borel plane labelled by the set σ^{m+K}, whose residues appear as non-perturbative contributions to the asymptotic series of $\Psi^{m+K}_r(\frac{1}{k})$:

$$\frac{1}{\sqrt{k}}\Psi^{m+K}_r(\tfrac{1}{k}) = -2\sqrt{i}\sum_{r'\in\sigma^{m+K}}\mathcal{S}^{m+K}_{rr'}c_{r'}\,e^{-2\pi i k\frac{r'^2}{4m}} + \text{perturbative expansion},$$
$$\text{where}\quad c_r := 2^{|K|}\sum_{\ell=1}^{m-1}P^{m+K}_{\ell r}\left(1-\frac{\ell}{m}\right). \tag{3.53}$$

Observe that we have recovered non-perturbative contributions from perturbative data, which is the key feature of resurgence analysis. Following [83], it is tempting to interpret them as the contributions of irreducible flat connections (can be either real or complex). We will observe several examples later when we *reverse-engineer* the topological data from the connection between homological blocks and false theta functions.

The same regularization procedure gives the radial limit:

$$\Psi^{m+K}_r(-k) = e\left(-k\frac{r^2}{4m}\right)c_r\ . \tag{3.54}$$

Therefore, we can write Equation (3.53) as follows:

$$\frac{1}{\sqrt{k}}\Psi^{m+K}_r(\tfrac{1}{k}) = \frac{2}{\sqrt{i}}\sum_{r'\in\sigma^{m+K}}\mathcal{S}^{m+K}_{r,r'}\Psi^{m+K}_{r'}(-k) + \text{perturbative expansion}, \tag{3.55}$$

which has an obvious interpretation as a modular S-transform. To be precise, Ψ_r^{m+K} exhibits a modular property but *only up to a smooth function.* In other words, Ψ_r^{m+K} gives rise to a quantum modular form. We will further explore the quantum modularity later in Section 3.4.

Let us conclude this section with a discussion about the relation between the integral in (3.49) and the Eichler integral (3.28), drawing on results in [147]. First of all, observe that we can write the integrand of (3.49) by the theory of partial fraction decompositions:

$$\frac{e^{-y^2/\tau}}{\sqrt{\tau}}\frac{\sinh((m-r)\pi y)}{\sinh(m\pi y)} = C_m \frac{e^{-y^2/\tau}}{\sqrt{\tau}} \lim_{n_*\to\infty} \sum_{n=-n_*}^{n_*} \frac{\sin(r\pi\frac{n}{m})}{y - i\frac{n}{m}}. \tag{3.56}$$

C_m is an unimportant constant that depends only on m. By the equality between two integrals

$$\int_{-\infty}^{\infty} \frac{e^{-\pi t y^2}}{y - ir} dy = \pi i r \int_0^{\infty} \frac{e^{-\pi r^2 u}}{\sqrt{u+t}} du \tag{3.57}$$

and exchanging the sum and the integral, we obtain[4]:

$$\int_0^{\infty} dy\, \frac{e^{-y^2/\tau}}{\sqrt{\tau}}\frac{\sinh((m-r)\pi y)}{\sinh(m\pi y)} = c\int_0^{\infty} du \frac{\theta^1_{m,r}(u)}{\sqrt{u+\tau}} \tag{3.58}$$

with some unimportant factor $c \in \mathbb{C}$. Therefore, we have recovered the Eichler integral from the Borel resummation. The above result extends to Ψ_r^{m+K}, which is a linear sum of $\Psi_{m,r}$.

Modularity dictionary

So far, we have defined homological blocks and false theta functions. In this section, we provide a "dictionary" by which the following identifications are made:

$$\widehat{Z}_b(M_3) \;=\; c\left(q^{\delta}\Psi_r^{m+K} + d\right), \qquad c \in \mathbb{C}, \quad \delta \in \mathbb{Q}, \quad d \in \mathbb{Z}[q]. \tag{3.59}$$

It turns out that the Weil representation $m+K$ is the same for all homological blocks of a given M_3. However, different "boundary conditions" b correspond to different vectors represented by $r \in \sigma^{m+K}$. Let us exhibit how the necessary ingredients are determined.

Determination of m. For 3-singular fibered Seifert manifolds, m is unambiguously determined by comparison of the q-power growth. If there were to be *any* identification between homological blocks and false theta functions, their q-series should

[4]The exchange of sum and integral can be delicate. See the proof for Lemma 3.3 [147].

exhibit the *same* q-power growth. The convergence criteria dictate that q-powers of homological blocks grow quadratically as $q^{-(M^{-1})_{v_0v_0}(\ell_{v_0})^2/4}$ over $\ell_{v_0} \in 2\mathbb{Z} + \delta_{v_0}$. False theta functions also exhibit quadratic growth, $q^{(2mn\pm r)^2/4m} \sim q^{mn^2}$ over $n \in \mathbb{Z}_{\geq 0}$. However, on the sublattices comprising b indices, $q^{-(M^{-1})_{v_0v_0}(\ell_{v_0})^2/4}$ may grow even faster. Therefore, we observe that (recall that $(M^{-1})_{v_0v_0}$ has to be negative for convergence):

$$M_3 \text{ is a 3-singular fibered Seifert manifold} \quad \Rightarrow \quad m \,\Big|\, |(M^{-1})_{v_0v_0}|. \tag{3.60}$$

One may also argue from a different topological viewpoint. The key observation is that if $\widehat{Z}_b(q) \leftrightarrow \Psi_r^{m+K}$, one can *reverse-engineer* the transseries expansion of Z_{CS}. In other words, the "non-perturbative" contributions (*c.f*, Equation (3.53)) and Chern-Simons invariants of abelian flat connections (*c.f.*, Equation (3.6)) must conspire to produce Chern-Simons invariants of non-abelian flat connections. Therefore, any $SU(2)$ flat connection α on M_3 must satisfy $CS(\alpha) = CS[a] - r^2/4m \pmod{\mathbb{Z}}$ for some $a \in \text{Coker}M$ and $r = 0, \cdots, m-1$:

$$\text{l.c.m}\left\{ \text{Denominators of } CS(\alpha) \;:\; \alpha \in \mathcal{M}_{flat}(M_3, SU(2)) \right\} \,\Big|\, 4m. \tag{3.61}$$

Both conditions will be useful. Explicitly for a Seifert manifold $M(b, \{q_i/p_i\}_{i=1}^n)$, the denominator of $CS(a)$ for a non-abelian is a l.c.m. of $4p_i$, where p_i are the orders of singular fibers [10]. As a result, we claim that for $M_3 = M(b, \{q_i/p_i\}_{i=1}^n)$,

$$4m = \text{l.c.m.}\Big(4\{p_i\}_{i=1}^n \;\cup\; \{\text{Denominators of CS}(a)\}_{0\neq a\in \text{Coker}M/\mathbb{Z}_2}\Big). \tag{3.62}$$

Later, we observe external automorphisms acting on the moduli space of connections. In presence of such extra symmetries, the above identity must be modified by appropriately modding them out.

Determination of $m + K$. Just as one searches through a dictionary in the lexicographic order, one can search through the irreps $m + K$ such that $|\sigma^{m+K}|$ equals the number of b-indices (modulo *center* symmetry and the Weyl group action). The component vectors Ψ_r^{m+K} are then compared with $\widehat{Z}_b(q)$ and are identified.

For practical usage, we define the following $S(M_3)$ and $T(M_3)$ matrices:

$$\begin{gathered} S(M_3) = S^{(A)}.\mathbf{Emb}.\left(S^{(B)}\right)^{-1}, \quad \mathbf{Emb}_{ar} = c, \\ T(M_3) = T^{(A)}.\mathbf{I}.\left(T^{(B)}\right)^{-1}, \quad \mathbf{I}_{ar} = 1, \\ a \in \text{Tor}H_1(M_3)/\mathbb{Z}_2, \quad \text{and} \quad r \in \sigma^{m+K}, \end{gathered} \tag{3.63}$$

where $S^{(A)}, T^{(B)}$ are simply the shorthand notations of (3.24). Then, one can compactly write:

$$Z_{CS} = \sum_{a,r} e^{2\pi i k CS[a]} S(M_3)_{ar} \Psi_r^{m+K}. \tag{3.64}$$

In the following examples, we will not only identify homological blocks with false theta functions, but also perform modular transform / resurgence analysis to obtain the transseries expansion of Z_{CS}. Let us elaborate on the procedure of *reverse-engineering* that was briefly mentioned before. We have seen that the non-perturbative contributions of Ψ_r^{m+K} involve $e^{-2\pi i k (r')^2/4m}$. They correspond to the poles in the Borel plane, and they can non-trivially contribute to Z_{CS} in three different ways, leading to three different topological interpretations (*c.f.* Table 3.2).

Type of	Transseries contributions		
connection	$\widehat{Z}_b$	Z_a	Z_{CS}
"renormalon"	∘	×	×
complex	∘	∘	×
real, irreducible	∘	∘	∘

Table 3.1: Transseries contribution of poles at different levels and the classification of flat connections.

The first case is when a pole contributes to some $\widehat{Z}_b$, but it does not contribute to:

$$Z_a := \sum_r S(M_3)_{ar} \Psi_r^{m+K}. \tag{3.65}$$

Recall that instanton contributions of Chern-Simons theory (either via analytic continuation or via resurgence analysis) would be reflected in Z_a's. Therefore, these poles do not even correspond to flat $SL(2,\mathbb{C})$ connections on M_3. Physically, they are invisible from Chern-Simons partition functions (or from Z_a), because Chern-Simons theory is *not* a realistic QFT, and thus, only instantons can contribute factorial divergence to the asymptotic series. However, its 3d-3d dual is a realistic QFT, and therefore, the 3d-2d coupled index Ψ_r^{m+K} may observe additional factorial divergences coming from the "renormalons." Thus by performing resurgence analysis for Ψ_r^{m+K}, we observe a new set of poles in the Borel plane, which were invisible for Z_a's.

Secondly, one may consider poles which contribute to some $\widehat{Z}_b$'s and Z_a's, but not to Z_{CS}. When contributions to Z_a's are observed, the poles correspond to the

saddle points of path integral for $\widehat{Z}_b$. A theorem [83] states that only non-abelian flat connections arise as non-perturbative contributions from asymptotic expansion around abelian flat connections. Therefore, these saddle points must represent non-abelian $SL(2,\mathbb{C})$ flat connections on M_3. Since their contributions are invisible in Z_{CS}, they can be safely regarded as "complex" flat connections which cannot be conjugated to $SU(2)$. By the same reasoning, the poles with non-zero contributions to Z_{CS} correspond to real, irreducible flat connections (for $SU(2)$, non-abelian = irreducible.)

We can cast the classification criteria in terms of $S(M_3)$ and $T(M_3)$ matrices. For complex flat connections, we can simply compute:

$$\boxed{\begin{aligned}&\{\, e(\mathrm{CS}(\mathfrak{a})) \mid \mathfrak{a} \text{ is a non-abelian } SL(2,\mathbb{C}) \text{ flat connection on } M_3 \,\} \\ &\quad = \{\, T(M_3)_{ar} \mid a, r \text{ such that } S(M_3)_{ar} \neq 0 \,\}\end{aligned}} \tag{3.66}$$

Let us denote the matrix elements $T(M_3)_{ar}$ which belongs to the RHS set by $e(\alpha)$, and write:

$$\sum_{a,r} T(M_3)_{a,r} S(M_3)_{a,r} c_r = \sum_{\alpha} e(\alpha)\, \mathbf{c}_\alpha, \quad \textit{i.e.}, \quad \mathbf{c}_\alpha = \sum_{(a,r)} S(M_3)_{a,r} c_r \tag{3.67}$$

where the summation $\sum_{(a,r)}$ ranges over the pairs (a, r) satisfying $T(M_3)_{ar} = e(\alpha)$.

Similarly for real, irreducible flat connections, we can write:

$$\boxed{\begin{aligned}&\{\, e(\mathrm{CS}(\mathfrak{a})) \mid \mathfrak{a} \text{ is a non-abelian } SU(2) \text{ flat connection on } M_3 \,\} \\ &\quad = \{\, e(\alpha) \mid \mathbf{c}_\alpha \neq 0 \,\}\end{aligned}} \tag{3.68}$$

Let us summarize the reverse-engineering procedure in Figure 3.6. A final and important remark is that by reverse-engineering, we can only compute the transseries coefficients, and thus, we cannot distinguish two different flat connections with the same Chern-Simons invariants (mod $\mathbb{Z}$).

3.3 Examples

In this section, we apply the "modularity dictionary" for various plumbed manifolds. Homological blocks are computed and identified with Eichler integrals. By virtue of their modular properties, we reverse-engineer the transseries expansion of Z_{CS}. It turns out that the transseries encode non-trivial information about the structure of moduli space.

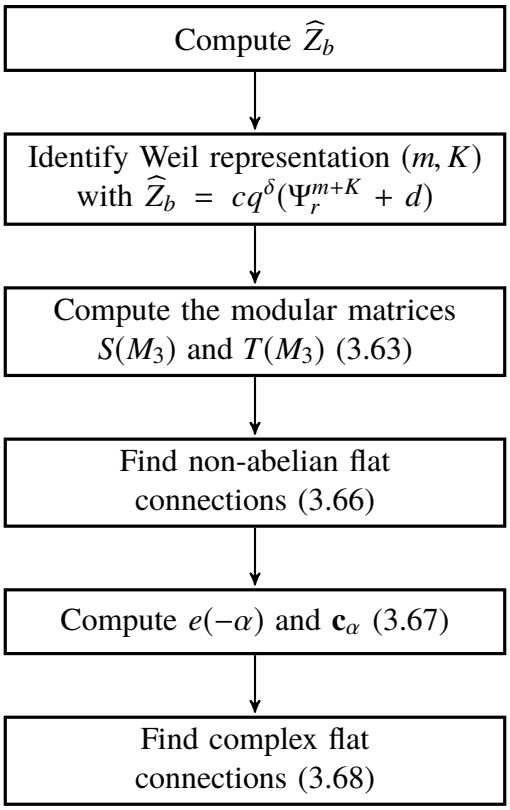

Figure 3.6: From plumbing data to flat connections.

Example: $M(-1; \frac{1}{2}, \frac{1}{3}, \frac{1}{9})$

The Seifert manifold has the following plumbing graph and linking matrix:

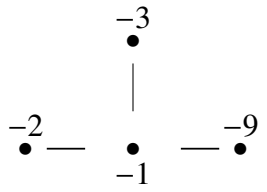

(3.69)

$$M = \begin{pmatrix} -1 & 1 & 1 & 1 \\ 1 & -2 & 0 & 0 \\ 1 & 0 & -3 & 0 \\ 1 & 0 & 0 & -9 \end{pmatrix}.$$

$$\mathrm{Coker}(M) = \mathbb{Z}^4/M\mathbb{Z}^4 = \big\langle (0,0,0,0), (1,0,-1,-6), (1,0,-2,-3) \big\rangle$$
$$\cong \mathrm{Tor}H_1(M(-1; \tfrac{1}{2}, \tfrac{1}{3}, \tfrac{1}{9})) = \mathbb{Z}_3. \quad (3.70)$$

Recall that the Weyl group acts by $a \leftrightarrow -a$. Therefore, the first element, $(0,0,0,0)$, is mapped to itself, while the others are conjugate to each other, *i.e.*, $(1,0,-1,-6) =$

$-(1,0,-2,-3) \in \mathbb{Z}^4/M\mathbb{Z}^4$. Thus,

$$\mathrm{Coker}(M)/\mathbb{Z}_2 = \big\langle (0,0,0,0), (1,0,-1,-6) \big\rangle \tag{3.71}$$

$$(2\mathrm{Coker}(M)+\delta)/\mathbb{Z}_2 = \big\langle (1,-1,-1,-1), (3,-1,-3,-13) \big\rangle \tag{3.72}$$

where $\delta = (1,-1,-1,-1)$ is given by $\delta_v = \deg_v -2$, as in [84]. Then, $\widehat{Z}_b(M_3)$ are given by (3.7):

$$\widehat{Z}_{(1,-1,-1,-1)}(q) = q + q^5 - q^6 - q^{18} + q^{20} + \dots \tag{3.73}$$

$$\widehat{Z}_{(3,-1,-3,-13)}(q) = -q^{4/3}(1 + q^2 - q^7 - q^{13} + q^{23} + \dots). \tag{3.74}$$

Weil representation: 18+9. From M^{-1}, one can read off $m = 18$, and the possible K (giving rise to irreducible representations) are $K = \{1,2\}$ and $K = \{1,9\}$. A simple calculation reveals that the relevant irreducible representation is $m + K = 18 + 9$:

$$\begin{aligned} \sigma^{18+9} &= \{1,3,5,7\} \\ \widehat{Z}_{(1,-1,-1,-1)}(q) &= q^{71/72}\Psi_1^{18+9}(\tau) \\ \widehat{Z}_{(3,-1,-3,-13)}(q) &= -q^{71/72}\Psi_5^{18+9}(\tau). \end{aligned} \tag{3.75}$$

$S(M_3)$ and $T(M_3)$ matrices. First of all, recall that $S^{(A)}$ is the linking pairing on $\mathrm{Tor}H_1(M_3)$ in (3.6). For $M_3 = M(-1;\frac{1}{2},\frac{1}{3},\frac{1}{9})$,

$$S^{(A)} = \frac{1}{\sqrt{3}}\begin{pmatrix} 1 & 1 \\ 2 & -1 \end{pmatrix}. \tag{3.76}$$

Next, from (3.59) and (3.75) we can easily read off:

$$\mathbf{Emb} = \begin{pmatrix} 1 & 0 & 0 & 0 \\ 0 & 0 & -1 & 0 \end{pmatrix}. \tag{3.77}$$

The S-matrix of the Weil representation is easily computed:

$$S^{(B)} = -\frac{2i}{3}\begin{pmatrix} A & \frac{3}{2} & B & C \\ \frac{1}{2} & 0 & \frac{1}{2} & -\frac{1}{2} \\ B & \frac{3}{2} & -C & -A \\ C & -\frac{3}{2} & -A & B \end{pmatrix} \tag{3.78}$$

where $A, B, C = \sin(\frac{\pi}{18}), \sin(\frac{5\pi}{18}), \sin(\frac{7\pi}{18})$, respectively. We can now combine $S^{(A)}$, **Emb**, and $S^{(B)}$ into $S(M_3)$:

$$S(M_3) = \begin{pmatrix} -0.23i & 0 & 0.66i & 0.43i \\ 0.43i & 1.73i & 0.23i & 0.66i \end{pmatrix}, \tag{3.79}$$

here evaluated numerically and rounded to the second decimal place.

Next, we compute the T matrices. $T^{(A)}$ is the diagonal matrix with $e^{2\pi i \mathrm{CS}(a)}$ on the diagonal:

$$T^{(A)} = \exp\ 2\pi i \begin{pmatrix} 0 & 0 \\ 0 & \frac{1}{3} \end{pmatrix}. \tag{3.80}$$

The Weil representation of T-matrix is:

$$T^{(B)} = \exp\ 2\pi i \begin{pmatrix} \frac{1}{72} & 0 & 0 & 0 \\ 0 & \frac{9}{72} & 0 & 0 \\ 0 & 0 & \frac{25}{72} & 0 \\ 0 & 0 & 0 & \frac{49}{72} \end{pmatrix}. \tag{3.81}$$

Combining all these elements, we obtain:

$$T(M_3) = \begin{pmatrix} e(-\frac{1}{72}) & e(-\frac{9}{72}) & e(-\frac{25}{72}) & e(-\frac{49}{72}) \\ e(-\frac{49}{72}) & e(-\frac{57}{72}) & e(-\frac{1}{72}) & e(-\frac{25}{72}) \end{pmatrix}. \tag{3.82}$$

Classifying flat connections. From $S(M_3)$ computed above,

$$\{T(M_3)_{ar} | a, r \text{ such that } S(M_3) \neq 0\} = \{e(-\tfrac{1}{72}), e(-\tfrac{25}{72}), e(-\tfrac{49}{72}), e(-\tfrac{57}{72})\}. \tag{3.83}$$

From the rule (3.66), we can identify (at least) four non-abelian $SL(2,\mathbb{C})$ flat connections, whose Chern-Simons invariants are $\{-\frac{1}{72}, -\frac{25}{72}, -\frac{49}{72}, -\frac{57}{72}\}$ modulo $\mathbb{Z}$.

To classify non-abelian flat connections, let us compute $\mathbf{c}_\alpha$ defined in (3.67), by summing over the pairs (a, r) such that $T(M_3)_{a,r} = e(\alpha)$. For example, when $\alpha = -\frac{1}{72}$, $(a, r) = (1, 1)$ and $(2, 4)$. Now, we can compute $\mathbf{c}_\alpha$:

$$\begin{cases} \mathbf{c}_{-\frac{1}{72}} & = 0 \\ \mathbf{c}_{-\frac{25}{72}} & = 1.17i \\ \mathbf{c}_{-\frac{49}{72}} & = 0.76i \\ \mathbf{c}_{-\frac{57}{72}} & = 1.03i. \end{cases} \tag{3.84}$$

So we conclude that $M(-1; \frac{1}{2}, \frac{1}{3}, \frac{1}{9})$ must admit one complex non-abelian flat connection with CS $= -\frac{1}{72}$, and three $SU(2)$ non-abelian flat connections with CS $= -\frac{25}{72}, -\frac{49}{72}, -\frac{57}{72}$.

Comparison with A-polynomial. We can cross-check our interpretation with a computation based on a *knot* surgery presentation of M_3. As explained in [76] and

[83, sec.5], when $M_3 = S^3_r(K)$ (*i.e.* M_3 is obtained by a rational r-surgery on a knot $K \subset S^3$), flat $SL(2,\mathbb{C})$ connections on M_3 are contained in the set of intersection points:

$$\text{flat connections} \quad \hookrightarrow \quad \{s(x,y) := yx^r - 1 = 0\} \cap \{A_K(x,y) = 0\} \tag{3.85}$$

in $(\mathbb{C}^* \times \mathbb{C}^*)/\mathbb{Z}_2$ parametrized by $(x,y) \sim (x^{-1}, y^{-1})$. Here, $A_K(x,y)$ is the so-called *A-polynomial* of the knot K.

In the present example, $M_3 = M(-1; \frac{1}{2}, \frac{1}{3}, \frac{1}{9}) = S^3_{-3}(\mathbf{3}^r)$, where $K = \mathbf{3}^r$ is the right-handed trefoil knot. The corresponding A-polynomial and the curve $s(x,y) = 0$ are:

$$A(x,y) = (y-1)(yx^6+1), \quad s(x,y) = yx^{-3} - 1. \tag{3.86}$$

Discarding the point $(x,y) = (-1,-1)$ that does not lift to a flat connection on M_3 [83], the intersection points (3.85) (modulo $(x,y) \sim (x^{-1}, y^{-1})$) are given by:

$$(x,y) \;=\; (1,1), (e^{\frac{2\pi i}{3}}, 1), (e^{\frac{\pi i}{3}}, -1), (e^{\frac{\pi i}{9}}, e^{\frac{\pi i}{3}}), (-e^{\frac{4\pi i}{9}}, e^{\frac{\pi i}{3}}), (e^{\frac{7\pi i}{9}}, e^{\frac{\pi i}{3}}). \tag{3.87}$$

All abelian flat connections have $y = 1$, and there are two such points in our list, in agreement with the above analysis. The remaining four points are candidates for non-abelian flat connections, either real or complex: it also agrees with the total number of non-abelian flat connections observed by reverse-engineering.

Let us remark that reverse-engineering (Figure 3.6) may underestimate the number of flat connections on M_3 due to the accidental cancellations among the transseries. On the other hand, some of the intersection points (3.85) may not lift to an actual representation $\rho : \pi_1 \to SL(2,\mathbb{C})$. Therefore, the two methods provide lower and upper bounds on the number of flat connections. In the present example, the two methods provide the same results, and we can conclude that there are two abelian flat connections, one complex flat connection, and three $SU(2)$ irreducible flat connections.

Asymptotic expansions. We conclude the analysis of this example by writing the asymptotic expansion of $Z_{CS}(M_3)$. Combining Equation (3.64), (3.75), $S(M_3)$ and $T(M_3)$ matrices, and the transseries expression for the false theta functions (3.53), we obtain the transseries expressions at large k. The results for various saddle points (flat connections on M_3) are tabulated in Table 3.2, where we omit the overall factor $-iq^{71/72}/2\sqrt{2}$.

CS action	stabilizer	type	transseries
0	$SU(2)$	central	$e^{2\pi i k\cdot 0}\left(\frac{4\pi i}{3\sqrt{3}}k^{-3/2}+\frac{203\pi^2}{27\sqrt{3}}k^{-5/2}+O(k^{-7/2})\right)$
$\frac{1}{3}$	$U(1)$	abelian	$e^{2\pi i k\frac{1}{3}}\left(\sqrt{3}k^{-1/2}-\frac{11\pi i}{4\sqrt{3}}k^{-3/2}+O(k^{-5/2})\right)$
$-\frac{25}{72}$	± 1	non-abelian, real	$e^{-2\pi i k\frac{25}{72}}e^{\frac{3\pi i}{4}}\left[\frac{4}{3\sqrt{3}}(\cos\frac{2\pi}{9}+2\sin\frac{\pi}{18})\right]$
$-\frac{49}{72}$	± 1	non-abelian, real	$e^{-2\pi i k\frac{49}{72}}e^{\frac{3\pi i}{4}}\left[\frac{4}{3\sqrt{3}}(2\cos\frac{\pi}{9}+\sin\frac{\pi}{18})\right]$
$-\frac{57}{72}$	± 1	non-abelian, real	$e^{-2\pi i k\frac{57}{72}}e^{\frac{3\pi i}{4}}\frac{2}{\sqrt{3}}$
$-\frac{1}{72}$	± 1	non-abelian, complex	0

Table 3.2: Transseries and classification of flat connections on $M(-2;\frac{1}{2},\frac{1}{3},\frac{1}{9})$.

Example: $M(-2;\frac{1}{2},\frac{1}{3},\frac{1}{2})$

Let us look at one more example in detail, the Seifert manifold $M_3 = M(-2;\frac{1}{2},\frac{1}{3},\frac{1}{2})$. This example will also play a role in Section 3.4, where we discuss the extension of $\widehat{Z}_b(q)$ (convergent on $\tau\in\mathbb{H}$) to the lower half-plane.

The current example also exhibits a "center symmetry." Distinguished from the familiar Weyl group action, it acts on representations $\rho:\pi_1(M_3)\to SL(2,\mathbb{C})$ by multiplying holonomies by the central elements $\pm\mathbf{1}$ of $G=SU(2)$ or its complexification $G_{\mathbb{C}}=SL(2,\mathbb{C})$. The role of this center symmetry will be discussed in further details later in this section.

The manifold of interest has $\mathrm{Tor}H_1(M_3,\mathbb{Z})=\mathbb{Z}_8$, the following plumbing graph, the linking matrix, $a\in\mathrm{Coker}(M)$ and $b\in 2\mathrm{Coker}(M)+\delta$:

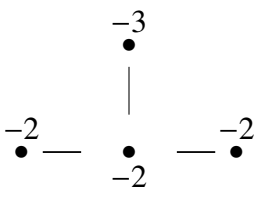

(3.88)

$$M=\begin{pmatrix}-2&1&1&1\\1&-2&0&0\\1&0&-3&0\\1&0&0&-2\end{pmatrix} \tag{3.89}$$

$$\begin{aligned}a\in\mathrm{Coker}(M)/\mathbb{Z}_2=&\big\langle(0,0,0,0),(1,-1,0,-1),\\&(0,-1,0,0),(0,0,-1,0),(0,0,0,-1)\big\rangle\end{aligned} \tag{3.90}$$

$$b \in (2\mathrm{Coker}(M) + \delta)/\mathbb{Z}_2 = \Big\langle (3,-1,-5,-3), (3,-3,-5,-1), \\ (1,-1,-1,-1), (3,-3,-1,-3), (1,-3,-1,-1) \Big\rangle. \tag{3.91}$$

Just as in the previous example, we compute 1) the Chern-Simons invariants of abelian flat connections, 2) its $S^{(A)}$ matrix, and 3) the homological blocks $\widehat{Z}_b(M_3)$:

$$\mathrm{CS}(a) = -(a, M^{-1}a) = \begin{cases} 0 & \mod \mathbb{Z} \quad \text{for} \quad a = (0,0,0,0), (1,-1,0,-1) \\ \frac{7}{8} & \mod \mathbb{Z} \quad \text{for} \quad a = (0,-1,0,0), (0,0,0,-1) \\ \frac{1}{2} & \mod \mathbb{Z} \quad \text{for} \quad a = (0,0,-1,0). \end{cases} \tag{3.92}$$

$$S^{(A)} = \frac{1}{\sqrt{8}} \begin{pmatrix} 1 & 1 & 1 & 1 & 1 \\ 1 & 1 & 1 & 1 & 1 \\ 2 & 2 & 0 & 0 & -2 \\ 2 & 2 & -2 & -2 & 2 \\ 2 & 2 & 0 & 0 & -2 \end{pmatrix} \tag{3.93}$$

$$\begin{aligned} \widehat{Z}_{(3,-1,-5,-3)}(q) &= q^{-1/4}(-1 + q^4 - q^8 + q^{20} - q^{28} + q^{48} + \ldots), \\ \widehat{Z}_{(3,-3,-5,-1)}(q) &= q^{-1/4}(-1 + q^4 - q^8 + q^{20} - q^{28} + q^{48} + \ldots), \\ \widehat{Z}_{(1,-1,-1,-1)}(q) &= q^{-3/8}(1 + q - q^2 + q^5 - q^7 + q^{12} + \ldots), \\ \widehat{Z}_{(3,-3,-1,-3)}(q) &= q^{-3/8}(-1 + q - q^2 + q^5 - q^7 + q^{12} + \ldots), \\ \widehat{Z}_{(1,-3,-1,-1)}(q) &= 2q^{1/4}(1 - q^2 + q^{10} - q^{16} + q^{32} - q^{42} + \ldots). \end{aligned} \tag{3.94}$$

Weil representation: 6+2. By Equation (3.62), we obtain:

$$4m = \text{l.c.m.}(8, 12, 1, 2, 8) = 24 \;\Rightarrow\; m = 6. \tag{3.95}$$

Since $\mathrm{Ex}_6 = \{1, 2, 3, 6\}$, K can be either $\{1\}$, $\{1, 2\}$ or $\{1, 3\}$. The latter two correspond to irreps. With $m + K = 6 + 2$,

$$\begin{aligned} \sigma^{6+2} &= \{1, 2, 4\}, \\ \widehat{Z}_{(3,-1,-5,-3)}(q) &= \widehat{Z}_{(3,-3,-5,-1)}(q) = -\frac{1}{2} q^{-5/12} \Psi_2^{6+2}(\tau), \\ \widehat{Z}_{(1,-1,-1,-1)}(q) &= q^{-5/12}(2q^{1/24} - \Psi_1^{6+2}(\tau)), \\ \widehat{Z}_{(3,-3,-1,-3)}(q) &= -q^{-5/12} \Psi_1^{6+2}(\tau), \\ \widehat{Z}_{(1,-3,-1,-1)}(q) &= q^{-5/12} \Psi_4^{6+2}(\tau). \end{aligned} \tag{3.96}$$

$S(M_3)$ and $T(M_3)$ matrices. Next, we proceed to compute the "composite" modular matrices $S(M_3)$ and $T(M_3)$. $S^{(A)}$ can be found in Equation (3.93). The embedding

matrix can be read off from Equation (3.96):

$$\mathbf{Emb} = \begin{pmatrix} 0 & -\frac{1}{2} & 0 \\ 0 & -\frac{1}{2} & 0 \\ -1 & 0 & 0 \\ -1 & 0 & 0 \\ 0 & 0 & 1 \end{pmatrix}. \tag{3.97}$$

The matrix $S^{(B)}$ can be computed from the projection matrices:

$$S^{(B)} = -\frac{i}{2}\begin{pmatrix} 0 & 1 & 1 \\ 2 & 1 & -1 \\ 2 & -1 & 1 \end{pmatrix}, \tag{3.98}$$

which can be compiled into:

$$S(M_3) = \frac{i}{\sqrt{2}}\begin{pmatrix} 0 & 1 & 0 \\ 0 & 1 & 0 \\ 2 & 0 & 0 \\ 0 & 0 & -2 \\ 2 & 0 & 0 \end{pmatrix}. \tag{3.99}$$

Next, we compute the T matrices. From Equation (3.92), we obtain

$$T^{(A)} = \exp\ 2\pi i \begin{pmatrix} 0 & 0 & 0 & 0 & 0 \\ 0 & 0 & 0 & 0 & 0 \\ 0 & 0 & \frac{7}{8} & 0 & 0 \\ 0 & 0 & 0 & \frac{1}{2} & 0 \\ 0 & 0 & 0 & 0 & \frac{7}{8} \end{pmatrix}. \tag{3.100}$$

On the other hand, $T^{(B)} = e^{2\pi i \frac{r^2}{4m}}\delta_{r,r'}$ for $r \in \sigma^{6+2} = \{1, 2, 4\}$:

$$T^{(B)} = \exp\ 2\pi i \begin{pmatrix} \frac{1^2}{24} & 0 & 0 \\ 0 & \frac{2^2}{24} & 0 \\ 0 & 0 & \frac{4^2}{24} \end{pmatrix}. \tag{3.101}$$

We combine $T^{(A)}$ and $T^{(B)}$ with $\mathbf{I}$ (= 3×5 matrix with all entries equal to 1),

$$T(M_3) = \begin{pmatrix} e(-\frac{1}{24}) & e(-\frac{4}{24}) & e(-\frac{16}{24}) \\ e(-\frac{1}{24}) & e(-\frac{4}{24}) & e(-\frac{16}{24}) \\ e(-\frac{4}{24}) & e(-\frac{7}{24}) & e(-\frac{19}{24}) \\ e(-\frac{13}{24}) & e(-\frac{4}{24}) & e(-\frac{4}{24}) \\ e(-\frac{4}{24}) & e(-\frac{7}{24}) & e(-\frac{19}{24}) \end{pmatrix}. \tag{3.102}$$

Classifying flat connections. From the $S(M_3)$ computed in the previous subsection, we observe that:

$$\{T(M_3)_{ar} | a, r \text{ such that } S(M_3) \neq 0\} = \{e(-\tfrac{1}{6})\}. \tag{3.103}$$

Therefore, using the rule (3.66), we predict (at least) one non-abelian $SL(2, \mathbb{C})$ flat connection with $CS = -\frac{4}{24}$. To determine whether it is real or complex, we compute $\mathbf{c}_{-\frac{1}{6}}$ via Equation (3.67):

$$\mathbf{c}_{-\frac{1}{6}} = 2i\sqrt{2}. \tag{3.104}$$

Since it is nonzero, it must be a $SU(2)$ non-abelian flat connection. In sum, we have one $SU(2)$ non-abelian flat connection with CS = $-\frac{4}{24}$, and there is no complex flat connection.

Asymptotic expansions. As in the previous example, we can assemble $\widehat{Z}_b$ into $Z_{CS}(M_3)$. Applying the modular S-transform yields transseries for $M_3 = M(-2; \frac{1}{2}, \frac{1}{3}, \frac{1}{2})$, summarized in Table 3.3. We omit an overall factor $-iq^{-5/12}/2\sqrt{2}$.

Center symmetry

Note the degeneracies in Equation (3.92)–(3.94). The degeneracy is due to an extra symmetry, *e.g.* $CS(a = (0, 0, 0, 0)) = CS(a = (1, -1, 0, -1))$. The corresponding rows of $S^{(A)}$ also enjoy the same symmetry. Therefore, the asymptotic expansions around these two abelian flat connections must be identical. Indeed, Table 3.3 explicitly shows several identical transseries.

In order to understand the origin of center symmetry and to remove the degeneracy from $S^{(A)}$, we first study its action on the holonomy representations. Then, we match the false theta functions with the "folded" version of the data (3.92)–(3.94), which are obtained by modding out the center symmetry.

CS action	stabilizer	type	transseries
0	$SU(2)$	central	$e^{2\pi i k\cdot 0}\left(\frac{\pi i}{4\sqrt{2}}k^{-3/2}+\frac{7\pi^2}{96\sqrt{2}}k^{-5/2}+O(k^{-7/2})\right)$
0	$SU(2)$	central	$e^{2\pi i k\cdot 0}\left(\frac{\pi i}{4\sqrt{2}}k^{-3/2}+\frac{7\pi^2}{96\sqrt{2}}k^{-5/2}+O(k^{-7/2})\right)$
$\frac{7}{8}$	$U(1)$	abelian	$e^{2\pi i k\frac{7}{8}}\left(-\sqrt{2}k^{-1/2}+\frac{2\sqrt{2}\pi i}{3}k^{-3/2}+O(k^{-5/2})\right)$
$\frac{7}{8}$	$U(1)$	abelian	$e^{2\pi i k\frac{7}{8}}\left(-\sqrt{2}k^{-1/2}+\frac{2\sqrt{2}\pi i}{3}k^{-3/2}+O(k^{-5/2})\right)$
$\frac{1}{2}$	$U(1)$	abelian	$e^{2\pi i k\frac{1}{2}}\left(-\frac{2\sqrt{2}}{3}k^{-1/2}-\frac{11\pi i}{54\sqrt{2}}k^{-3/2}+O(k^{-5/2})\right)$
$-\frac{4}{24}$	± 1	non-abelian, real	$e^{-2\pi i k\frac{4}{24}}e^{\frac{3\pi i}{4}}2\sqrt{2}$

Table 3.3: Transseries for $M(-2;\frac{1}{2},\frac{1}{3},\frac{1}{2})$.

The fundamental group of a Seifert manifold $M_3 = M(b,\{q_i/p_i\}_{i=1}^n)$ is given by

$$\pi_1(M_3) = \langle x_1, x_2, x_3, h \mid h \text{ central},\ x_i^{p_i} = h^{-q_i},\ x_1x_2x_3 = h^b\rangle. \tag{3.105}$$

We can classify $SU(2)$ flat connections by the $SU(2)$ representations of the fundamental group into $SU(2)$:

$$\rho : \big(\pi_1(M_3) \longrightarrow SU(2)\big)/\mathcal{G}. \tag{3.106}$$

Concretely, we can characterize such representations by the images of $\pi_1(M_3)$ generators. In the present example,

$$\begin{aligned}\rho(x_i) &= g_i\begin{pmatrix} e(\lambda_i) & 0\\ 0 & e(-\lambda_i)\end{pmatrix}g_i^{-1},\quad i=1,2,3\\ \rho(h) &= \begin{pmatrix} e(\lambda) & 0\\ 0 & e(-\lambda)\end{pmatrix}\end{aligned} \tag{3.107}$$

where g_i's represent arbitrary gauge transformations compatible with the group structure of $\pi_1(M_3)$. The Weyl group acts on each $\rho(x_i)$ via conjugation by $\left(\begin{smallmatrix}0 & -1\\ 1 & 0\end{smallmatrix}\right)$, hence $\lambda_i \leftrightarrow -\lambda_i$. Table 3.4 shows holonomy variables $(\lambda,\lambda_1,\lambda_2,\lambda_3)$ which classify the group homomorphisms ρ and their Chern-Simons invariants computed as in [10].

Apart from the Weyl group, we conjecture an outer automorphism acting on the moduli space, which permutes different components of the moduli space. In terms of the holonomy angles λ_i, it acts by

$$(\lambda,\lambda_1,\lambda_2,\lambda_3) = (\lambda,\lambda_1+\tfrac{1}{2},\lambda_2,\lambda_3+\tfrac{1}{2}). \tag{3.108}$$

CS invariant	type	$(,_1,_2,_3)$	center symmetry
0	abelian	$(0,0,0,0)$	$(0,0,0,0) \mapsto (0,\frac{1}{2},0,\frac{1}{2})$
0	abelian	$(0,\frac{1}{2},0,\frac{1}{2})$	$(0,\frac{1}{2},0,\frac{1}{2}) \mapsto (0,0,0,0)$
$\frac{1}{2}$	abelian	$(\frac{1}{2},\frac{1}{4},\frac{1}{2},\frac{1}{4})$	$(\frac{1}{2},\frac{1}{4},\frac{1}{2},\frac{1}{4}) \mapsto (\frac{1}{2},\frac{1}{4},\frac{1}{2},\frac{1}{4})$
$\frac{7}{8}$	abelian	$(\frac{1}{4},\frac{5}{8},\frac{1}{4},\frac{1}{8})$	$(\frac{1}{4},\frac{5}{8},\frac{1}{4},\frac{1}{8}) \mapsto (\frac{1}{4},\frac{1}{8},\frac{1}{4},\frac{5}{8})$
$\frac{7}{8}$	abelian	$(\frac{1}{4},\frac{1}{8},\frac{1}{4},\frac{5}{8})$	$(\frac{1}{4},\frac{1}{8},\frac{1}{4},\frac{5}{8}) \mapsto (\frac{1}{4},\frac{5}{8},\frac{1}{4},\frac{1}{8})$
$-\frac{4}{24}$	non-abelian	$(\frac{1}{2},\frac{1}{4},\frac{1}{6},\frac{1}{4})$	$(\frac{1}{2},\frac{1}{4},\frac{1}{6},\frac{1}{4}) \mapsto (\frac{1}{2},\frac{1}{4},\frac{1}{6},\frac{1}{4})$

Table 3.4: Holonomy variables and Chern-Simons invariants of $SU(2)$ flat connections on $M(-2;\frac{1}{2},\frac{1}{3},\frac{1}{2})$, along with the action of center symmetry on them.

For instance, this maps one abelian flat connection to another as

$$\left(\tfrac{1}{4},\tfrac{1}{8},\tfrac{1}{4},\tfrac{5}{8}\right) + \left(0,\tfrac{1}{2},0,\tfrac{1}{2}\right) \sim \left(\tfrac{1}{4},\tfrac{5}{8},\tfrac{1}{4},\tfrac{1}{8}\right), \tag{3.109}$$

where we have taken the action of the Weyl group into account. The orbits of center symmetry are shown in Table 3.4.

We claim that the outer automorphism acts on the entire moduli space of all connections. First, the center symmetry can be easily identified from the data of the abelian flat connections Equation (3.92)–(3.94). One observes degenerate values of $CS(a)$ and rows of $S^{(A)}$ *e.g.*, for $a = (0,0,0,0)$ and $a = (1,-1,0,-1)$. As a result, not only the values $CS(a)$, but also the perturbative expansions around $a = (0,0,0,0)$ and $a = (1,-1,0,-1)$ are identical. As the two transseries are identical, we claim that the center symmetry is a symmetry of the moduli space.

Next, let us identify flat connections related by the center symmetry. The data of

the abelian flat connections become:

$$\mathrm{CS}(a) = \begin{cases} 0 & \mod \mathbb{Z} \quad \text{for} \quad a = (0,0,0,0) \sim (1,-1,0,-1) \\ \frac{7}{8} & \mod \mathbb{Z} \quad \text{for} \quad a = (0,-1,0,0) \sim (0,0,0,-1) \\ \frac{1}{2} & \mod \mathbb{Z} \quad \text{for} \quad a = (0,0,-1,0) \end{cases}$$

$$S^{(A)} = \frac{1}{\sqrt{2}} \begin{pmatrix} 2 & 2 & 1 \\ 4 & 0 & -2 \\ 2 & -2 & 1 \end{pmatrix} \tag{3.110}$$

$$\widehat{Z}_0(q) = \widehat{Z}_{(3,-1,-5,-3)}(q) + \widehat{Z}_{(3,-3,-5,-1)}(q) = -q^{-5/12}\Psi_2^{6+2}(\tau)$$
$$\widehat{Z}_1(q) = \widehat{Z}_{(1,-1,-1,-1)}(q) + \widehat{Z}_{(3,-3,-1,-3)}(q) = 2q^{-5/12}(1 - \Psi_1^{6+2}(\tau))$$
$$\widehat{Z}_2(q) = \widehat{Z}_{(1,-3,-1,-1)}(q) = q^{-5/12}\Psi_4^{6+2}(\tau).$$

After modding out the center symmetry, $S^{(A)}$ is non-degenerate and, furthermore, vectors of the irrep $6+2$ are in 1-1 correspondence with the "folded" homological blocks. Therefore, we may conclude that the modularity dictionary can be utilized without ambiguity *after* we mod out by the center symmetry.

Example: $M(-1; \frac{1}{2}, \frac{1}{3}, \frac{1}{10})$

We present another example with the center symmetry. The example shows that it is *necessary* to mod out the center symmetry in order to find an appropriate Weil representation $m + K$.

CS invariant	type	holonomy angles	center symmetry
0	abelian	$(0,0,0,0)$	$(0,0,0,0) \mapsto (0,\frac{1}{2},0,\frac{1}{2})$
0	abelian	$(0,\frac{1}{2},0,\frac{1}{2})$	$(0,\frac{1}{2},0,\frac{1}{2}) \mapsto (0,0,0,0)$
$\frac{1}{4}$	abelian	$(\frac{1}{2},\frac{1}{4},\frac{1}{2},\frac{1}{4})$	$(\frac{1}{2},\frac{1}{4},\frac{1}{2},\frac{1}{4}) \mapsto (\frac{1}{2},\frac{1}{4},\frac{1}{2},\frac{1}{4})$
$-\frac{25}{60}$	non-abelian	$(\frac{1}{2},\frac{1}{4},\frac{1}{6},\frac{1}{4})$	$(\frac{1}{2},\frac{1}{4},\frac{1}{6},\frac{1}{4}) \mapsto (\frac{1}{2},\frac{1}{4},\frac{1}{6},\frac{1}{4})$
$-\frac{49}{60}$	non-abelian	$(\frac{1}{2},\frac{1}{4},\frac{1}{6},\frac{3}{20})$	$(\frac{1}{2},\frac{1}{4},\frac{1}{6},\frac{3}{20}) \mapsto (\frac{1}{2},\frac{1}{4},\frac{1}{6},\frac{7}{20})$
$-\frac{49}{60}$	non-abelian	$(\frac{1}{2},\frac{1}{4},\frac{1}{6},\frac{7}{20})$	$(\frac{1}{2},\frac{1}{4},\frac{1}{6},\frac{7}{20}) \mapsto (\frac{1}{2},\frac{1}{4},\frac{1}{6},\frac{3}{20})$

Table 3.5: Holonomy angles and Chern-Simons invariants of $SU(2)$ flat connections on $M(-1; \frac{1}{2}, \frac{1}{3}, \frac{1}{10})$, along with the action of center symmetry.

As before, we characterize flat connections by holonomy angles λ. The angles and their Chern-Simons invariants are summarized in Table 3.5. The center symmetry

acts by

$$(\lambda, \lambda_1, \lambda_2, \lambda_3) \ \mapsto \ (\lambda, \lambda_1 + \tfrac{1}{2}, \lambda_2, \lambda_3 + \tfrac{1}{2}).$$

The manifold of interest has $\mathrm{Tor}H_1(M_3) = \mathbb{Z}_4$ with the following plumbing graph:

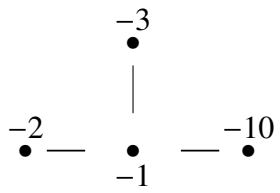

(3.111)

From its adjacency matrix, we can compute:

$$a \in \mathrm{Coker}M/\mathbb{Z}_2 = \langle (0,0,0,0), (1,-1,0,-5), (1,0,-1,-7) \rangle$$
$$b \in (2\mathrm{Coker}M + \delta)/\mathbb{Z}_2 = \langle (1,-1,-1,-1), (3,-3,-1,-11), (3,-1,-3,-15) \rangle$$

$$\mathrm{CS}(a) = -(a, M^{-1}a) = \begin{cases} 0 \mod \mathbb{Z} & \text{for} \quad a = (0,0,0,0), (1,-1,0,-5) \\ \frac{1}{4} \mod \mathbb{Z} & \text{for} \quad (1,0,-1,-7) \end{cases} \tag{3.112}$$

$$S^{(A)} = \frac{1}{2}\begin{pmatrix} 1 & 1 & 1 \\ 1 & 1 & 1 \\ 2 & 2 & -2 \end{pmatrix} \tag{3.113}$$

$$\widehat{Z}_{(1,-1,-1,-1)}(q) = q^{5/4}(1 + q^6 - q^{28} + q^{62} + \cdots) \tag{3.114}$$

$$\widehat{Z}_{(3,-3,-1,-11)}(q) = q^{13/4}(-1 - q^{12} + q^{14} + q^{38} - q^{82} + \cdots) \tag{3.115}$$

$$\widehat{Z}_{(3,-1,-3,-15)}(q) = -q^{3/2}(1 - q^3 + q^4 - q^{11} + q^{19} - q^{32} - q^{52} + \cdots). \tag{3.116}$$

"Folding" the center symmetry. Unlike what happens in the previous example, here the homological blocks (3.114)–(3.116) do not correspond to any level 30 false theta function (although they do correspond to certain level 60 false theta functions). Furthermore, while Equation (3.62) dictates:

$$4m = \text{l.c.m.}(8, 12, 40, 1, 4) = 120 \ \Rightarrow \ m = 30, \tag{3.117}$$

Equation (3.60) gives $m = 15$. Such an ambiguity can be resolved by modding out the center symmetry.

First, note that the center symmetry is manifest in Equations (3.112)–(3.116): the values $\mathrm{CS}(a)$ are equal for $a = (0,0,0,0)$ and $a = (1,-1,0,-5)$, and the corresponding rows of $S^{(A)}$ are identical. As a result, the asymptotic expansions around

$a = (0,0,0,0)$ and $a = (1,-1,0,-5)$ must be identical, indicating the presence of center symmetry.

Next, we mod out the center symmetry:

$$\mathrm{CS}(a) = \begin{cases} 0 & \mod \quad \mathbb{Z} \quad \text{for} \quad a = (0,0,0,0) \sim (1,-1,0,-5) \\ \frac{1}{4} & \mod \quad \mathbb{Z} \quad \text{for} \quad a = (1,0,-1,-7) \end{cases}$$

$$S^{(A)} = \begin{pmatrix} 1 & 1 \\ 1 & -1 \end{pmatrix}$$

$$\begin{aligned} \widehat{Z}_0(q) &= \widehat{Z}_{(1,-1,-1,-1)}(q) + \widehat{Z}_{(3,-3,-1,-11)}(q) = q^{5/4}(1 - q^2 + q^6 - q^{14} + q^{16} + \cdots) \\ \widehat{Z}_1(q) &= \widehat{Z}_{(3,-1,-3,-15)}(q) = -q^{3/2}(1 - q^3 + q^4 - q^{11} + q^{19} - q^{32} - q^{52} + \cdots). \end{aligned} \tag{3.118}$$

As expected, $S^{(A)}$ is non-degenerate. Furthermore, false theta functions from $m+K = 15+5$ perfectly match the "folded" $\widehat{Z}_b(M_3)$'s.

$$\begin{aligned} \sigma^{15+5} &= \{1,2,4,5,7,10\} \ \text{(irrep, genus 0)} \\ \widehat{Z}_0(q) &= q^{37/30}\Psi_1^{15+5}(\tau) \\ \widehat{Z}_1(q) &= -q^{37/30}\Psi_4^{15+5}(\tau)\,. \end{aligned} \tag{3.119}$$

This supports our proposal for applying the modularity dictionary *after* modding out the symmetries of the moduli space.

$S(M_3)$ and $T(M_3)$ matrices and asymptotic expansions.

$$\mathbf{Emb} = \begin{pmatrix} 1 & 0 & 0 & 0 & 0 & 0 \\ 0 & 0 & -1 & 0 & 0 & 0 \end{pmatrix}, \quad T^{(A)} = \exp\ 2\pi i \begin{pmatrix} 0 & 0 \\ 0 & \frac{1}{4} \end{pmatrix}$$

$$S^{(B)} = i \begin{pmatrix} 0.20 & -0.51 & -0.20 & -0.32 & -0.51 & -0.32 \\ -0.51 & -0.20 & -0.51 & -0.32 & 0.20 & 0.32 \\ -0.20 & -0.51 & -0.20 & 0.32 & 0.51 & -0.32 \\ -0.63 & -0.63 & 0.63 & 0.32 & -0.63 & 0.32 \\ -0.51 & 0.20 & 0.51 & -0.32 & 0.20 & -0.32 \\ -0.63 & 0.63 & -0.63 & 0.32 & -0.63 & -0.32 \end{pmatrix} \tag{3.120}$$

$$T^{(B)} = \exp\ 2\pi i \cdot \mathrm{diag}\left(\tfrac{1}{60}, \tfrac{4}{60}, \tfrac{16}{60}, \tfrac{25}{60}, \tfrac{49}{60}, \tfrac{100}{60}\right)$$

It follows that

$$\begin{aligned} S(M_3) &= i \begin{pmatrix} -0.39 & 0 & 0 & 0.63 & 1.02 & 0 \\ 0 & 1.02 & 0.39 & 0 & 0 & 0.63 \end{pmatrix} \\ T(M_3) &= \begin{pmatrix} e(-\frac{1}{60}) & e(-\frac{4}{60}) & e(-\frac{16}{60}) & e(-\frac{25}{60}) & e(-\frac{49}{60}) & e(-\frac{100}{60}) \\ e(-\frac{46}{60}) & e(-\frac{49}{60}) & e(-\frac{1}{60}) & e(-\frac{10}{60}) & e(-\frac{34}{60}) & e(-\frac{25}{60}) \end{pmatrix}, \end{aligned} \tag{3.121}$$

from which we conclude that the Chern-Simons invariants of non-abelian flat connections are $-\frac{1}{60}, -\frac{25}{60}, -\frac{49}{60}$. Since $\mathbf{c}_{-\frac{1}{60}}$ vanishes, we predict one complex flat connection with CS $= -\frac{1}{60}$. Of course, the complex flat connection may represent two complex connections identified under the folding procedure. We will rule out this possibility shortly, via comparison with A-polynomial analysis.

The other two non-abelian flat connections are real, with CS $= -\frac{25}{60}, -\frac{49}{60}$. The asymptotic expansions are computed and summarized in Table 3.6, where we have omitted the overall factor $-iq^{-37/30}/2\sqrt{2}$.

CS action	stabilizer	type	transseries
0	$SU(2)$	central	$e^{2\pi ik\cdot 0}\left(\pi i k^{-3/2} + \frac{283\pi^2}{60}k^{-5/2} + O(k^{-7/2})\right)$
$\frac{1}{4}$	$U(1)$	abelian	$e^{2\pi ik\frac{1}{4}}\left(\frac{4}{3}k^{-1/2} - \frac{49\pi i}{135}k^{-3/2} + O(k^{-5/2})\right)$
$-\frac{25}{60}$	± 1	non-abelian, real	$e^{-2\pi ik\frac{25}{60}}e^{\frac{3\pi i}{4}}\cdot\frac{1}{\sqrt{10}}$
$-\frac{49}{60}$	± 1	non-abelian, real	$e^{-2\pi ik\frac{49}{60}}e^{\frac{3\pi i}{4}}\cdot\frac{4\sqrt{2}}{\sqrt{15}}(\cos\frac{\pi}{30} + \sin\frac{2\pi}{15})$
$-\frac{1}{60}$	± 1	non-abelian, complex	0

Table 3.6: Transseries and classification of flat connections on $M(-1; \frac{1}{2}, \frac{1}{3}, \frac{1}{10})$, *after* modding out the center symmetry.

Note that Table 3.6 is obtained *after* modding out the center symmetry. In particular, the transseries of the "central" flat connection stands for the sum of two identical transseries related by the center symmetry. In order to recover the contribution from each of the two central flat connections, we must multiply the above answer by a factor of $\frac{1}{2}$.

Likewise, there are two real non-abelian flat connections identified by the center symmetry. As a check, we compute the Chern-Simons invariants from the holonomy variables [10]:

$$\begin{aligned}\mathrm{CS}[(\lambda,\lambda_i); M(b,\{q_i/p_i\}_{i=1}^n)] &= -\Big(\sum_{i=1}^{3} p_i r_i \lambda_i^2 - q_i s_i \frac{1}{2^2}\Big) \\ &= \begin{cases} -\frac{49}{60} & \text{for } (\lambda_1,\lambda_2,\lambda_3) = (\frac{1}{4},\frac{1}{6},\frac{3}{20}) \text{ and } (\frac{1}{4},\frac{1}{6},\frac{7}{20}) \\ -\frac{25}{60} & \text{for } (\lambda_1,\lambda_2,\lambda_3) = (\frac{1}{4},\frac{1}{6},\frac{5}{20}). \end{cases}\end{aligned} \tag{3.122}$$

In the first line, r_i and s_i are any integers satisfying $p_i s_i - q_i r_i = 1$. It follows that degenerate non-abelian flat connections have CS $= -\frac{49}{60}$. As a result, we predict that our manifold has

- one complex flat connection with CS $= -\frac{1}{60}$,
- two real non-abelian flat connections with CS $= -\frac{49}{60}$,
- one real non-abelian flat connection with CS $= -\frac{25}{60}$.

Comparison with A-polynomial. It remains to determine the number of complex flat connections. Since $M_3 = M(-1; \frac{1}{2}, \frac{1}{3}, \frac{1}{10})$ is a $-4/1$ surgery along the right-handed trefoil, we can utilize the A-polynomial analysis. Counting the intersection points of

$$A(x, y) = (y - 1)(yx^6 + 1) \quad \text{and} \quad s(x, y) = yx^{-4} - 1,$$

we find a total of *four* non-abelian flat connections, which agrees with their total number found in the previous section. Therefore, there is only one complex flat connection, and we can finalize the transseries as in Table 3.7. (Again, the overall factor $-iq^{-37/30}/2\sqrt{2}$ is omitted.)

CS action	stabilizer	type	transseries
0	$SU(2)$	central	$e^{2\pi i k \cdot 0}\left(\frac{\pi i}{2}k^{-3/2} + \frac{283\pi^2}{120}k^{-5/2} + O(k^{-7/2})\right)$
0	$SU(2)$	central	$e^{2\pi i k \cdot 0}\left(\frac{\pi i}{2}k^{-3/2} + \frac{283\pi^2}{120}k^{-5/2} + O(k^{-7/2})\right)$
$\frac{1}{4}$	$U(1)$	abelian	$e^{2\pi i k \frac{1}{4}}\left(\frac{4}{3}k^{-1/2} - \frac{49\pi i}{135}k^{-3/2} + O(k^{-5/2})\right)$
$-\frac{25}{60}$	± 1	non-abelian, real	$e^{-2\pi i k \frac{25}{60}} e^{\frac{3\pi i}{4}} \cdot \frac{1}{\sqrt{10}}$
$-\frac{49}{60}$	± 1	non-abelian, real	$e^{-2\pi i k \frac{49}{60}} e^{\frac{3\pi i}{4}} \cdot \frac{2\sqrt{2}}{\sqrt{15}}(\cos\frac{\pi}{30} + \sin\frac{2\pi}{15})$
$-\frac{49}{60}$	± 1	non-abelian, real	$e^{-2\pi i k \frac{49}{60}} e^{\frac{3\pi i}{4}} \cdot \frac{2\sqrt{2}}{\sqrt{15}}(\cos\frac{\pi}{30} + \sin\frac{2\pi}{15})$
$-\frac{1}{60}$	± 1	non-abelian, complex	0

Table 3.7: Transseries and classification of flat connections on $M(-1; \frac{1}{2}, \frac{1}{3}, \frac{1}{10})$.

Example: 3-singular fibered Brieskorn spheres

Let us extend our analysis to a specific class of 3-manifolds, the 3-singular fibered Brieskorn spheres:

$$\Sigma(p_1, p_2, p_3) := S^5 \cap \{(x, y, z) \in \mathbb{C}^3 \mid x^{p_1} + y^{p_2} + z^{p_3} = 0\}. \tag{3.123}$$

The manifolds are naturally labeled by a triple of relatively prime integers (p_1, p_2, p_3). As discussed in [119], one can easily translate to the Seifert data $M\left(-1; \frac{q_1}{p_1}, \frac{q_2}{p_2}, \frac{q_3}{p_3}\right)$, satisfying [5]

$$\frac{q_1}{p_1} + \frac{q_2}{p_2} + \frac{q_3}{p_3} = 1 - \frac{1}{p_1 p_2 p_3}. \tag{3.124}$$

We choose the standard choice of orientation, viewing Brieskorn spheres as boundaries of negative definite plumbings. False theta functions were observed in the WRT invariants of Brieskorn spheres in [87], building on [146]. Our goal in this section is to understand their Weil representations and to perform the resurgence analysis.

Weil representation $m + K$	$m = p_1p_2p_3$ and $K = \{1, p_1p_2, p_2p_3, p_1p_3\}$
q-series invariant $\widehat{Z}_0(q)$	Ψ_r^{m+K}, where $r = m - p_1p_2 - p_2p_3 - p_1p_3$
Number of (real and complex) non-abelian flat connections	$\lvert\sigma^{m+K}\rvert = \frac{1}{4}(p_1 - 1)(p_2 - 1)(p_3 - 1)$
CS invariants of (real or complex) non-abelian flat connections	$\text{CS} = -\frac{r^2}{4m}\ \forall\ r \in \sigma^{m+K}$
CS invariants of complex non-abelian flat connections	$\text{CS} = -\frac{r^2}{4m}\ s.t.\ \sum_{\ell=1}^{m-1} P_{\ell r}^{m+K}(1 - \frac{\ell}{m}) = 0$

Table 3.8: The modularity dictionary for Brieskorn spheres $\Sigma(p_1, p_2, p_3)$.

All Brieskorn spheres are integral homology spheres, so there is only one homological block $\widehat{Z}_0(q)$. The modularity dictionary therefore operates in a particularly simple way, as summarized in Table 3.8. Some of them also exhibit connection with quantum modularity via q-hypergeometric series (see [38] and [146] for further details.)

[5] This holds for all $\frac{1}{p_1} + \frac{1}{p_2} + \frac{1}{p_3} < 1$. There is only one exception, which is the Poincaré homology sphere $\Sigma(2, 3, 5)$ which has Seifert data $M(-2; \frac{1}{2}, \frac{2}{3}, \frac{4}{5})$.

Example: D-type manifolds

In this section, we consider a class of manifolds with the following plumbing graph:

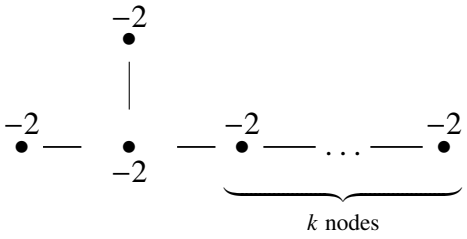

(3.125)

The plumbing graph is negative-definite and has a shape of a D_{k+3}, $k \geq 1$ Dynkin diagram. Its Seifert invariant is $M\left(-2; \frac{1}{2}, \frac{1}{2}, \frac{k}{k+1}\right)$. This manifold can also be represented as an intersection of a D_{k+3} singularity with a unit sphere in $\mathbb{C}^3$:

$$M\left(-2; \frac{1}{2}, \frac{1}{2}, \frac{k}{k+1}\right) := S^5 \cap \{(x, y, z) \in \mathbb{C}^3 \mid x^k + xy^2 + z^2 = 0\}. \tag{3.126}$$

Already in [90], false theta functions appeared in their WRT invariants. In this section, we study their Weil representations and perform resurgence analysis.

The relevant Weil representation is $m + K = k + 1$, with $m = k + 1$ and $K = \{1\}$ being the trivial group. Whenever m is a prime to some power ($m = p^N$), $m + K$ is an irrep. As we will see in Section 3.4, this includes optimal examples for $m = 2, 3, 4, 5, 6, 7, 8, 9, 10, 12, 13, 16, 18, 25$. Following the modularity dictionary, one can identify homological blocks with false theta functions, observe center symmetries, and perform modular transform / resurgence analysis to obtain transseries expansions. See [38] for the results.

Example: four-singular fibered Seifert manifolds

So far, we have restricted ourselves to the three-singular fibered Seifert manifolds and identified their homological blocks with false theta functions. In this section, we consider four-singular fibered Seifert manifolds and exhibit that their homological blocks consist of the Eichler integrals of weight-$1/2$ and weight-$3/2$ theta functions. We call such combinations the "building blocks" of homological blocks, defined as follows:

$$\begin{aligned} B_{m,r}(\tau) &\equiv \frac{1}{2m}\left[\Phi_{m,r}(\tau) - r\Psi_{m,r}(\tau)\right] \\ B_r^{m+K}(\tau) &= 2^{|K|-1} \sum_{r' \bmod 2m} P_{rr'}^{m+K} B_{m,r'}(\tau). \end{aligned} \tag{3.127}$$

By the end of this section, we provide a non-spherical example $M(-2; \frac{1}{2}, \frac{2}{3}, \frac{2}{5}, \frac{2}{5})$ and compute its asymptotic expansion.

The building blocks can be deduced from the examples of 4-singular fibered Brieskorn homology spheres [86, 89]. To delineate the procedure, we first consider the 3-singular fibered cases. As we have seen above, $Z_{CS}[\Sigma(p_1, p_2, p_3)]$ decompose into false theta functions. The projectors can also be expressed as [90, 91]:

$$Z_{CS}(\Sigma(p_1, p_2, p_3)) = \frac{q^{-\phi/4}}{i\sqrt{8k}}\Bigg[\sum_{r=1}^{m-1} \chi_{2m}^{(1,1,1)}(r)\Psi_{m,r}(\tau) + H\Big(-1 + \sum_{j=1}^{3}\frac{1}{p_j}\Big)q^{1/120}\Bigg], \tag{3.128}$$

where $m = \prod_j p_j$, and H is the Heaviside step-function. One can see that the false theta functions serve as the "building blocks" for the homological blocks, whose contributions are controlled by the projector $\chi_{2m}^{(1,1,1)}(r)$.

In general, we can define a $2m$-periodic projector $\chi_{2m}^{\vec{l}}(r)$ from an n-dimensional vector $\vec{l} = (l_1, \cdots, l_n)$ and $\vec{p} = (p_1, \cdots, p_n)$ such that $0 < l_j < p_j$:

$$\chi_{2m}^{\vec{l}}(r) = \begin{cases} -\prod_{j=1}^{n}\epsilon_j & \text{if } r \equiv m\Big(1 + \sum_j \frac{\epsilon_j l_j}{p_j}\Big) \bmod 2m, \text{ where } \epsilon_j = \pm 1 \\ 0 & \text{otherwise.} \end{cases}$$

For four-singularly fibered Seifert homology spheres $\Sigma(p_1, p_2, p_3, p_4)$, the quantity $Z_{CS}(M_3)$ can be expressed in terms of false theta functions and a weight $1/2$ Eichler integral [86, 89]. From the expressions, one can extract building blocks by pulling out $\chi_{2m}^{(p_1-1,1,1,1)}(r)$:

$$\begin{aligned} Z_{CS}(\Sigma(p_1, p_2, p_3, p_4)) = \\ \frac{q^{-\phi/4}}{i\sqrt{8k}}\Bigg[\sum_{r=1}^{m-1} \chi_{2m}^{(p_1-1,1,1,1)}(r)\frac{1}{2m}\Big(\Phi_{m,r}(\tau) - r\Psi_{m,r}(\tau)\Big) \\ + H\Big(-1 + \sum_j \frac{1}{p_j}\Big)\Psi_{m,(2m-\sum_j m/pj)}(\tau)\Bigg], \end{aligned} \tag{3.129}$$

where $\Phi_{m,r}(\tau)$ are the weight-$1/2$ Eichler integrals (3.28) of the weight 1/2 theta functions (cf. (3.27))

$$\theta_{m,r}^{0}(\tau) := \theta_{m,r}(\tau, z)|_{z=0} = \sum_{\substack{\ell\in\mathbb{Z} \\ \ell = r \bmod 2m}} q^{\ell^2/4m}.$$

Explicitly,

$$\Phi_{m,r}(\tau) = \sum_{n\geq 0} n\,\psi_{2m}^{\prime(r)}(n)q^{n^2/4m}, \quad \psi_{2m}^{\prime(r)}(n) = \begin{cases} 1 & \text{if } \quad n \equiv \pm r \mod 2m \\ 0 & \text{otherwise.} \end{cases} \tag{3.130}$$

In terms of projectors, $\psi'^{(r)}_{2m}(n) = 2(P^+_m(m))_{r,n}$. Observe the appearance of buliding blocks in Equation (3.129). While $\Psi_{m,r} = -\Psi_{m,-r}$, the building blocks satisfy $B_{m,r} = B_{m,-r}$. As a result, we must require $m \in K$.

The building blocks $B_{m,r}$ inherit their modular properties from $\Psi_{m,r}$ and $\Phi_{m,r}$:

$$\begin{aligned}
&\frac{1}{\sqrt{k}}\Psi_{m,r}(1/k) + \frac{1}{\sqrt{i}}\sum_{r'=1}^{m-1}\sqrt{\frac{2}{m}}\sin\frac{rr'\pi}{m}\Psi_{m,r'}(-k) = \sum_{n\geq 0}\frac{c_n}{n!}\left(\frac{\pi i}{2m}\right)^n k^{-n-\frac{1}{2}},\\
&\Psi_{m,r}(-k) = \left(1-\frac{r}{m}\right)e^{-2\pi i k r^2/4m}, \quad \text{where} \quad \frac{\sinh(m-r)z}{\sinh mz} = \sum_{n=0}^{\infty}\frac{c_n}{2n!}z^{2n}.
\end{aligned} \tag{3.131}$$

$$\begin{aligned}
&\frac{1}{\sqrt{k}}\Phi_{m,r}(1/k) + \frac{k}{\sqrt{i^3}}\sum_{r'=1}^{m-1}\sqrt{\frac{2}{m}}\frac{r'(m-r')}{m}\cos\frac{rr'\pi}{m}e^{-2\pi i k\frac{(r')^2}{4m}}\\
&\quad = \frac{mk}{\pi i}\sum_{n=0}^{\infty}\frac{c'_n}{n!}\left(\frac{\pi i}{2m}\right)^n k^{-n-\frac{1}{2}}, \quad \text{where} \quad \frac{\partial}{\partial r}\frac{\sinh(m-r)z}{\sinh mz} = \sum_{n=0}^{\infty}\frac{c'_n}{2n!}z^{2n}.
\end{aligned} \tag{3.132}$$

Later, we will explore the relation between the homological blocks of three-singular fibered Seifert manifolds and the characters of singlet $(1, p)$ logarithmic vertex algebras. The relation extends to the present case, where one can observe a close relation between characters of singlet (p_+, p_-) vertex algebras [3, 18].

Let us apply the modularity dictionary to a non-spherical example with four singular fibers. The subject manifold is $M(-2; \frac{1}{2}, \frac{2}{3}, \frac{2}{5}, \frac{2}{5})$ with the following plumbing graph:

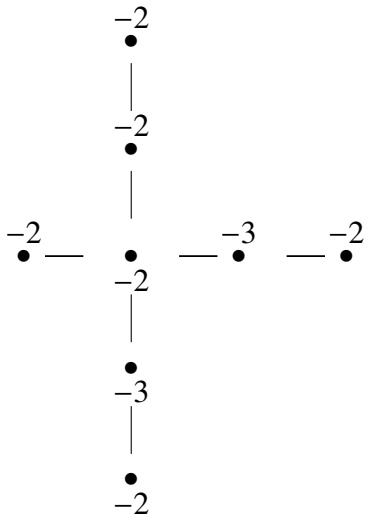

(3.133)

As before, we compute homological blocks and $S^{(A)}$:

$$\begin{gathered}\mathrm{CS}(a)=\begin{pmatrix}1 & \frac{1}{5} & \frac{9}{5}\end{pmatrix},\quad S^{(A)}=\frac{1}{\sqrt{5}}\begin{pmatrix}1 & 1 & 1\\ 2 & \frac{-1-\sqrt{5}}{2} & \frac{-1+\sqrt{5}}{2}\\ 2 & \frac{-1+\sqrt{5}}{2} & \frac{-1-\sqrt{5}}{2}\end{pmatrix},\\ \widehat{Z}_0(q)=q^{7/2}(1-q^{11}+q^{14}-q^{19}-q^{33}+q^{40}-q^{45}+2q^{53}+q^{74}+\cdots),\\ \widehat{Z}_1(q)=0,\\ \widehat{Z}_2(q)=2q^{93/10}(-1+q^{15}+q^{25}-q^{50}-2q^{65}+2q^{120}-2q^{165}-3q^{190}+\cdots).\end{gathered}\tag{3.134}$$

By the prescription of modularity dictionary, we can identify $m=30$ and $\sigma=30+5,6,30$. The relevant projector is (mark the projector $P^{-}_{30}(15)$ exhibiting the "Fricke" property):

$$\begin{aligned}P^{30+5,6,30}&=P^{+}_{30}(5)P^{+}_{30}(6)P^{-}_{30}(15),\\ B_7^{30+5,6,30}(\tau)&=\left(B_{30,7}-B_{30,13}+B_{30,17}-B_{30,23}\right)(\tau),\\ B_5^{30+5,6,30}(\tau)&=\left(B_{30,5}-B_{30,23}\right)(\tau).\end{aligned}\tag{3.135}$$

The homological blocks are now identified with the LHS:

$$\begin{aligned}\widehat{Z}_0(q)&=q^{-109/120}\left(\Psi_{30,23}(\tau)-B_7^{30+5,6,30}(\tau)\right)\\ \widehat{Z}_1(q)&=0\\ \widehat{Z}_2(q)&=2q^{-109/120}B_5^{30+5,6,30}(\tau).\end{aligned}\tag{3.136}$$

By Equations (3.131) and (3.132), we can compute the transseries summarized in Table 3.9. An overall factor of $-iq^{-109/120}/2\sqrt{2}$ is omitted as usual.

3.4 Quantum modularity of homological blocks

In this section, we explore the behavior of $\widehat{Z}_b(M_3)$ upon the orientation-reversal. Viewing it as a 3d-2d coupled index on a solid torus, it fits into the conjectured "factorization" property of 3d $\mathcal{N}=2$ SCFT index [84, 85]:

$$\begin{aligned}\mathcal{I}(q)&:=\mathrm{Tr}_{\mathcal{H}_{S^2}}(-1)^F q^{R/2+J_3}=Z_{T[M_3]}(S^2\times_q S^1)\\ &=\quad\text{(}\bar{\mathrm{A}}\text{ – twist)}\quad\text{(A – twist)}\quad=\sum_b|\mathcal{W}_b|\widehat{Z}_b(q)\widehat{Z}_b(q^{-1}).\end{aligned}\tag{3.137}$$

where $\mathcal{W}_b$ is the Weyl orbit of b. Physically, the RHS has the interpretation of gluing two 2d-3d coupled systems with $T[M_3]$ in the bulk, supported on two solid tori with opposite orientations [84]. Due to the opposite orientation, the two theories are related by a parity transform, in which the bulk 3d $\mathcal{N}=2$ theory $T[M_3]$ changes the

CS action	stabilizer	type	transseries
0	$SU(2)$	central	$e^{2\pi i k\cdot 0}\left(\frac{4\pi i}{5}k^{-3/2}+O(k^{-5/2})\right)$
$\frac{1}{5}$	$U(1)$	abelian	$e^{2\pi i k\frac{1}{5}}\left(\frac{5-\sqrt{5}}{6}k^{-1/2}+O(k^{-3/2})\right)$
$\frac{9}{5}$	$U(1)$	abelian	$e^{2\pi i k\frac{9}{5}}\left(\frac{5+\sqrt{5}}{6}k^{-1/2}+O(k^{-3/2})\right)$
$-\frac{1}{120}$	± 1	non-abelian, real	$e^{-2\pi i k\frac{1}{120}}\frac{e^{3\pi i/4}}{150\sqrt{15}}(-25+5\sqrt{5}+24\sqrt{3}\cos\frac{\pi}{10})$
$-\frac{4}{120}$	± 1	non-abelian, real	$-e^{-2\pi i k\frac{4}{120}}\frac{e^{3\pi i/4}}{4}(1+\sqrt{5})$
$-\frac{16}{120}$	± 1	non-abelian, real	$e^{-2\pi i k\frac{16}{120}}\frac{e^{3\pi i/4}}{4}(1-\sqrt{5})$
$-\frac{25}{120}$	± 1	non-abelian, real	$e^{-2\pi i k\frac{25}{120}}\frac{4e^{3\pi i/4}}{5}\sqrt{1-\frac{2}{\sqrt{5}}}$
$-\frac{40}{120}$	± 1	non-abelian, real	$e^{-2\pi i k\frac{40}{120}}e^{3\pi i/4}$
$-\frac{49}{120}$	± 1	non-abelian, real	$-e^{-2\pi i k\frac{49}{120}}\frac{e^{3\pi i/4}}{30\sqrt{15}}(25+5\sqrt{5}+24\sqrt{3}\cos\frac{3\pi}{10})$
$-\frac{73}{120}$	± 1	non-abelian, real	$-e^{-2\pi i k\frac{73}{120}}\frac{8e^{3\pi i/4}}{5\sqrt{5}}\cos\frac{3\pi}{10}$
$-\frac{76}{120}$	± 1	non-abelian, real	$e^{-2\pi i k\frac{76}{120}}\frac{e^{3\pi i/4}}{4}(1-\sqrt{5})$
$-\frac{81}{120}$	± 1	non-abelian, real	$e^{-2\pi i k\frac{81}{120}}\frac{e^{3\pi i/4}}{3\sqrt{3}}(1-\sqrt{5})$
$-\frac{97}{120}$	± 1	non-abelian, real	$e^{-2\pi i k\frac{97}{120}}\frac{8e^{3\pi i/4}}{5\sqrt{5}}\cos\frac{\pi}{10}$
$-\frac{105}{120}$	± 1	non-abelian, real	$e^{-2\pi i k\frac{105}{120}}\frac{4e^{3\pi i/4}}{3\sqrt{3}}$
$-\frac{9}{120}$	± 1	non-abelian, complex	0
$-\frac{64}{120}$	± 1	non-abelian, complex	0
$-\frac{100}{120}$	± 1	non-abelian, complex	0

Table 3.9: Transseries and classification of flat connections on $M(-2;\frac{1}{2},\frac{2}{3},\frac{2}{5},\frac{2}{5})$.

signs of all Chern-Simons terms. For the boundary 2d $\mathcal{N}=(0,2)$ theory, the parity transform acts as follows:

$$\text{parity}: \quad \mathcal{B}_a \;\mapsto\; \widetilde{\mathcal{B}}_a. \tag{3.138}$$

Let us denote resultant half-indices (which are q-series) as $\widehat{Z}_b(q)$ and $\widehat{Z}_b(q^{-1})$ for reasons to become clear.

From the vantage point of 3d-3d correspondence, the parity transform of $T[M_3]$ is equivalent to the orientation reversal of M_3, $M_3 \leftrightarrow -M_3$. As we will discuss shortly, $\widehat{Z}_b(-M_3)$ is related to $\widehat{Z}_b(M_3)$ by a change of variable, $q \leftrightarrow q^{-1}$. Therefore, we observe a non-trivial equality between q^{-1}-series and q-series, which can be

interpreted as extending the definition of $\widehat{Z}_b(q)$ across the unit circle $|q| = 1$:

$$\widehat{Z}_b(-M_3, q^{-1}) \overset{\text{re-expand}}{=\!=} \widehat{Z}_b(M_3, q). \tag{3.139}$$

One may understand the above equality from the exact Chern-Simons partition function, presented in the form of Equation (3.6). Under the "CP" transform $(M_3, k) \leftrightarrow -(M_3, k)$, the combination $2\pi i k CS[a]$ remains invariant because $C : k \leftrightarrow -k$ and $P : CS[a] \leftrightarrow -CS[a]$. On the other hand, $\widehat{Z}_b$ is also invariant, because $C : q \leftrightarrow q^{-1}$ and $P : M \leftrightarrow -M$.

The parity transform was also studied in the context of perturbative Chern-Simons theory with gauge group $G_{\mathbb{C}}$ [52]. Besides the path integral presentation of the *quantum* Chern-Simons partition function (k is quantum corrected) which is manifestly invariant under the CP transform, one observes that the phase space is also CP-invariant. In particular, it preserves the symplectic form given by variations around the flat connections α. As a result, the parity transform relates $Z^{(\alpha)}_{\text{pert}}(M_3, \hbar) = Z^{(\alpha)}_{\text{pert}}(-M_3, -\hbar)$, where

$$Z^{(\alpha)}_{\text{pert}}(M_3, \hbar) \;=\; \sum_n a_n \hbar^n, \quad q \;=\; e^{\hbar} \tag{3.140}$$

and

$$Z^{(\alpha)}_{\text{pert}}(-M_3, \hbar) \;=\; \sum_n (-1)^n a_n \hbar^n. \tag{3.141}$$

Therefore, the extension problem can be cast into the subject of resurgence analysis of Equation (3.141) with respect to $\hbar$. However, when Equation (3.140) admits a relatively simple Borel resummation (*e.g.*, the asymptotic expansion of false theta functions), the Borel resummation of its parity dual can be much more complicated [116]. In this sense, the convergence criteria of homological blocks play an important role to determine on which side of the τ-plane one can perform the simpler Borel resummation.

The above observation suggests that $\widehat{Z}_b(q)$ and $\widehat{Z}_b(q^{-1})$ may look completely different, even when they asymptotically agree on the unit circle. To be more precise for the $SU(2)$ Chern-Simons partition function, it is only required that they agree on the rational points of the unit circle, which is precisely the statement of *quantum modularity* introduced by Zagier [145]. Indeed, we will soon study the extension problem of $\widehat{Z}_b(q)$'s when they are false theta functions, which naturally fits into the study of (mock) modular objects by Rademacher [126] and his followers. Accordingly, we propose that $\widehat{Z}_b(M_3)$'s from three-singular fibered Seifert manifolds form

mock-false pairs with $\widehat{Z}_b(-M_3)$'s. The latter are mock modular forms with shadows that we will shortly discuss.

False theta functions and q-hypergeometric series

Before proceeding to the general proposal, let us consider some special cases of homological blocks. They are special in a sense that the associated false theta functions admit expressions as q-hypergeometric series which converges for *both* $|q| < 1$ and $|q| > 1$. Across the unit disk $|q| = 1$, one observes Ramanujan's famous mock theta functions. However, the extension procedure naturally involves certain ambiguities which we will dicuss in the end of this section.

In (3.96), we have observed (recall that $q = e^{2\pi i\tau}$):

$$\begin{aligned}\widehat{Z}_{(1,-1,-1,-1)}(q) &= q^{-5/12}(2q^{1/24} - \Psi_1^{6+2}(\tau))\\ \widehat{Z}_{(3,-3,-1,-3)}(q) &= -q^{-5/12}\Psi_1^{6+2}(\tau)\end{aligned} \tag{3.142}$$

for the Seifert manifold $M(-2; \frac{1}{2}, \frac{1}{3}, \frac{1}{2})$.

The false theta function can be written in terms of *q-Pochhammer symbols* for $|q| < 1$ (or equivalently, when τ lies in the upper half-plane $\mathbb{H}$) [20]:

$$\Psi_1^{6+2}(\tau) = \psi_1^{6+2}(q), \quad \psi_1^{6+2}(q) = \frac{q^{\frac{1}{24}}}{2}\left(1 - \sum_{n\geq 1}\frac{(-1)^n q^{\frac{n(n-1)}{2}}}{(-q;q)_n}\right), \tag{3.143}$$

where $(a;x)_n := \prod_{k=0}^{n-1}(1 - ax^k)$. In this form, the false theta function naturally has an interpretation as a q-hypergeometric series due to the following property of q-Pochhammer symbols:

$$(a;q^{-1})_n = (-1)^n a^n q^{-\frac{n(n-1)}{2}}(a^{-1};q)_n. \tag{3.144}$$

Due to Equation (3.144), it is easy to see that ψ_1^{6+2} converges for both $|q| > 1$ and $|q| < 1$:

$$\psi_1^{6+2}(q^{-1}) = \frac{q^{-\frac{1}{24}}}{2}\left(1 - \sum_{n\geq 1}\frac{(-1)^n q^n}{(-q;q)_n}\right). \tag{3.145}$$

It turns out that the RHS is a mock modular form, related to the celebrated order three mock theta function $f(q)$:

$$2q^{\frac{1}{24}}\psi_1^{6+2}(q^{-1}) = f(q) = 1 + q - 2q^2 + 3q^3 + O(q^4). \tag{3.146}$$

Following the previous discussions, we proposed $f(q)$ as a homological block of $-M_3$. In Section 3.4, we show that it belongs to a family of special vector-valued mock modular forms $h^{m+K} = (h_r^{m+K})$. For more examples, see [38].

The ambiguity. This example also illustrates the intrinsic ambiguity in the q-hypergeometric approach. Consider the following two q-hypergeometric series

$$\begin{aligned}\psi'(q) &= \frac{q^{1/24}}{2}\left(1+\sum_{n\geq 1}\frac{q^n}{(-q;q)_n^2}\right)\\ \psi''(q) &= q^{1/24}\sum_{n\geq 0}\frac{q^n}{(-q^2;q^2)_n},\end{aligned} \tag{3.147}$$

which are defined both inside and outside the unit disk. It turns out that they are related to $\psi_1^{6+2}(q)$ for $|q|<1$ via:

$$\begin{aligned}\psi_1^{6+2}(q) &= \psi'(q)+\frac{1}{2}S(\tau) = \psi''(q)\\ \psi_1^{6+2}(q^{-1}) &= \psi'(q^{-1}) = \psi''(q^{-1})-\frac{1}{2}T(\tau+1/2)\end{aligned} \tag{3.148}$$

$$\text{where}\quad S(\tau) := \frac{1}{\eta^2(\tau)}\Psi_{2,1}(\tau),\quad T(\tau) := \frac{\eta^7(2\tau)}{\eta^3(\tau)\eta^3(4\tau)}. \tag{3.149}$$

Observe that the two q-hypergeometric series coincide in the upper half-plane, but they extend to two different functions in the lower half-plane. Such an ambiguity is commonly found. See for instance [61] where the Rogers-Fine false theta functions give rise to mock forms which differ from those which are obtained from the machineries described in Section 3.4-3.4.

False, mock, and quantum

So far, we have observed the appearances of false theta functions from homological blocks, and mock theta functions upon their extensions to the other side of the τ-plane. The relation can be understood from the viewpoint of quantum modular forms [145] (see also Ch 21 of [22] for a recent account.) In this section, we propose the (strong) quantum modularity of the false and mock theta functions which appear as homological blocks.

Let us first recall the definition [145]: A function $Q:\mathbb{Q}\to\mathbb{C}$ is a *quantum modular form* of weight k and multiplier χ on Γ, if the "period function"

$$p_\gamma : \mathbb{Q}\backslash\{\gamma^{-1}(\infty)\}\to\mathbb{C},\quad p_\gamma(x) := Q(x)-\left(Q|_{k,\chi}\gamma\right)(x) \tag{3.150}$$

has some property of continuity or analyticity $\forall\gamma\in\Gamma$.[6]

[6] In our examples, $\Gamma = SL(2,\mathbb{Z})$ or $\Gamma_0(N)$, the Hecke congruence subgroup of level N. The latter is defined by $\Gamma_0(N) = \left\{\left(\begin{smallmatrix}a & b\\ c & d\end{smallmatrix}\right)\in SL(2,\mathbb{Z}) \mid c\equiv 0 \bmod N\right\}$.

In the above, we have used the "slash operator" for weight k and multiplier χ on Γ, acting on the space of holomorphic functions on the upper half-plane:

$$\left(f|_{k,\chi}\gamma\right)(\tau) := f\left(\frac{a\tau+b}{c\tau+d}\right)\chi(\gamma)(c\tau+d)^{-k}, \quad \gamma = \left(\begin{smallmatrix} a & b \\ c & d \end{smallmatrix}\right) \in \Gamma. \tag{3.151}$$

Moreover, Q is said to be a *strong quantum modular form* if it has images in formal power series (say, $\in \mathbb{C}[[\epsilon]]$) instead of complex numbers. Then it is often convenient to denote it by $Q(x+i\epsilon)$. Accordingly, Equation (3.150) is interpreted as an identity between countable collections of formal power series.

Example: Eichler integrals. The holomorphic Eichler integrals (Equation (3.28)) are examples of quantum modular forms. Consider a weight w cusp form g with multiplier χ. Its non-holomorphic Eichler integral is given by:

$$\tilde{g}^* : \mathbb{H}^- \to \mathbb{C}, \quad \tilde{g}^*(z) := C\int_{\bar{z}}^{i\infty} g(z')(z'-z)^{w-2}dz'. \tag{3.152}$$

The constant C is the same as in Equation (3.28). For our purposes, it suffices to consider the cusp forms with real coefficients, *i.e.* $\overline{g(-\bar{\tau})} = g(\tau)$. In [19, 146] it was shown that holomorphic / non-holomorphic Eichler integrals agree around all $x \in \mathbb{Q}$ order-by-order (see Figure 3.7):

$$\tilde{g}(x+it) \sim \sum_{n\geq 0}\alpha_n t^n, \quad \tilde{g}^*(x-it) \sim \sum_{n\geq 0}\alpha_n(-t)^n, \quad t>0. \tag{3.153}$$

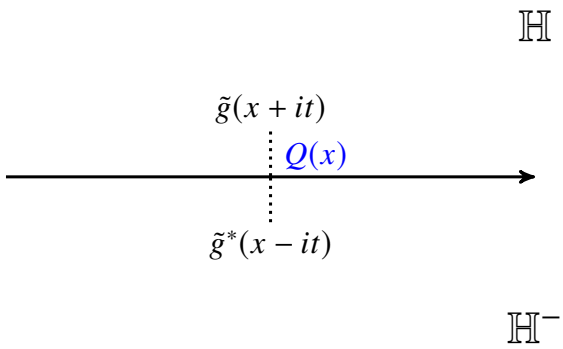

Figure 3.7: The upper and lower half-planes and quantum modular forms.

Furthermore, $\tilde{g}^*$ is nearly modular of weight $2-w$ in $\mathbb{H}^-$, and the discrepancy is precisely the period function:

$$\tilde{g}^*(z) - \left(\tilde{g}^*|_{2-w,\chi}\gamma\right)(z) = C\int_{\gamma^{-1}(i\infty)}^{i\infty} g(z')(z'-z)^{w-2}dw. \tag{3.154}$$

Therefore, the holomorphic Eichler integral $\tilde{g}$ is a quantum modular form of weight $2-w$, multiplier system χ, and the period function:

$$p_\gamma(x) = C \int_{\gamma^{-1}(i\infty)}^{i\infty} g(z')(z'-x)^{w-2} dw. \tag{3.155}$$

The quantum modularity is reflected in the analyticity of p_γ: it is smooth on $\mathbb{R} \setminus \{\gamma^{-1}(i\infty)\}$, and it has an analytic extension (see Lemma 3.3 in [39].)

In particular, the false theta functions $\Psi_{m,r}$ are quantum modular forms of weight 1/2, associated to the cusp form $\theta^1_{m,r}$. In association with topological invariants, it shows the quantum modularity of homological blocks. We now proceed to study the behavior on the other side of the plane.

Mock modular forms. Let us recall the definition of *mock modular forms* [148]:[7] A holomorphic function $f : \mathbb{H} \to \mathbb{C}$ is a *mock modular form* of weight k and multiplier χ on Γ, if and only if there is a weight $(2-k)$ cusp form g on Γ such that:

$$\forall \gamma \in \Gamma, \quad \hat{f} = \hat{f}|_{k,\chi}\gamma \quad \text{(the non-holomorphic completion of } f\text{)},$$
$$\text{where} \quad \begin{cases} \hat{f}(\tau) := f(\tau) - g^*(\tau), \\ g^*(\tau) := C \int_{-\bar{\tau}}^{i\infty} (\tau'+\tau)^{-k} \overline{g(-\bar{\tau}')}\, d\tau'. \end{cases} \tag{3.156}$$

Note the normalization ambiguity in the shadow $g^*(\tau)$. We will choose a normalization which is suitable for comparing mock modular forms and Eichler integrals. The *shadow map* is defined by $\xi : f \mapsto g$.

Mock modular forms give rise to quantum modular forms, in a way that is closely related to the case of Eichler integrals [39]. Suppose a group Γ has t inequivalent cusps, $\{q_1, \ldots, q_t\} \subset \mathbb{Q} \cup \{i\infty\}$. Then, we can "carve out" the singularities of f by subtracting a collection $\{G_j\}_{j=1}^t$ of weakly holomorphic modular forms. In other words, the *modular subtractions* $\{G_j\}_{j=1}^t$ can be chosen such that $f - G_j$ is bounded near the cusps equivalent to q_j. Beyond the boundedness, we have the following non-trivial equality among asymptotic series:

$$(f - G_x)(x+it) \sim \sum_{n\geq 0} \beta_n t^n, \quad \text{and} \quad g^*(x+it) \sim \sum_{n\geq 0} \beta_n t^n. \tag{3.157}$$

Given a mock modular form f and the *modular subtractions* $\{G_j\}_{j=1}^t$, therefore, one can define:

$$Q_f : \mathbb{Q} \to \mathbb{C}, \quad Q_f(x) := \lim_{t\to 0^+} (f - G_x)(x+it), \tag{3.158}$$

[7] The definition identifies holomorphic part of certain harmonic Maass forms with mock modular forms, and the non-holomorphic part (a modular form itself) as *shadows*. For our purposes, we restrict ourselves to the mock modular forms whose shadows are cusp forms.

where $G_x = G_j$ when $x \sim q_j$ under the Γ-action. Then, Q_f is a (strong) quantum modular form, because of (1) the equality (3.157), (2) the analyticity (3.155) of the period function associated to $\tilde{g}^*$, (3) the fact that $g^*(\tau) = \tilde{g}^*(-\tau)$, and (4) the reality condition $\overline{g(-\bar{\tau})} = g(\tau)$ imposed for our examples.

It is important to remark that the choice of $\{G_j\}_{j=1}^t$ is *not unique*, but at present, we do not know how to classify all possible choices. Nevertheless, the limiting values and the asymptotic series are independent of the choices.

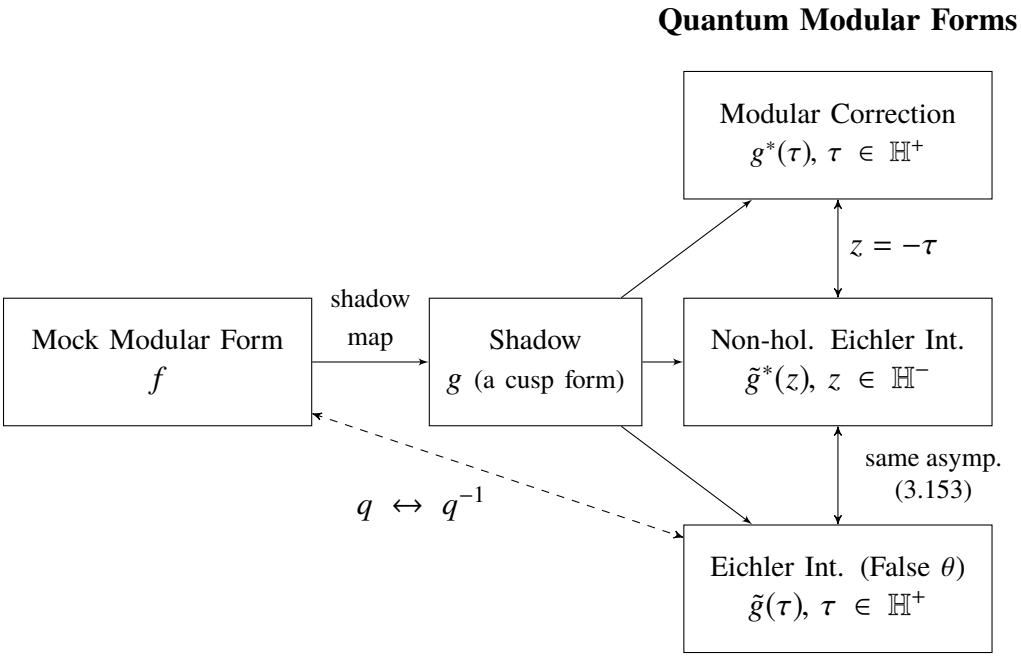

Figure 3.8: Relations among different modular objects with weight k, multiplier χ, and the group Γ. The dashed line denotes that the relation is not 1-1 in both directions.

We have therefore observed that the mock modular form f and the Eichler integrals of its shadow g have the same asymptotic series at the cusps, although they belong to two different sides of the plane. We summarize the extension procedure in Figure 3.8.

Lastly, let us comment that such a "leaking" behavior is precisely what we have expected from the topological invariants, upon $k \leftrightarrow -k$. Also, since homological blocks are labeled by vectors of Weil representations, we need a vector-valued version of the above discussions, for $\Gamma = SL(2, \mathbb{Z})$. This is left for future works.

Rademacher sums

Besides the q-hypergeometric approach and quantum modularity, there is yet another systematic way to connect mock-false pairs: the method of Rademacher sums. By adding up all modular transforms (with weight k and multiplier χ) of a given τ-dependent quantity, one can obtain a modular form. When $k \leq 2$, however, the sum diverges, and one must regularize it. The Rademacher sum precisely does this job by introducing a regularization factor and constraining the summation range to a subgroup of the modular group (see [33] for a review.) Since the summation range is now constrained, the Rademacher sum exhibits "spoiled" modularity that we are after. Indeed, the technique was applied to various weights, multipliers and modular groups, and later, it produced weight 1/2 mock modular forms [32, 49, 50]. This is not a coincidence, because the Rademacher sum in the lower-half plane is related to Eichler integral of the shadow. Therefore, Rademacher sum provides a systematic way to extend across the unit circle (although such extension may not be unique.) The examples we will discuss in the next section serve as examples of Rademacher sums. For further details about the Rademacher sums in the present context, see [38].

The "optimal" examples

Here we present 39 examples of the mock–false pairs. They are interesting, because (1) they can be obtained by Rademacher sums in a particularly simple way, (2) they appear as homological blocks of Seifert manifolds, and (3) some of them are finite in the limit $q \to 1$. They are studied and classified in [34] as the only *optimal mock Jacobi forms of weight one* with non-transcendental coefficients.

Recall that homological blocks of our interest are false theta functions, which are Eichler integrals of weight 3/2 unary theta functions which are grouped into Weil representations. On the other side of the plane, they would then correspond to weight 1/2 modular forms which are vector-valued and transforming in the dual Weil representations. Mock Jacobi forms of weight one are ideal candidates. Given a vector-valued mock modular form $h = (h_r)_{r=1}^{m-1}$, we say that its combination with the index m theta functions (cf. (3.16))

$$\psi(\tau, z) = \sum_{r=1,\dots,m-1} h_r(\tau) \left(\theta_{m,r} - \theta_{m,-r}\right)(\tau, z) \tag{3.159}$$

is a *mock Jacobi form* of index m and weight one if its non-holomorphic completion

$$\hat{\psi}(\tau, z) = \sum_{r=1,\dots,m-1} \hat{h}_r(\tau) \left(\theta_{m,r} - \theta_{m,-r}\right)(\tau, z) \tag{3.160}$$

$m+K$	σ^{m+K}	M_3	$H_1(M_3)$	$r \in \sigma^{m+K}$
2	$\{1\}$	$M(-2;1/2,1/2,1/2)$	$\mathbb{Z}_2 \oplus \mathbb{Z}_2$	$r = 1$
3	$\{1,2\}$	$M(-2;1/2,1/2,2/3)$	$\mathbb{Z}_4$	$r = 1,2$
4	$\{1,2,3\}$	$M(-2;1/2,1/2,3/4)$	$\mathbb{Z}_2 \oplus \mathbb{Z}_2$	$r = 1,3$
5	$\{1,2,3,4\}$	$M(-2;1/2,1/2,4/5)$	$\mathbb{Z}_4$	$r = 1,4$
6	$\{1,\dots,5\}$	$M(-2;1/2,1/2,5/6)$	$\mathbb{Z}_2 \oplus \mathbb{Z}_2$	$r = 1,5$
6+3	$\{1,3\}$	$M(-2;1/2,2/3,2/3)$	$\mathbb{Z}_3$	$r = 1,3$
7	$\{1,\dots,6\}$	$M(-2;1/2,1/2,6/7)$	$\mathbb{Z}_4$	$r = 1,6$
8	$\{1,\dots,7\}$	$M(-2;1/2,1/2,7/8)$	$\mathbb{Z}_2 \oplus \mathbb{Z}_2$	$r = 1,7$
9	$\{1,\dots,8\}$	$M(-2;1/2,1/2,8/9)$	$\mathbb{Z}_4$	$r = 1,8$
10	$\{1,\dots,9\}$	$M(-2;1/2,1/2,9/10)$	$\mathbb{Z}_2 \oplus \mathbb{Z}_2$	$r = 1,9$
10+5	$\{1,3,5\}$	$M(-1;1/2,1/5,1/5)$	$\mathbb{Z}_3$	$r = 1,5$
		$M(-4;1/2,1/2,1/2)$	$\mathbb{Z}_2 \oplus \mathbb{Z}_2 \oplus \mathbb{Z}_5$	$r = 1,3,5$
12	$\{1,\dots,11\}$	$M(-2;1/2,1/2,11/12)$	$\mathbb{Z}_2 \oplus \mathbb{Z}_2$	$r = 1,11$
12+4	$\{1,4,5\}$	$M(-1;1/2,2/3,3/4)$	$\mathbb{Z}_2$	$r = 1,5$
13	$\{1,\dots,12\}$	$M(-2;1/2,1/2,12/13)$	$\mathbb{Z}_4$	$r = 1,12$
14+7	$\{1,3,5,7\}$	$M(-5;1/2,1/2,1/2)$	$\mathbb{Z}_2 \oplus \mathbb{Z}_2 \oplus \mathbb{Z}_7$	$r = 1,3,5,7$
		$M(-1;1/2,1/7,2/7)$	$\mathbb{Z}_7$	$r = 3,7$
16	$\{1,\dots,15\}$	$M(-2;1/2,1/2,15/16)$	$\mathbb{Z}_2 \oplus \mathbb{Z}_2$	$r = 1,15$
18	$\{1,\dots,17\}$	$M(-2;1/2,1/2,17/18)$	$\mathbb{Z}_2 \oplus \mathbb{Z}_2$	$r = 1,17$
18+9	$\{1,3,5,7\}$	$M(-1;1/2,1/3,1/9)$	$\mathbb{Z}_3$	$r = 1,5$
		$M(-2;1/2,1/3,2/3)$	$\mathbb{Z}_9$	$r = 1,3,5,7$
		$M(-6;1/2,1/2,1/2)$	$\mathbb{Z}_2 \oplus \mathbb{Z}_2 \oplus \mathbb{Z}_9$	$r = 1,3,5,7$
25	$\{1,\dots,24\}$	$M(-2;1/2,1/2,24/25)$	$\mathbb{Z}_4$	$r = 1,24$
22+11	$\{1,3,5,7,9,11\}$	$M(-7;1/2,1/2,1/2)$	$\mathbb{Z}_2 \oplus \mathbb{Z}_2 \oplus \mathbb{Z}_{11}$	$r = 1,3,5,7,9,11$
		$M(-1;1/2,1/11,4/11)$	$\mathbb{Z}_{11}$	$r = 7,11$
30+6,10,15	$\{1,7\}$	$\Sigma(2,3,5)$	0	$r = 1$
30+15	$\{1,3,\dots,15\}$	$M(-9;1/2,1/2,1/2)$	$\mathbb{Z}_2 \oplus \mathbb{Z}_2 \oplus \mathbb{Z}_{15}$	$r = 1,3,\dots,15$
		$M(-1;1/2,2/5,1/15)$	$\mathbb{Z}_5$	$r = 7,11$
46+23	$\{1,3,\dots,23\}$	$M(-13;1/2,1/2,1/2)$	$\mathbb{Z}_2 \oplus \mathbb{Z}_2 \oplus \mathbb{Z}_{23}$	$r = 1,3,\dots,23$

Table 3.10: Optimal mock Jacobi thetas of Niemeier type and examples of the relevant 3-manifolds.

transforms as a usual Jacobi form (of index m and weight one) [34, 48, 53].

Recall the ambiguities in the Rademacher sums. However, weight one mock Jacobi forms are special, because they are uniquely determined by their poles [48, 131]. For us, it is important that the mock modular form is bounded at each pole, so we make *optimal* choices, *i.e.*, for a given index m,

$$q^{\frac{1}{4m}} h_r = O(1). \tag{3.161}$$

$m+K$	σ^{m+K}	M_3	$H_1(M_3)$	$r \in \sigma^{m+K}$
6+2	$\{1,2,4\}$	$M(-2;1/2,1/2,1/3)$	$\mathbb{Z}_8$	$r=1,2,4$
10+2	$\{1,2,3,4,6,8\}$	$M(-2;1/2,1/2,3/5)$	$\mathbb{Z}_8$	$r=1,4,6$
12+3	$\{1,2,3,5,6,9\}$	$M(-1;1/3,1/3,1/4)$	$\mathbb{Z}_3$	$r=1,9$
		$M(-2;1/2,1/2,1/4)$	$\mathbb{Z}_2\oplus\mathbb{Z}_2\oplus\mathbb{Z}_3$	$r=1,3,5,9$
15+5	$\{1,2,4,5,7,10\}$	$M(-1;1/2,1/3,1/10)$	$\mathbb{Z}_4$	$r=1,4$
		$M(-1;1/3,1/5,2/5)$	$\mathbb{Z}_5$	$r=4,10$
		$M(-3;1/2,1/2,1/3)$	$\mathbb{Z}_{20}$	$r=1,2,4,5,10$
18+2	$\{1,\ldots,8,10,12,14,16\}$	$M(-2;1/2,1/2,7/9)$	$\mathbb{Z}_8$	$r=1,8,10$
20+4	$\{1,3,4,7,8,11\}$	$M(-1;1/2,1/4,1/5)$	$\mathbb{Z}_2$	$r=1,11$
21+3	$\{1,\ldots,6,8,9,11,12,15,18\}$	$M(-2;1/2,1/2,4/7)$	$\mathbb{Z}_8$	$r=1,6,8,15$
24+8	$\{1,2,5,7,8,13\}$	$M(-1;1/2,1/3,1/8)$	$\mathbb{Z}_2$	$r=1,7$
28+7	$\{1,2,3,5,6,7,9,$ $10,13,14,17,21\}$	$M(-1;1/4,1/7,4/7)$	$\mathbb{Z}_7$	$r=13,21$
30+3,5,15	$\{1,3,5,7,9,15\}$			
33+11	$\{1,2,4,5,7,8,10,$	$M(-5;1/2,1/2,1/3)$	$\mathbb{Z}_{44}$	$r=$ all
	$11,13,16,19,22\}$	$M(-1;1/3,1/11,6/11)$	$\mathbb{Z}_{11}$	$r=16,22$
36+4	$\{1,3,4,5,7,8,11,$ $12,15,16,19,23\}$			
42+6,14,21	$\{1,5,11\}$	$\Sigma(2,3,7)$	0	$r=1$
60+12,15,20	$\{1,2,7,11,13,14\}$	$\Sigma(3,4,5)$	0	$r=13$
70+10,14,35	$\{1,3,9,11,13,23\}$	$\Sigma(2,5,7)$	0	$r=11$
78+6,26,39	$\{1,5,7,11,17,23\}$	$\Sigma(2,3,13)$	0	$r=7$

Table 3.11: Optimal mock Jacobi thetas of non-Niemeier type and examples of the relevant 3-manifolds.

In [34], it was shown that the space of weight one mock Jacobi forms with (1) optimal poles and (2) non-transcendental coefficients is finite dimensional. There are 39 special vectors in this space, which span the space. They are labeled by the same pair (m,K) which characterize the Weil (sub-)representations. Let's denote the corresponding vector-valued mock modular forms by

$$\psi^{m+K} = \sum_{r=1,\ldots,m-1} h_r^{m+K}(\tau)(\theta_{m,r} - \theta_{m,-r}). \tag{3.162}$$

Then the group K dictates the symmetry of Ψ^{m+K} that it is invariant under $\theta_{m,r} \mapsto \theta_{m,ra(n)}$ for every $n \in K$. In particular, since $a(m) = -1$ we will never have a non-vanishing ψ^{m+K} unless $m \notin K$.

Therefore, we obtain 39 distinguished mock Jacobi forms ψ^{m+K}, which can be expressed as Rademacher sums. Furthermore, they can be expressed as theta function

shadows and most importantly for us, have integral coefficients. The integral coefficients further divide 39 examples into two sub-classes. In the first case of 23 examples, called the *Niemeier type*, the coefficients are nonnegative for all non-polar terms in the q-expansion.[8] The remaining 16 involve both positive and negative coefficients. The Weil representations $m + K$ of the two groups are summarized in Table 3.10 and 3.11 respectively.

Finally, it is possible to show that some of them exhibit boundedness, which is crucial for the connection with perturbative data:

$$\lim_{\tau\to 0} h_r^{m+K}(\tau) = O(1), \quad \text{for} \quad \begin{cases} m+K = 6+2, & r = 1 \\ m+K = 10+2, & r = 1,3 \\ m+K = 18+2, & r = 1,3,5,7 \end{cases} \tag{3.163}$$

which can easily be verified from the known behavior (3.161) of h_r^{m+K} near $\tau \to i\infty$ and the S-matrix of the Weil representation.

3.5 $S_{ab}^{(A)}$ and logarithmic CFTs

So far, we have discussed the integrality and modularity of homological blocks. In this section, we focus on the "modularity" of the $S_{ab}^{(A)}$ matrix which was shown in Equation (3.6). In ordinary, rational CFTs, one would expect modular S-transforms to be represented as a "sin" representation of the modular group. This is when rational vertex operator algebras (VOAs) have semi-simple modular tensor categories (MTCs) as their representation categories.

However, $S_{ab}^{(A)}$ is a "cos" representation of $SL(2,\mathbb{Z})$, due to the Weyl group action $a \leftrightarrow -a$:

$$S_{ab}^{(A)} = \frac{\cos\frac{2\pi ab}{p}}{1+\delta_{a,0}}. \tag{3.164}$$

In fact, such S-matrices appear in non-semisimple MTCs, and it is the logarithmic VOAs which have non-semisimple MTCs as their representation categories [112, 113]. They are *logarithmic* in a sense that their Hamiltonian operator L_0 is non-diagonalizable over the Hilbert space. As a result, log behavior is observed not only from the correlation functions of certain operator, but also in their characters, hence $\chi \in \mathbb{Z}[[q]][\log q]$. After formal manipulations, one can often turn the latter into a

[8] The name comes from the fact that they are in 1-1 correspondence with the 23 Niemeier lattices and play the role of the graded dimensions of the finite group modules for umbral moonshine [35, 37].

q-series, but then it exhibits precisely the "spoiled" modular behavior which we are after.[9]

In particular, we will observe that the homological blocks are the characters of reducible, yet indecomposable modules which are new features of log VOAs. Considering their MTC structure, one observes the above "cosine" S-matrix.

Singlet and triplet $(1,p)$ models

Simple examples of logarithmic VOAs constructed from free fields and screening operators are the singlet and triplet $(1,p)$ models [1, 57, 58, 63, 118], originally introduced in [98]. They are *logarithmic* in a sense that the Hilbert space is non-diagonalizable in L_0.

Let us start with a free scalar field with OPE. We mostly follow [63] for this lightning review.

$$\varphi(z)\varphi(w) \sim \log(z-w).$$

whose primary fields are represented by the vertex operators $e^{j(1,s)\varphi}$, where we define:

$$j(r,s) := \frac{1-r}{2}\alpha_+ + \frac{1-s}{2}\alpha_-, \quad \alpha_+ = \sqrt{2p}, \quad \text{and} \quad \alpha_- = -\sqrt{\frac{2}{p}}.$$

Their conformal dimensions (weights) of $e^{j(r,s)\varphi}$ are

$$\Delta(r,s) := \frac{1}{2}(j(r,s)^2 - 2\alpha_0 j(r,s)) = \frac{r^2-1}{4}p + \frac{s^2-1}{4p} + \frac{1-rs}{2}.$$

The energy-momentum tensor is given by:

$$T = \frac{1}{2}\partial\varphi\partial\varphi + \frac{\alpha_0}{2}\partial^2\varphi, \quad \alpha_0 = \alpha_+ + \alpha_-.$$

Notice that the central charge is:

$$c \;=\; 1 - 3\alpha_0^2 \;=\; 1 - 6\frac{(1-p)^2}{p}. \tag{3.165}$$

Also, there are two screening operators

$$S_+ := \oint e^{\alpha_+\varphi}, \quad S_- := \oint e^{\alpha_-\varphi} \quad \Rightarrow \quad [S_\pm, T(z)] = 0$$

which are respectively called "long" and "short" screening operators.

[9] Such formal manipulations were already discussed in the context of the analytic continuation of WRT invariants [84, 124].

As usual, the modes of $\partial\varphi(z)$ generate the Heisenberg algebra $[a_m, a_n] = m\delta_{m+n,0}\mathbf{1}$, while the modes of the energy-momentum tensor generate the Virasoro algebra with the central charge (3.165). Then, one can consider the Fock modules $\mathcal{F}_{j(r,s)}$ generated by the Heisenberg algebra acting on the highest weight vector provided by the vertex operator $e^{j(1,s)\varphi}$.[10] Observe that in this notation, the Heisenberg algebra itself is $\mathcal{F}_0$. Further define:

$$\mathcal{F} := \bigoplus_{\substack{r\in\mathbb{Z}\\ s=1,\cdots,p}} \mathcal{F}_{j(r,s)}, \quad \mathcal{F}_{[s]} := \mathcal{F}_{j(1,s)}. \tag{3.166}$$

Observe that the kernel of S_- acting on $\mathcal{F}$ comprises an algebra, $\mathcal{A}(p)$. This algebra is generated by $e^{-\alpha_+\varphi/2}$ and $[S_+, e^{-\alpha_+\varphi/2}]$, hence determined by the lattice $\frac{\alpha_+}{2}\mathbb{Z}$. It is in fact non-local, as scalar products of lattice vectors are valued in $\frac{1}{2}\mathbb{Z}$.

Considering the maximal local subalgebra in $\mathcal{A}(p)$, one obtains the *triplet* $(1,p)$ vertex algebra (denoted either $\mathcal{W}_p$ or $\mathcal{W}(2,(2p-1)^{\otimes 3})$), which is an extension of the Virasoro algebra by the $\mathfrak{sl}(2)$ triplet of the Virasoro primary fields $W^{\pm,0}(z)$ of conformal dimension $2p-1$ [63]:

$$W^-(z) \;=\; e^{-\alpha_+\varphi}(z), \qquad W^0(z) \;=\; [S_+, W^-(z)], \qquad W^+(z) \;=\; [S_+, W^0(z)].$$

By construction, the triplet algebra is given by:

$$\mathcal{W}_p \;=\; \mathrm{Ker}_{\mathcal{V}_L} S_- \tag{3.167}$$

on the lattice VOA $\mathcal{V}_L$ for $L = \alpha_+\mathbb{Z} = \sqrt{2p}\mathbb{Z}$. Considering $\mathcal{M}_p = \mathcal{F}_0 \cap \mathcal{W}_p$, one obtains the *singlet* $(1,p)$ vertex algebra:

$$\mathcal{M}_p \;=\; \mathrm{Ker}_{\mathcal{F}_0} S_-. \tag{3.168}$$

Both algebras $\mathcal{M}_p$ and $\mathcal{W}_p$ have the central charge (3.165).

Having defined the vertex algebras, let us study their representations. First of all, the singlet algebra admits Fock modules $\mathcal{F}_\lambda$ labeled by the highest weight $\lambda \in \mathbb{C}$. Besides them, there are Feigin-Fuchs modules $M_{1,s}$ obtained from $e^{j(1,s)\varphi}$ with $1 \le s < p$, and their characters take the form [2, 60]:

$$\begin{aligned} \chi_{\mathcal{F}_\lambda} \;&=\; \frac{q^{\frac{1}{2}(\lambda-\frac{\alpha_0}{2})^2}}{\eta(q)}, \\ \chi_{M_{1,s}} \;&=\; \frac{1}{\eta(q)}\sum_{n\ge 0}\left(q^{\frac{1}{4p}(2pn+p-s)^2} - q^{\frac{1}{4p}(2pn+p+s)^2}\right) \;=\; \frac{\Psi_{p,p-s}(q)}{\eta(q)}. \end{aligned} \tag{3.169}$$

[10] As modules of Virasoro algebras, these are also Feigin-Fuchs modules.

The $\mathcal{W}_p$ generators shift $e^{j(r,s)\varphi} \to e^{j(r+2n,s)\varphi}$ for some integer n. As a result, for each fixed $s = 1, \cdots, p$, we can define two $\mathcal{W}_p$ modules, $\mathcal{X}_s^{\pm}$ generated from $e^{j(1,s)\varphi}$ and $e^{j(1,s)\varphi}$ respectively. Altogether, we have $2p$ irreducible representations $\{\mathcal{X}_s^{\pm}\}_{s=1}^{p}$ of $\mathcal{W}_p$, whose conformal dimensions are:

$$\Delta(\mathcal{X}_s^{+}) \;=\; \frac{(p-s)^2}{4p} + \frac{c-1}{24} \tag{3.170}$$

$$\Delta(\mathcal{X}_s^{-}) \;=\; \frac{(2p-s)^2}{4p} + \frac{c-1}{24} \tag{3.171}$$

Next, we consider the characters. We often obtain them by modular transforms on the vacuum character. We can do the same here [60], but unlike in rational CFTs, the characters of the irreducible representations $\mathcal{X}_s^{\pm}$,

$$\begin{aligned}\chi_s^{+}(q) \;:=\; \mathrm{Tr}_{\mathcal{X}_s^{+}} q^{L_0-\frac{c}{24}} \;&=\; \frac{q^{-1/24}}{\prod_{n=1}^{\infty}(1-q^n)} \sum_{n\in\mathbb{Z}} (2n+1) q^{p(n+\frac{p-s}{2p})^2} \;= \\ &=\; \frac{1}{\eta(q)}\left(\frac{s}{p}\theta_{p-s}(q) + 2\theta'_{p-s}(q)\right)\end{aligned} \tag{3.172}$$

$$\begin{aligned}\chi_s^{-}(q) \;:=\; \mathrm{Tr}_{\mathcal{X}_s^{-}} q^{L_0-\frac{c}{24}} \;&=\; \frac{q^{-1/24}}{\prod_{n=1}^{\infty}(1-q^n)} \sum_{n\in\mathbb{Z}} 2n q^{p(-n+\frac{s}{2p})^2} \;= \\ &=\; \frac{1}{\eta(q)}\left(\frac{s}{p}\theta_{s}(q) - 2\theta'_{s}(q)\right)\end{aligned} \tag{3.173}$$

do not close under the action of the modular group $SL(2,\mathbb{Z})$. The modularity is restored once we introduce $(p-1)$ "pseudo-characters."

Due to the logarithmic nature of the CFT, we observe indecomposable representations. They are constructed as (iterative) extensions of the $2p$ irreducible representations. In the end of this process, one finds projective modules with the following structure ($1 \le s \le p-1$):

$$\mathcal{P}_s^{\pm}: \tag{3.174}$$

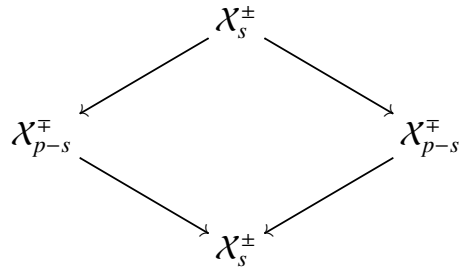

where, following [57, 58], we denote extensions by

$$\mathcal{X}_s^{\pm} \bullet \longrightarrow \bullet \mathcal{X}_{p-s}^{\mp} \tag{3.175}$$

$\widehat{Z}_a(M_3)$ as characters of log-VOAs

Notice the appearance of a false theta function in Equation (3.169). Then, we can identify the homological blocks as the characters of triplet $(1, p)$ models up to a Dedekind eta function. In fact, the eta function corresponds to the Cartan part of the adjoint chiral multiplet in the bulk, which is suppressed in the homological block [84, 85]:

$$\widehat{Z}_a^{(\text{unred})}(q) \;=\; \frac{\widehat{Z}_a(q)}{(q;q)_\infty}. \tag{3.176}$$

Recovering the eta function, we obtain the *unreduced* physical index, which can be now identified with the characters of the indecomposable representations:

$$\widehat{Z}_a^{(\text{unred})}(q) \;=\; \chi\left(M_{1,p-s_1} \oplus M_{1,p-s_2} \oplus \ldots\right) \tag{3.177}$$

for $p - s_i \in \sigma^{p+K}$. Some spherical examples are provided in Table 3.12, but the correspondence of course extends to all Seifert manifolds with three singular fibers that we have observed so far.

3-manifold	$m + K$	**module of a singlet log-VOA**
$\Sigma(2,3,5)$	$30 + 6, 10, 15$	$M_{1,1} \oplus M_{1,11} \oplus M_{1,19} \oplus M_{1,29}$
$\Sigma(2,3,7)$	$42 + 6, 14, 21$	$M_{1,1} \oplus M_{1,13} \oplus M_{1,29} \oplus M_{1,41}$

Table 3.12: Weil representations and the corresponding modules of the logarithmic $(1, p)$ singlet CFT for simple homology spheres.

The cosine S-matrix

The $2p$ irreps and $(p-1)$ pseudo-characters of the $\mathcal{W}_p$ algebra comprise a $(3p-1)$-dimensional projective representation $\mathfrak{Z}$ of $SL(2,\mathbb{Z})$ [58]:

$$\mathfrak{Z} \;=\; \mathcal{R}_{p+1} \;\oplus\; \mathbb{C}^2 \otimes \mathcal{R}_{p-1}. \tag{3.178}$$

As we have briefly mentioned above, the $2p$ irreps of VOAs are not closed under the modular transformations, and we must reorganize them. For instance, $\mathcal{R}_{p+1}$ is spanned by the Verma modules over $\mathcal{W}_p$ whose characters are:

$$\begin{aligned} N_0(\tau) &= \chi_p^-(\tau) \\ N_s(\tau) &= \chi_s^+(\tau) + \chi_{p-s}^-(\tau), \quad s = 1, \cdots, p-1 \\ N_p(\tau) &= \chi_p^+(\tau). \end{aligned} \tag{3.179}$$

In fact, $\mathfrak{Z}$ can be interpreted as the space of conformal blocks on a torus, or equivalently, the endomorphisms of the identity functor in the representation category of VOA.

Mark the "plus" sign in N_s. The sign results in the "$\cos\frac{\pi rs}{p}$" factor in the modular S-transform of N_s. This is precisely the $S^{(A)}_{ab}$ matrix that we were after. Therefore, $\mathcal{R}_{p+1}$ corresponds to a non-unitary $(p+1)$-dimensional representation of $SL(2,\mathbb{Z})$. On the other hand, $\mathcal{R}_{p-1}$ is the $(p-1)$-dimensional "$\sin\frac{\pi rs}{p}$" representation of $SL(2,\mathbb{Z})$ on the unitary $\widehat{\mathfrak{sl}(2)}_{p-2}$ characters, and $\mathbb{C}^2$ is the defining two-dimensional representation of $SL(2,\mathbb{Z})$.

3.6 Quantum grups via Kazhdan-Lusztig correspondence

Just as defects of Chern-Simons theory and their categorifications were controlled by quantum groups, the $SL(2,\mathbb{Z})$ representation $\mathfrak{Z}$ and its categorification are controlled by quantum groups as well. The relation is given by the so-called Kazhdan-Lusztig correspondence [99–101].

In general, the *Kazhdan-Lusztig* correspondence between a VOA and a quantum group states:

1. a suitable representation category of the VOA is equivalent to the category of finite-dimensional quantum group representations;
2. the fusion algebra associated with the CFT coincides with the Grothendieck ring of the quantum group;
3. the modular group representation of conformal blocks on T^2 is equivalent to that of the quantum group center.

It is relatively well known that fusion rules of a WZW model are related to the representation theory of a quantum group at a primitive root of unity (see *e.g.*, [64].) To achieve the correspondence, however, one must quotient the quantum group representation category by certain ideal. The procedure is called *semisimplification*, and it is crucial to describe the semisimple MTC which describes the semisimple fusion algebra in rational CFTs.

In logarithmic CFTs, however, the associated MTC is not semisimple, and the extra semisimplification procedure is irrelevant. For $\widehat{Z}_b(q)$, this implies that in the limit q goes to roots of unity, it may require certain corrections (*c.f.*, Table 3.13). In this section, we compare the representations and characters of triplet $(1,p)$ models with their counterparts in quantum group representations.

The quantum group of interest is a restricted version of quantum group $U_q(\mathfrak{sl}_2)$. The restricted quantum groups $\overline{\mathcal{U}}_q(\mathfrak{sl}_2)$ at the primitive $2p$-th root of unity $q = e^{\frac{i\pi}{p}}$ is

3-manifolds	**Logarithmic CFTs**
flat connections	modules
invariants $\widehat{Z}_b(q)$	characters $\chi(q)$
"mock side"	KL "positive zone"
"false side"	KL "negative zone"
"corrections" at roots of unity	semisimplification

Table 3.13: Mysterious duality between 3-manifolds and logarithmic CFTs.

defined by supplementing the usual $U_q(\mathfrak{sl}_2)$ relations

$$[E,F] \;=\; \frac{K-K^{-1}}{q-q^{-1}}, \qquad KEK^{-1} \;=\; q^2E, \qquad KFK^{-1} \;=\; q^{-2}F \tag{3.180}$$

with

$$E^p \;=\; 0 \;=\; F^p, \quad \text{and} \quad K^{2p} \;=\; \mathbf{1}. \tag{3.181}$$

It is spanned by $E^iK^jF^l$ with $0 \le i,l \le p-1$ and $0 \le j \le 2p-1$. Consequently, the restricted quantum group is $2p^3$-dimensional, and this "regular" representation has the following decomposition:

$$\text{Reg} \;=\; \bigoplus_{s=1}^{p-1} s\mathcal{P}_s^+ \oplus \bigoplus_{s=1}^{p-1} s\mathcal{P}_s^- \oplus p\mathcal{X}_p^+ \oplus p\mathcal{X}_p^-. \tag{3.182}$$

We will describe the shown representations next. To find the center of the quantum group, we consider the bimodule endomorphisms of the regular representation. As a result, one observes $(3p-1)$-dimensional center generated by the following elements satisyfing an associative commutative algebra:

$$\begin{aligned} &e_se_{s'} = \delta_{s,s'}e_s, && s,s' = 0,\cdots,p,\\ &e_sw_{s'}^{\pm} = \delta_{s,s'}w_{s'}^{\pm}, && 0 \le s \le p,\ 1 \le s' \le p-1,\\ &w_s^{\pm}w_{s'}^{\pm} = w_s^{\pm}w_{s'}^{\mp}, && 1 \le s,s' \le p-1. \end{aligned} \tag{3.183}$$

There are $2(p-1)$ elements $w_s^{\pm}$ $(1 \le s \le p-1)$ and $(p+1)$ primitive idempotents. This is exactly the structure of $\mathfrak{Z}$ that we have observed in Equation (3.178).

Besides the observed agreement in the center, we can see the correspondence in representations. First of all, there are $2p$ irreducible representations $\mathcal{X}_s^{\pm}$ for $s = 1,\cdots,p$. Each $\mathcal{X}_s^{\pm}$ is s-dimensional and spanned by elements $|s,n\rangle^{\pm}$, where $|s,0\rangle^{\pm}$

is the highest-weight vector and the generators of $\overline{\mathcal{U}}_q(\mathfrak{sl}_2)$ act by:

$$\begin{aligned} K|s,n\rangle^{\pm} &= \pm q^{s-1-2n}|s,n\rangle^{\pm}, \\ E|s,n\rangle^{\pm} &= \pm[n][s-n]|s,n\rangle^{\pm} \\ F|s,n\rangle^{\pm} &= |s,n\rangle^{\pm} \end{aligned} \tag{3.184}$$

where $|s,s\rangle^{\pm} = |s,-1\rangle^{\pm} = 0$.

Besides the irreducible representations, there are also non-trivial exensions: (1) $2p$ Verma modules $\mathcal{V}_s^{\pm}$, $1 \le s \le p$ and (2) the projective modules $\mathcal{P}_s^{+}$ and $\mathcal{P}_s^{-}$ of dimensions ($1 \le s \le p$):

$$\dim \mathcal{P}_s^{\pm} \;=\; 2p, \qquad\qquad \mathrm{qdim}\mathcal{P}_s^{\pm} \;=\; 0 \qquad\qquad (1 \le s \le p-1) \tag{3.185}$$

For generic $s \neq p$, they are given by extensions

$$0 \to \mathcal{X}_{p-s}^{\mp} \to \mathcal{V}_s^{\pm} \to \mathcal{X}_s^{\pm} \to 0 \tag{3.186}$$

and

$$0 \to \mathcal{V}_{p-s}^{\mp} \to \mathcal{P}_s^{\pm} \to \mathcal{V}_s^{\pm} \to 0, \tag{3.187}$$

respectively. This is precisely the structure depicted in (3.174). When $s = p$, the two modules

$$\mathcal{X}_p^{\pm} \;=\; \mathcal{V}_p^{\pm} \;=\; \mathcal{P}_p^{\pm} \tag{3.188}$$

are irreducible, Verma, and projective simultaneously. They are called *Steinberg modules* by analogy with what happens in the quantum group over $\mathbb{F}_p$.

Finally, the Grothendieck ring of $\overline{\mathcal{U}}_q(\mathfrak{sl}_2)$ match the fusion algebra of log CFT. The Grothendieck ring is generated by over $\mathbb{Z}$ by $x = \mathcal{X}_2^{+}$ [58]:

$$\mathrm{Gr} \;=\; \mathbb{Z}[x]/\,(x-2)(x+2)\prod_{j=1}^{p-1}\left(x - 2\cos\tfrac{\pi j}{p}\right)^2. \tag{3.189}$$

Note: in the Grothendieck ring, there is no difference between direct sums and non-trivial extensions, so that $[\mathcal{P}_s^{\pm}] = 2[\mathcal{X}_s^{\pm}] + 2[\mathcal{X}_{p-s}^{\mp}]$, etc.

Among other things, this offers a new way of looking at logarithmic CFTs, connecting them to supersymmetric 3d $\mathcal{N} = 2$ theories, including theories $T[M_3]$ coming from 3-manifolds. We hope that, in the future, this new perspective will help to shed light on the still rather mysterious nature of log-CFTs.

3.7 Generalizations and discussions

So far, we have studied Chern-Simons partition functions as a 3d-2d coupled system. Bridged by their modular properties, we have also observed their interpretations as log VOA characters. There are several knobs we can turn, but most obviously, we can study higher rank gauge groups and more general class of 3-manifolds. Indeed, homological blocks for higher rank gauge groups were suggested in [44], and are waiting for the analysis of its modularity and interpretation as log VOA characters. In terms of 3-manifolds, we have only discussed Seifert manifolds with three or four singular fibers. We have observed that a different number of singular fibers leads to different building blocks, hence different modular behaviors. The correspondence also extends to the characters of log VOA, and for the four singular fibered examples, one can often identify the homological blocks with characters of (p_+, p_-) singlet models. It would be therefore interesting to explore the modularity of higher-rank and higher-fiber examples. With evidences in [18], the project is in progress. On the other hand, Seifert manifolds of the above discussion have discrete first homology groups. Therefore, it would be also interesting to explore the examples with $b_1 \geq 1$.

It is also interesting to find the precise characterization of the boundary conditions $\mathcal{B}_a$ for the homological blocks. To approach their physical descriptions, one may consider the 3-manifold M_3 as a boundary of a 4-manifold M_4. Then, one would obtain a 2d theory labeled by M_4, while $T[M_3]$ in the bulk. The idea was originally introduced in [66] and further extended to define vertex algebras VOA$[M_4]$ labeled by the closed 4-manifolds [51, 56]. It would be interesting to understand the precise relation between the log VOAs which arise from the 3d-2d coupled system and VOA$[M_4]$. Also, as a 3d-2d coupled index, $\widehat{Z}_a(q)$ are "counting" BPS states, and it would be interesting to find relations (dualities) to other systems where similar modular structures are observed, e.g. [5, 7, 36, 48, 132].

In the modularity dictionary, we have identified $m + K$ essentially via searching through the valid candidates. So we may ask for the explicit relation between the choice of K and the topology of 3-manifold: or equivalently, the embedding of Weil representations in the topological / physical data.

Identification of $\widehat{Z}_a$ on the mock side requires further study, because of the ambiguities we have discussed. First of all, as we have seen in the q-hypergeometric approaches, there can be two q-hypergeometric series which agree on one side of the plane while looking completely different on the other side. Secondly, even

when a mock function is identified, there are ambiguities coming from the modular subtractions. All of these ambiguities are invisible from perturbative Chern-Simons invariants, but they are indeed crucial in the identifications with the exact partition function.

Furthermore, the "optimal" homological blocks suggest the 39 optimal mock Jacobi theta functions on the other side. At the same time, these mock functions also play the role of the graded dimensions of finite group representations in the context of the umbral moonshine [35, 37]. Therefore, it would be also interesting to explore the relation between homological blocks and the moonshine finite groups.

It would be also interesting to find the dictionary between log VOA characters and the homological blocks. Existence of such a dictionary is advocated by the fact that modularities of homological blocks and unitarities of log VOA characters are spoiled in a similar manner. Recall that the modularity in the boundary 2d system is spoiled by the 3d system in the bulk. As a result, we observe false, mock, and quantum modular forms. On the other hand, log CFTs can be thought as "deformations" of ordinary CFTs such as free field theories or lattice VOAs. Indeed, we have above constructed them as kernels of screening operators in lattice VOAs [57, 58], which are larger compared to the BRST cohomologies of the same screenings used in the construction of minimal models [59, 95]. Regarding the connection, we may associate the boundary conditions $\mathcal{B}_a$ with free fields or lattice VOAs, and realize the screening operators from the bulk 3d $\mathcal{N} = 2$ theory $T[M_3]$. This is also a subject for future works.

In a parallel line of development, there are "logarithmic" 3-manifold invariants based on non-semisimple MTCs [14, 16, 17]. The 3-manifold invariants are logarithmic extensions of the so-called "Hennings invariants," which encode WRT invariants in the semisimple case. Although the naive attempts would yield only trivial TQFTs, by taking the modified trace, one can obtain non-trivia results. Observe that the log behavior is required precisely when one generalizes to non-semisimple MTCs. Furthermore, the construction is based on deformed quantum groups, and it would be extremely interesting to understand their relations with $\widehat{Z}_a(q)$.

Appendix A

DERIVATION OF *N*WEB RELATIONS VIA WILSON LINES

In this section, we show that the relations of Figure 2.7 are satisfied by Wilson lines in $SU(N)$ Chern-Simons theory.

A.1 The normalization ambiguity and associativity relation

Before proceeding to the derivations, however, it is necessary to resolve an ambiguity in our normalization. The ambiguity is resolved so that it satisfies the "associativity" relation (Figure 2.7(a)). There is a remaining overall sign ambiguity, but this is invisible.

One might be worried whether our choice of normalization could be inconsistent. However, the consistency is guaranteed by a Theorem in MOY calculus [143] which states that the relations in Figure 2.7, together with the expectation values of Wilson loops supported on a k-colored unknot, form the complete set of relations which uniquely determines the MOY graph polynomials $P_N(\Gamma; q) \in \mathbb{Z}[q, q^{-1}]$. Therefore, it suffices to fix the normalizations such that they satisfy Figure 2.7.

To exhibit the normalization ambiguity, first recall that we have already fixed the normalization of gauge invariant tensors (ϵ_{k_1,k_2} and $\tilde{\epsilon}_{k_1,k_2}$) placed at the junctions of Figure 2.4. However, the condition only fixes the normalization of their product. Thus, there is an ambiguity in the "relative" normalization among the invariant tensors from different types of junctions.

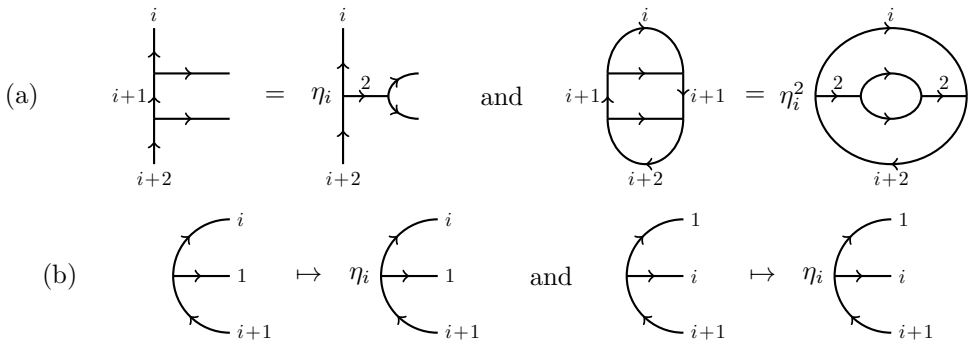

Figure A.1: Resolving normalization ambiguities. (a) Definition of η_i and the closed Wilson lines which determine the value of η_i^2. (b) Renormalization of junctions which involve the Wilson lines in $\square$.

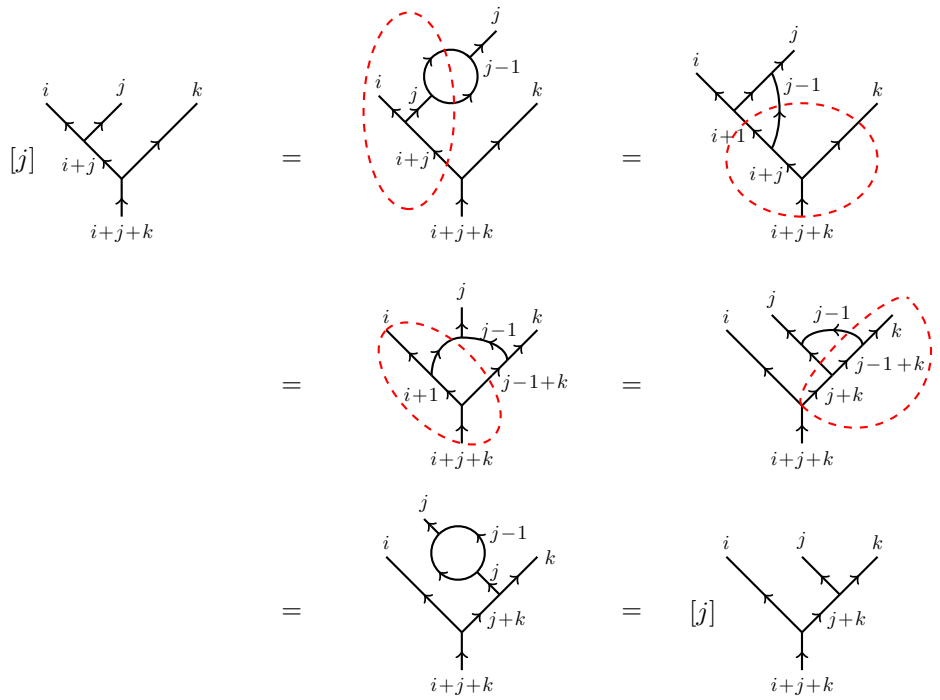

Figure A.2: Induction on j. Apply the base case $j = 1$ and the induction hypothesis for $j - 1$ in the red dashed cirlces.

Let us first normalize the gauge invariant tensors $\epsilon_{i,1}$ and $\tilde{\epsilon}_{i,1}$. The open Wilson lines of Figure A.1(a) are proportional to each other, since the associated Hilbert space is 1-dimensional. Renormalize the invariant tensor $\epsilon_{i,1}$ via multiplication by η_i (*c.f.* Figure A.1(b)), and renormalize $\tilde{\epsilon}_{i,1}$ and $\tilde{\epsilon}_{1,i}$ accordingly via multiplication by $1/\eta_i$. This proves Figure 2.7(a) for $j = k = 1$.

Inductively renormalize the junctions of higher rank representations. Consider Wilson lines of Figure 2.7(a) with $j = 1$, and assume WLOG that $i \geq k$. Since the associated Hilbert space is 1-dimensional, the Wilson lines on each side are proportional to each other. Renormalizing $\epsilon_{i,k+1}$ by absorbing the proportionality constant, we have turned the relation into an identity and determined the relative normalization between $\epsilon_{i,k+1}$ and $\epsilon_{i+1,k}$. Proceed recursively until we reach $\epsilon_{i+k,1}$, whose normalization is fixed by Figure A.1(b). Applying this procedure for all $i + k$, the relative normalizations among the invariant tensors can be determined such that Figure 2.7(a) holds for $j = 1$. Finally, induction on j shows that Figure 2.7(a) holds for any i, j and k (*c.f.* Figure A.2.)

A.2 "$[E, F]$" relation

In this section, we prove Figure 2.7(e). Consider the three configurations of Wilson lines in Figure 2.7(e). The path integral in these systems gives three vectors in $H_{S^2,\{m,j,\bar{m},\bar{j}\}}$. Since the dimensions of this space is greater than 2 for general m and j, it is not *a priori* clear whether the three vectors should satisfy a linear relation. In order to obtain it, we start with the relations among networks in Figure A.3(a). That such relations (with some coefficients) have to hold follows from the fact that

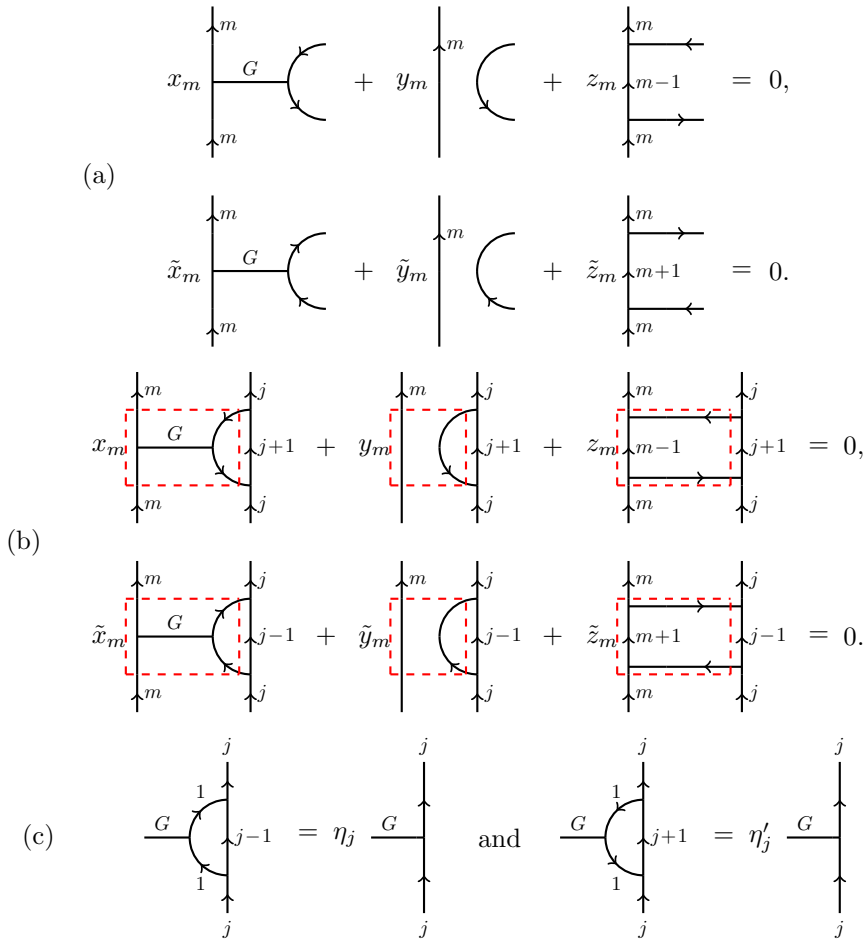

Figure A.3: Relations needed to set up the $[E, F]$ relation. (a) Two linear relations among three Wilson lines in $H_{S^2,\{1,m,\bar{1},\bar{m}\}}$, (b) two linear relations among three Wilson lines containing those of (a) in the red dashed box, and (c) proportionality relations between two vectors in $H_{S^2,\{G,j,\bar{j}\}}$.

$H_{S^2,\{1,m,\bar{1},\bar{m}\}}$ is 2-dimensional. Here, G stands for the adjoint representation, and we have chosen non-trivial vertices at the end-points of the Wilson lines colored by G. (The actual choice will not play a role in the following.) Inserting these relations into larger networks of Wilson lines leads to relations of Figure A.3(b).

Next, from the 1-dimensionality of $H_{S^2,\{G,j,\bar{j}\}}$ one derives the relations in Figure A.3(c). (Again, we have chosen non-trivial junction fields.) This allows us to relate the first two terms in the identities of Figure A.3(b), and hence to eliminate them from the relations. One arrives at the new relation depicted in Figure A.4, which is a linear relation of the type we are after. To deduce (e) of Figure 2.7, it remains to determine the coefficients α and β. We will do this in two steps. First we join

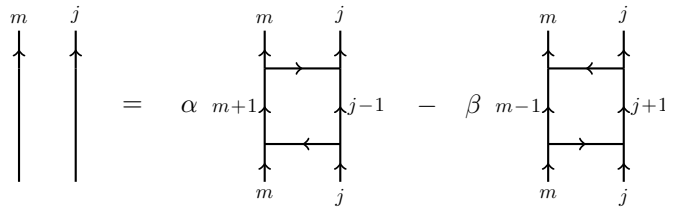

Figure A.4: A linear relation among three vectors in $\mathcal{H}_{S^2,\{j,m,\bar{j},\bar{m}\}}$. The coefficients α and β are functions of $x_m, y_m, z_m, \tilde{x}_m, \tilde{y}_m, \tilde{z}_m, \eta_j, \eta'_j$.

the ends of the m- and j-colored Wilson lines in Figure A.4. Using the expectation values of all the resulting networks of Wilson lines that have been determined earlier, we obtain the following relation

$$[N] = \alpha\,[N-j]\,[m] - \beta\,[N-m]\,[j]\ . \tag{A.1}$$

Another relation can be found by connecting the incoming m- and j-colored Wilson lines in Figure A.4 with a junction to an incoming $j+m$ Wilson line. Since $H_{S^2,\{j,m,\overline{j+m}\}}$ is one-dimensional, the vectors associated to all three configurations of Wilson lines are proportional to one another. The constants of proportionality can be easily found: close off Wilson lines in relation of Figure 2.7(a) in a way shown in Figure A.5(a), then insert the identity of Figure 2.7(b), and finally apply the resulting identity twice. The result is depicted in Figure A.5(b), from which we obtain another relation on the coefficients α and β:

$$1 = \alpha\,[m]\,[j+1] - \beta\,[m+1]\,[j]\ . \tag{A.2}$$

Together with (A.1) this fixes the sought-after coefficients to be

$$\frac{1}{\alpha} = [m-j] = \frac{1}{\beta}\,, \tag{A.3}$$

finally proving the relation of Figure 2.7(e).

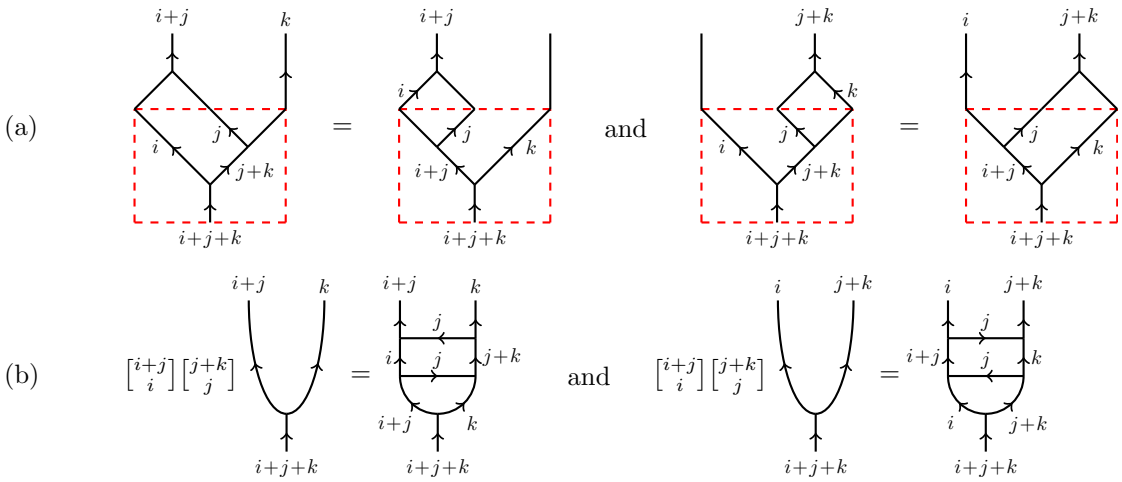

Figure A.5: Relations to fix the coefficients of the $[E, F]$ relation. (a) Capping off the "associativity identity." (b) Relations in $H_{S^2,\{j,m,\overline{j+m}\}}$.

A.3 The remaining relations

The remaining relations follow from Figure 2.7(a) and Figure 2.7(e).

First of all, Figure 2.7(b) is rather straightforward. The two Wilson lines are proportional as the associated Hilbert space is one-dimensional. Once we close the open ends by connecting them, the normalization condition fixes the proportionality constant.

The three vectors of Figure 2.7(c) satisfy a linear relation, as the associated Hilbert space is 2-dimensional. Close the open ends in two inequivalent ways (*c.f.* Figure A.4.) The resulting closed Wilson lines have computable expectation values via the direct sum formula, Figure 2.7(a), and Figure 2.7(b).

Figure 2.7(d) follows from Figures 2.7(a), (b) and (e). First, apply Figure 2.7(a) and 2.7(b) to replace the right-moving Wilson line labeled by $\wedge^n\square$ (the left-moving Wilson line labeled by $\wedge^{l+n-1}\square$) with n parallel right-moving Wilson lines labeled by $\square$ (l+n−1 left-moving Wilson lines labeled by $\square$). Recursively apply Figure 2.7(e) until the resulting Wilson lines are those of the RHS, and the coefficients follow.

Figure 2.7(f) also follows from Figures 2.7(a), (b) and (e). First, apply Figure 2.7(a) on LHS with $(i, j, k) = (m-2, 1, 1)$. Use Figure 2.7(a) and (b) to replace the upper Wilson line labeled by $\wedge^j\square$ by j Wilson lines labeled by $\square$. Then, recursively apply Figure 2.7(e) until the resulting Wilson lines differ from those of the RHS only by a single right-moving Wilson line labeled by $\wedge^2\square$. Use Figure 2.7(a) and (b) to replace the latter with two Wilson lines labeled by $\square$, and the coefficients follow.

This concludes our proof of Figure 2.7.

BIBLIOGRAPHY

[1] Dražen Adamović. Classification of irreducible modules of certain subalgebras of free boson vertex algebra. *J. Algebra*, 270.

[2] Dražen Adamović and Antun Milas. Logarithmic intertwining operators and W(2,2p-1)-algebras. *J. Math. Phys.*, 48:073503, 2007. doi: 10.1063/1.2747725.

[3] Dražen Adamović and Antun Milas. The doublet vertex operator superalgebras $\mathcal{A}(p)$ and $\mathcal{A}_{2,p}$,. *Recent developments in algebraic and combinatorial aspects of representation theory*, 602, 2013.

[4] Sharad Agnihotri and Chris Woodward. Eigenvalues of products of unitary matrices and quantum Schubert calculus. *arXiv e-prints*, art. alg-geom/9712013, Dec 1997.

[5] Sergei Alexandrov and Boris Pioline. Black holes and higher depth mock modular forms. 2018.

[6] Mark G. Alford, Kai-Ming Lee, John March-Russell, and John Preskill. Quantum field theory of nonAbelian strings and vortices. *Nucl.Phys.*, B384: 251–317, 1992. doi: 10.1016/0550-3213(92)90468-Q.

[7] Murad Alim, Babak Haghighat, Michael Hecht, Albrecht Klemm, Marco Rauch, and Thomas Wotschke. Wall-crossing holomorphic anomaly and mock modularity of multiple M5-branes. *Commun. Math. Phys.*, 339(3): 773–814, 2015. doi: 10.1007/s00220-015-2436-3.

[8] George E. Andrews. *Partitions: yesterday and today*. New Zealand Mathematical Society, 1979. ISBN 9780959757903. URL `https://books.google.com/books?id=zfHuAAAAMAAJ`.

[9] Philip C. Argyres and Mithat Unsal. The semi-classical expansion and resurgence in gauge theories: new perturbative, instanton, bion, and renormalon effects. *JHEP*, 08:063, 2012. doi: 10.1007/JHEP08(2012)063.

[10] David R. Auckly. Topological methods to compute chern-simons invariants. *Mathematical Proceedings of the Cambridge Philosophical Society*, 115(2): 229–251, 1994. doi: 10.1017/S0305004100072066.

[11] Vijay Balasubramanian, Jackson R. Fliss, Robert G. Leigh, and Onkar Parrikar. Multi-Boundary Entanglement in Chern-Simons Theory and Link Invariants. 2016.

[12] Dror Bar-Natan. Khovanov's homology for tangles and cobordisms. *arXiv Mathematics e-prints*, art. math/0410495, Oct 2004.

[13] Alexander. A Beilinson, George Lusztig, and Robert MacPherson. A geometric setting for the quantum deformation of gl(n). *Duke Math. J.*, 61(2): 655–677, 1990. ISSN 0012-7094. doi: 10.1215/S0012-7094-90-06124-1. URL http://dx.doi.org/10.1215/S0012-7094-90-06124-1.

[14] Anna Beliakova, Christian Blanchet, and Nathan Geer. Logarithmic Hennings invariants for restricted quantum sl(2). *arXiv e-prints*, art. arXiv:1705.03083, May 2017.

[15] Prakash Belkale. Local systems on p(1)-s for s a finite set. *Compositio Math.*, 129(1):67–86, 2001. ISSN 0010-437X. doi: 10.1023/A:1013195625868. URL http://dx.doi.org/10.1023/A:1013195625868.

[16] Christian Blanchet, Francesco Costantino, Nathan Geer, and Bertrand Patureau-Mirand. Non semi-simple TQFTs, Reidemeister torsion and Kashaev's invariants. *arXiv e-prints*, art. arXiv:1404.7289, Apr 2014.

[17] Christian Blanchet, Francesco Costantino, Nathan Geer, and Bertrand Patureau-Mirand. Non semi-simple TQFTs from unrolled quantum $sl(2)$. *arXiv e-prints*, art. arXiv:1605.07941, May 2016.

[18] Kathrin Bringmann and Antun Milas. $\mathcal{W}$-Algebras, False Theta Functions and Quantum Modular Forms, I. *International Mathematics Research Notices*, 2015(21):11351–11387, 02 2015. ISSN 1073-7928. doi: 10.1093/imrn/rnv033. URL https://doi.org/10.1093/imrn/rnv033.

[19] Kathrin Bringmann and Larry Rolen. Half-integral weight Eichler integrals and quantum modular forms. *arXiv e-prints*, art. arXiv:1409.3781, Sep 2014.

[20] Kathrin Bringmann, Amanda Folsom, and Robert C. Rhoades. Partial theta functions and mock modular forms as q-hypergeometric series. *arXiv e-prints*, art. arXiv:1109.6560, Sep 2011.

[21] Kathrin Bringmann, Amanda Folsom, and Antun Milas. Asymptotic behavior of partial and false theta functions arising from Jacobi forms and regularized characters. *Journal of Mathematical Physics*, 58(1):011702, Jan 2017. doi: 10.1063/1.4973634.

[22] Kathrin Bringmann, Amanda Folsom, Ken Ono, and Larry Rolen. *Harmonic Maass forms and mock modular forms: theory and applications*, volume 64. American Mathematical Society Colloquium Publications, American Mathematical Society, Providence, RI, 2017.

[23] Ilka Brunner and Daniel Roggenkamp. B-type defects in Landau-Ginzburg models. *JHEP*, 08:093, 2007. doi: 10.1088/1126-6708/2007/08/093.

[24] Ilka Brunner and Daniel Roggenkamp. B-type defects in Landau-Ginzburg models. *JHEP*, 0708:093, 2007. doi: 10.1088/1126-6708/2007/08/093.

[25] Ilka Brunner and Daniel Roggenkamp. Defects and bulk perturbations of boundary Landau-Ginzburg orbifolds. *JHEP*, 0804:001, 2008. doi: 10.1088/1126-6708/2008/04/001.

[26] Ilka Brunner, Manfred Herbst, Wolfgang Lerche, and Bernhard Scheuner. Landau-Ginzburg realization of open string TFT. *JHEP*, 0611:043, 2006. doi: 10.1088/1126-6708/2006/11/043.

[27] Ilka Brunner, Hans Jockers, and Daniel Roggenkamp. Defects and D-Brane Monodromies. *Adv.Theor.Math.Phys.*, 13:1077–1135, 2009. doi: 10.4310/ATMP.2009.v13.n4.a4.

[28] Andrea Cappelli, Claude Itzykson, and Jean-Bernard Zuber. The A-D-E classification of minimal and A1(1) conformal invariant theories. *Communications in Mathematical Physics*, 113:1–26, 03 1987. doi: 10.1007/BF01221394.

[29] Nils Carqueville and Daniel Murfet. Computing Khovanov-Rozansky homology and defect fusion. *Topology*, 14:489–537, 2014. doi: 10.2140/agt.2014.14.489.

[30] Sabin Cautis, Joel Kamnitzer, and Scott Morrison. Webs and quantum skew Howe duality. *Math. Ann.*, 360(1-2):351–390, 2014. ISSN 0025-5831. doi: 10.1007/s00208-013-0984-4. URL `http://dx.doi.org/10.1007/s00208-013-0984-4`.

[31] Sergio Cecotti and Cumrun Vafa. On classification of N=2 supersymmetric theories. *Commun.Math.Phys.*, 158:569–644, 1993. doi: 10.1007/BF02096804.

[32] Miranda C. N. Cheng and John F. R. Duncan. On Rademacher Sums, the Largest Mathieu Group, and the Holographic Modularity of Moonshine. *Commun. Num. Theor. Phys.*, 6:697–758, 2012. doi: 10.4310/CNTP.2012.v6.n3.a4.

[33] Miranda C. N. Cheng and John F. R. Duncan. Rademacher Sums and Rademacher Series. *Contrib. Math. Comput. Sci.*, 8:143–182, 2014. doi: 10.1007/978-3-662-43831-2_6.

[34] Miranda C. N. Cheng and John F. R. Duncan. Optimal Mock Jacobi Theta Functions. *arXiv e-prints*, art. arXiv:1605.04480, May 2016.

[35] Miranda C. N. Cheng, John F. R. Duncan, and Jeffrey A. Harvey. Umbral Moonshine and the Niemeier Lattices. 2013.

[36] Miranda C. N. Cheng, Xi Dong, John F. R. Duncan, Sarah Harrison, Shamit Kachru, and Timm Wrase. Mock Modular Mathieu Moonshine Modules. 2014. doi: 10.1186/s40687-015-0034-9. [Res. Math. Sci.2,13(2015)].

[37] Miranda C. N. Cheng, John F. R. Duncan, and Jeffrey A. Harvey. Umbral Moonshine. *Commun. Num. Theor. Phys.*, 08:101–242, 2014. doi: 10.4310/CNTP.2014.v8.n2.a1.

[38] Miranda C. N. Cheng, Sungbong Chun, Francesca Ferrari, Sergei Gukov, and Sarah M. Harrison. 3d Modularity. 2018.

[39] Dohoon Choi, Subong Lim, and Robert C. Rhoades. Mock modular forms and quantum modular forms. *Proc. Amer. Math. Soc.*, 144, 2016.

[40] Sungbong Chun. Junctions of refined Wilson lines and one-parameter deformation of quantum groups. 2017.

[41] Sungbong Chun. A resurgence analysis of the $SU(2)$ Chern-Simons partition functions on a Brieskorn homology sphere $\Sigma(2, 5, 7)$. 2017.

[42] Sungbong Chun and Ning Bao. Entanglement entropy from SU(2) Chern-Simons theory and symmetric webs. 2017.

[43] Sungbong Chun, Sergei Gukov, and Daniel Roggenkamp. Junctions of surface operators and categorification of quantum groups. 2015.

[44] Hee-Joong Chung. BPS Invariants for Seifert Manifolds. 2018.

[45] Ovidiu Costin and Stavros Garoufalidis. Resurgence of the kontsevich-zagier series. 61(3):1225–1258, 2011. URL `http://eudml.org/doc/219786`.

[46] Louis Crane and Igor Frenkel. Four-dimensional topological field theory, Hopf categories, and the canonical bases. *J. Math. Phys.*, 35:5136–5154, 1994. doi: 10.1063/1.530746.

[47] Thomas Creutzig and Antun Milas. False Theta Functions and the Verlinde formula. *Adv. Math.*, 262:520–545, 2014. doi: 10.1016/j.aim.2014.05.018.

[48] Atish Dabholkar, Sameer Murthy, and Don Zagier. Quantum Black Holes, Wall Crossing, and Mock Modular Forms. 2012.

[49] Wladimir de Azevedo Pribitkin. The fourier coefficients of modular forms and niebur modular integrals having small positive weight, i. *Acta Arithmetica*, 91(4):291–309, 1999. URL `http://eudml.org/doc/207357`.

[50] Wladimir de Azevedo Pribitkin. The fourier coefficients of modular forms and niebur modular integrals having small positive weight, ii. *Acta Arithmetica*, 93(4):343–358, 2000. URL `http://eudml.org/doc/207418`.

[51] Mykola Dedushenko, Sergei Gukov, and Pavel Putrov. Vertex algebras and 4-manifold invariants. In *Proceedings, Nigel Hitchin's 70th Birthday Conference : Geometry and Physics : A Festschrift in honour of Nigel Hitchin : 2 volumes: Aarhus, Denmark, Oxford, UK, Madrid, Spain, September 5-16, 2016*, volume 1, pages 249–318, 2018. doi: 10.1093/oso/9780198802013.003.0011.

[52] Tudor Dimofte, Sergei Gukov, Jonatan Lenells, and Don Zagier. Exact Results for Perturbative Chern-Simons Theory with Complex Gauge Group. *Commun. Num. Theor. Phys.*, 3:363–443, 2009. doi: 10.4310/CNTP.2009.v3.n2.a4.

[53] Martin Eichler and Don Zagier. *The theory of Jacobi forms*. Birkhäuser, 1985.

[54] David Eisenbud. Homological algebra on a complete intersection, with an application to group representations. *Trans. Amer. Math. Soc.*, 260:35–64, 1980.

[55] Ross Elliot and Sergei Gukov. Exceptional knot homology. 2015.

[56] Boris L. Feigin and Sergei Gukov. VOA[M_4]. 2018.

[57] Boris L. Feigin, Azat M. Gainutdinov, Aleksei M. Semikhatov, and I. Yu. Tipunin. Kazhdan-Lusztig correspondence for the representation category of the triplet W-algebra in logarithmic CFT. *Theor. Math. Phys.*, 148:1210–1235, 2006. doi: 10.1007/s11232-006-0113-6. [Teor. Mat. Fiz.148,398(2006)].

[58] Boris L. Feigin, Azat M. Gainutdinov, Aleksei M. Semikhatov, and I. Yu. Tipunin. Modular group representations and fusion in logarithmic conformal field theories and in the quantum group center. *Commun. Math. Phys.*, 265: 47–93, 2006. doi: 10.1007/s00220-006-1551-6.

[59] Giovanni Felder. BRST approach to minimal models. *Nucl. Phys. B*, 317, 1989.

[60] Michael A. I. Flohr. On modular invariant partition functions of conformal field theories with logarithmic operators. *Int. J. Mod. Phys.*, A11:4147–4172, 1996. doi: 10.1142/S0217751X96001954.

[61] Amanda Folsom, Ken Ono, and Robert C. Rhoades. Mock theta functions and quantum modular forms. *Forum of Mathematics, Pi*, 1:e2, 2013. doi: 10.1017/fmp.2013.3.

[62] Daniel S. Freed and Robert E. Gompf. Computer calculation of witten's 3-manifold invariant. *Comm. Math. Phys.*, 141(1):79–117, 1991. URL `https://projecteuclid.org:443/euclid.cmp/1104248195`.

[63] Jürgen Fuchs, Stephen Hwang, Aleksei M. Semikhatov, and I. Yu. Tipunin. Nonsemisimple fusion algebras and the Verlinde formula. *Commun. Math. Phys.*, 247:713–742, 2004. doi: 10.1007/s00220-004-1058-y.

[64] Matthias R. Gaberdiel. An explicit construction of the quantum group in chiral WZW-models. *Comm. Math. Phys.*, 173(2):357–377, 1995. URL `https://projecteuclid.org:443/euclid.cmp/1104274733`.

[65] Abhijit Gadde and Sergei Gukov. 2d Index and Surface operators. *JHEP*, 1403:080, 2014. doi: 10.1007/JHEP03(2014)080.

[66] Abhijit Gadde, Sergei Gukov, and Pavel Putrov. Fivebranes and 4-manifolds. 2013.

[67] Abhijit Gadde, Sergei Gukov, and Pavel Putrov. Walls, Lines, and Spectral Dualities in 3d Gauge Theories. *JHEP*, 05:047, 2014. doi: 10.1007/JHEP05(2014)047.

[68] Stavros Garoufalidis. Chern-Simons theory, analytic continuation and arithmetic. *ArXiv e-prints*, November 2007.

[69] Stavros Garoufalidis, Thang T. Q. Le, and Marcos Marino. Analyticity of the Free Energy of a Closed 3-Manifold. *SIGMA*, 4:080, 2008. doi: 10.3842/SIGMA.2008.080.

[70] Robert E. Gompf and András I. Stipsicz. *4-Manifolds and Kirby Calculus*. Graduate studies in mathematics. American Mathematical Society, 1999. ISBN 9780821809945. URL https://books.google.com/books?id=ahLKzRUTBbUC.

[71] Rajesh Gopakumar and Cumrun Vafa. M-theory and topological strings-i. Jan 1998. URL http://arxiv.org/abs/hep-th/9809187v1.

[72] Rajesh Gopakumar and Cumrun Vafa. M-theory and topological strings-ii. Jan 1998. URL http://arxiv.org/abs/hep-th/9812127v1.

[73] Rajesh Gopakumar and Cumrun Vafa. On the gauge theory / geometry correspondence. *Adv. Theor. Math. Phys.*, 3:1415–1443, 1999. doi: 10.4310/ATMP.1999.v3.n5.a5. [AMS/IP Stud. Adv. Math.23,45(2001)].

[74] Jonathan Grant. The moduli problem of Lobb and Zentner and the colored sl(n) graph invariant. *J. Knot Theory Ramifications*, 22(10):1350060, 16, 2013. ISSN 0218-2165. doi: 10.1142/S0218216513500600. URL http://dx.doi.org/10.1142/S0218216513500600.

[75] Enore Guadagnini, Maurizio Martellini, and Mihail Mintchev. Wilson Lines in Chern-Simons Theory and Link Invariants. *Nucl. Phys.*, B330:575–607, 1990. doi: 10.1016/0550-3213(90)90124-V.

[76] Sergei Gukov. Three-dimensional quantum gravity, Chern-Simons theory, and the A polynomial. *Commun. Math. Phys.*, 255:577–627, 2005. doi: 10.1007/s00220-005-1312-y.

[77] Sergei Gukov. Gauge theory and knot homologies. *Fortsch.Phys.*, 55:473–490, 2007. doi: 10.1002/prop.200610385.

[78] Sergei Gukov and Marko Stošić. Homological Algebra of Knots and BPS States. *Proc.Symp.Pure Math.*, 85:125–172, 2012. doi: 10.1090/pspum/085/1377.

[79] Sergei Gukov and Johannes Walcher. Matrix factorizations and Kauffman homology. 2005.

[80] Sergei Gukov and Johannes Walcher. Matrix factorizations and Kauffman homology. 2005.

[81] Sergei Gukov and Edward Witten. Gauge Theory, Ramification, And The Geometric Langlands Program. 2006.

[82] Sergei Gukov, Albert S. Schwarz, and Cumrun Vafa. Khovanov-Rozansky homology and topological strings. *Lett. Math. Phys.*, 74:53–74, 2005. doi: 10.1007/s11005-005-0008-8.

[83] Sergei Gukov, Marcos Marino, and Pavel Putrov. Resurgence in complex Chern-Simons theory. 2016.

[84] Sergei Gukov, Du Pei, Pavel Putrov, and Cumrun Vafa. BPS spectra and 3-manifold invariants. 2017.

[85] Sergei Gukov, Pavel Putrov, and Cumrun Vafa. Fivebranes and 3-manifold homology. *JHEP*, 07:071, 2017. doi: 10.1007/JHEP07(2017)071.

[86] Kazuhiro Hikami. Quantum Invariant, Modular Form, and Lattice Points. *arXiv e-prints*, art. math-ph/0409016, Sep 2004.

[87] Kazuhiro Hikami. On the Quantum Invariant for the Brieskorn Homology Spheres. *arXiv e-prints*, art. math-ph/0405028, May 2004.

[88] Kazuhiro Hikami. Mock (False) Theta Functions as Quantum Invariants. *Regular and Chaotic Dynamics*, 10(4):509, Jan 2005. doi: 10.1070/RD2005v010n04ABEH000328.

[89] Kazuhiro Hikami. Quantum invariants, modular forms, and lattice points II. *Journal of Mathematical Physics*, 47(10):102301–102301, Oct 2006. doi: 10.1063/1.2349484.

[90] Kazuhiro Hikami. On the Quantum Invariants for the Spherical Seifert Manifolds. *Communications in Mathematical Physics*, 268(2):285–319, Dec 2006. doi: 10.1007/s00220-006-0094-1.

[91] Kazuhiro Hikami. Decomposition of Witten-Reshetikhin-Turaev invariant: Linking pairing and modular forms. *AMS/IP Stud. Adv. Math.*, 50:131–151, 2011.

[92] Kentaro Hori and Johannes Walcher. F-term equations near Gepner points. *JHEP*, 0501:008, 2005. doi: 10.1088/1126-6708/2005/01/008.

[93] Lisa C. Jeffrey. Chern-simons-witten invariants of lens spaces and torus bundles, and the semiclassical approximation. *Comm. Math. Phys.*, 147(3): 563–604, 1992. URL https://projecteuclid.org:443/euclid.cmp/1104250751.

[94] Lisa C. Jeffrey and Jonathan Weitsman. Bohr-Sommerfeld orbits in the moduli space of flat connections and the Verlinde dimension formula. *Comm. Math. Phys.*, 150(3):593–630, 1992. ISSN 0010-3616. URL http://projecteuclid.org/euclid.cmp/1104251961.

[95] Yukihiro Kanie and Akihiro Tsuchiya. Fock space representations of virasoro algebra and intertwining operators. *Proc. Japan Acad. Ser. A Math. Sci.*, 62 (1):12–15, 1986. doi: 10.3792/pjaa.62.12. URL https://doi.org/10.3792/pjaa.62.12.

[96] Anton Kapustin and Yi Li. Topological correlators in Landau-Ginzburg models with boundaries. *Adv. Theor. Math. Phys.*, 7(4):727–749, 2003. doi: 10.4310/ATMP.2003.v7.n4.a5.

[97] Amir-Kian Kashani-Poor. Quantization condition from exact WKB for difference equations. *JHEP*, 06:180, 2016. doi: 10.1007/JHEP06(2016)180.

[98] Horst G. Kausch. Extended conformal algebras generated by a multiplet of primary fields. *Phys. Lett. B*, 259, 1991.

[99] David Kazhdan and George Lusztig. Tensor structures arising from affine Lie algebras. i, ii. *J. Amer. Math. Soc.*, 6, 1993.

[100] David Kazhdan and George Lusztig. Tensor structures arising from affine lie algebras. iii. *J. Amer. Math. Soc.*, 7, 1994.

[101] David Kazhdan and George Lusztig. Tensor structures arising from affine lie algebras. iv. *J. Amer. Math. Soc.*, 7, 1994.

[102] Mikhail Khovanov. A categorification of the Jones polynomial. *Duke Math. J.*, 101:359–426, 2000.

[103] Mikhail Khovanov. sl(3) link homology. *arXiv Mathematics e-prints*, art. math/0304375, Apr 2003.

[104] Mikhail Khovanov and Lev Rozansky. Matrix factorizations and link homology. *arXiv Mathematics e-prints*, art. math/0401268, Jan 2004.

[105] Mikhail Khovanov and Lev Rozansky. Topological Landau-Ginzburg models on the world-sheet foam. *Adv. Theor. Math. Phys.*, 11(2):233–259, 2007. ISSN 1095-0761. URL http://projecteuclid.org/euclid.atmp/1185303945.

[106] Mikhail Khovanov and Lev Rozansky. Virtual crossings, convolutions and a categorification of the so(2n) Kauffman polynomial. *J. Gökova Geom. Topol. GGT*, 1:116–214, 2007. ISSN 1935-2565.

[107] Mikhail Khovanov and Lev Rozansky. Matrix factorizations and link homology. II. *Geom. Topol.*, 12(3):1387–1425, 2008. ISSN 1465-3060. doi: 10.2140/gt.2008.12.1387. URL `http://dx.doi.org/10.2140/gt.2008.12.1387`.

[108] Maxim Kontsevich. Resurgence from the path integral perspective. Lectures at Perimeter Institute, 2012.

[109] Maxim Kontsevich. Exponential integrals. Lectures at SCGP and at IHES, 2014 and 2015.

[110] Maxim Kontsevich. Resurgence and wall-crossings via complexified path integral. Lectures at TFC Sendai, 2016.

[111] Andrew Lobb and Raphael Zentner. The quantum sl(n) graph invariant and a moduli space. *Int. Math. Res. Not. IMRN*, (7):1956–1972, 2014. ISSN 1073-7928.

[112] Volodimir Lyubashenko. Modular properties of ribbon abelian categories. In *Symposia Gaussiana, Proc. of the 2nd Gauss Symposium, Munich, 1993, Conf. A (Berlin, New York), Walter de Ruyter, 1995, pp. 529-579*, pages 529–579, 1994.

[113] Volodimir V. Lyubashenko. Invariants of three manifolds and projective representations of mapping class groups via quantum groups at roots of unity. *Commun. Math. Phys.*, 172:467–516, 1995. doi: 10.1007/BF02101805.

[114] Marco Mackaay and Pedro Vaz. The universal sl3-link homology. *arXiv Mathematics e-prints*, art. math/0603307, Mar 2006.

[115] Marco Mackaay, Marko Stosic, and Pedro Vaz. Sl(N) link homology using foams and the Kapustin-Li formula. *arXiv e-prints*, art. arXiv:0708.2228, Aug 2007.

[116] Marcos Marino. Lectures on non-perturbative effects in large N gauge theories, matrix models and strings. *Fortsch. Phys.*, 62:455–540, 2014. doi: 10.1002/prop.201400005.

[117] Scott Morrison and Ari Nieh. On Khovanov's cobordism theory for su(3) knot homology. *arXiv Mathematics e-prints*, art. math/0612754, Dec 2006.

[118] Kiyokazu Nagatomo and Akihiro Tsuchiya. The Triplet Vertex Operator Algebra W(p) and the Restricted Quantum Group at Root of Unity. *arXiv e-prints*, art. arXiv:0902.4607, Feb 2009.

[119] Walter Neumann and Frank Raymond. *Seifert manifolds, plumbing, μ-invariant and orientation reversing maps*, volume 664, pages 163–196. 01 1970. doi: 10.1007/BFb0061699.

[120] Tomotada Ohtsuki. A polynomial invariant of integral homology 3-spheres. *Mathematical Proceedings of the Cambridge Philosophical Society*, 117(1): 83–112, 1995. doi: 10.1017/S0305004100072935.

[121] Tomotada Ohtsuki. A polynomial invariant of rational homology 3-spheres. *Inventiones Mathematicae*, 123:241, 1996. doi: 10.1007/BF01232375.

[122] Hirosi Ooguri and Cumrun Vafa. Knot invariants and topological strings. *Nucl. Phys.*, B577:419–438, 2000. doi: 10.1016/S0550-3213(00)00118-8.

[123] Peter Ozsvath and Zoltan Szabo. Holomorphic disks and knot invariants. *Adv. Math.*, 186:58–116, 2004.

[124] Du Pei and Ke Ye. A 3d-3d appetizer. *JHEP*, 11:008, 2016. doi: 10.1007/JHEP11(2016)008.

[125] Hoel Queffelec and David E. V. Rose. The sl_n foam 2-category: a combinatorial formulation of khovanov-rozansky homology via categorical skew howe duality. 2014.

[126] Hans Rademacher. A convergent series for the partition function $p(n)$. *Proceedings of the National Academy of Sciences of the United States of America*, 1937.

[127] Jacob Rasmussen. Floer homology and knot complements. 2003.

[128] Lev Rozansky. A large k asymptotics of witten's invariant of seifert manifolds. *Comm. Math. Phys.*, 171(2):279–322, 1995. URL `https://projecteuclid.org:443/euclid.cmp/1104273564`.

[129] Lev Rozansky. Topological A models on seamed Riemann surfaces. *Adv.Theor.Math.Phys.*, 11, 2007.

[130] Grant Salton, Brian Swingle, and Michael Walter. Entanglement from Topology in Chern-Simons Theory. *Phys. Rev.*, D95(10):105007, 2017. doi: 10.1103/PhysRevD.95.105007.

[131] Nils-Peter Skoruppa. *Über den Zusammenhang zwischen Jacobiformen und Modulformen halbganzen Gewichts*. PhD thesis, Universität Bonn Mathematisches Institut, Bonn, 1985. Dissertation, Rheinische Friedrich-Wilhelms-Universität, Bonn, 1984.

[132] Jan Troost. The non-compact elliptic genus: mock or modular. *JHEP*, 06: 104, 2010. doi: 10.1007/JHEP06(2010)104.

[133] Daniel Tubbenhauer, Pedro Vaz, and Paul Wedrich. Super q-Howe duality and web categories. *arXiv e-prints*, art. arXiv:1504.05069, Apr 2015.

[134] Edward Witten. Quantum field theory and the jones polynomial. *Comm. Math. Phys.*, 121(3):351–399, 1989. URL https://projecteuclid.org:443/euclid.cmp/1104178138.

[135] Edward Witten. Quantum Field Theory and the Jones Polynomial. *Comm.Math.Phys.*, 121:351–399, 1989. doi: 10.1007/BF01217730.

[136] Edward Witten. Gauge Theories and Integrable Lattice Models. *Nucl.Phys.*, B322:629, 1989. doi: 10.1016/0550-3213(89)90232-0.

[137] Edward Witten. Gauge Theories, Vertex Models, and Quantum Groups. *Nucl.Phys.*, B330:285, 1990. doi: 10.1016/0550-3213(90)90115-T.

[138] Edward Witten. The Verlinde algebra and the cohomology of the Grassmannian. 1993.

[139] Edward Witten. Chern-Simons gauge theory as a string theory. *Prog. Math.*, 133:637–678, 1995.

[140] Edward Witten. Solutions of four-dimensional field theories via M theory. *Nucl.Phys.*, B500:3–42, 1997. doi: 10.1016/S0550-3213(97)00416-1.

[141] Edward Witten. Fivebranes and Knots. 2011.

[142] Edward Witten. Analytic Continuation Of Chern-Simons Theory. *AMS/IP Stud. Adv. Math.*, 50:347–446, 2011.

[143] Hao Wu. A colored sl(N)-homology for links in $S\hat{3}$. *arXiv e-prints*, art. arXiv:0907.0695, Jul 2009.

[144] Yasuyoshi Yonezawa. Quantum $(\mathfrak{sl}_n, \wedge v_n)$ link invariant and matrix factorizations. *Nagoya Math. J.*, 204:69–123, 12 2011. doi: 10.1215/00277630-1431840. URL https://doi.org/10.1215/00277630-1431840.

[145] Don Zagier. Quantum modular forms. *Clay Math. Proc.*, 11, 2010.

[146] Don Zagier and Ruth Lawrence. Modular forms and quantum invariants of 3-manifolds. *Asian J. Math*, 3, 01 1999. doi: 10.4310/AJM.1999.v3.n1.a5.

[147] Sander P. Zwegers. Mock θ-functions and real analytic modular forms. *Contemp. Math.*, 291, 01 2001. doi: 10.1090/conm/291/04907.

[148] Sander P. Zwegers. Mock Theta Functions. *arXiv e-prints*, art. arXiv:0807.4834, Jul 2008.